Report
R-19-03
April 2019

Modelling of the near-field hydrogeology – temperate climate conditions

Report for the safety evaluation SE-SFL

Elena Abarca
Diego Sampietro
Jorge Molinero
Henrik von Schenck

SVENSK KÄRNBRÄNSLEHANTERING AB

SWEDISH NUCLEAR FUEL
AND WASTE MANAGEMENT CO

Box 3091, SE-169 03 Solna
Phone +46 8 459 84 00
skb.se

SVENSK KÄRNBRÄNSLEHANTERING

ISSN 1402-3091
SKB R-19-03
ID 1571321
April 2019

Modelling of the near-field hydrogeology – temperate climate conditions

Report for the safety evaluation SE-SFL

Elena Abarca, Diego Sampietro, Jorge Molinero,
Henrik von Schenck
Amphos 21 Consulting S. L.

This report concerns a study which was conducted for Svensk Kärnbränslehantering AB (SKB). The conclusions and viewpoints presented in the report are those of the authors. SKB may draw modified conclusions, based on additional literature sources and/or expert opinions.

A pdf version of this document can be downloaded from www.skb.se.

© 2019 Svensk Kärnbränslehantering AB

Summary

The present work is part of the SFL safety evaluation (SE-SFL) and deals with the hydrological conditions in the repository near-field. The term near-field refers to the rock vaults, their components and barriers, as well as the surrounding rock in the vicinity of the repository.

Geological data from the Laxemar area has been used to represent a granitic host rock for SFL. The area is well characterised with high data density, having been considered as a potential site for the final repository for spent nuclear fuel (SKB 2011). Preliminary modelling of the SFL near-field hydrogeology explored the influence of host rock characteristics and barrier properties (Abarca et al. 2016). Near-field simulations were performed sampling two rock domains at three different depths (300 m, 500 m, and 700 m depth). This work focusses on the near-field host rock at location 500_1, selected as representative granitic host rock for SFL. The regional hydrogeological model of Joyce et al. (2019) has been used as input to supply initial and boundary conditions to the near-field hydrology model.

A central objective has been to perform near-field simulations under different scenarios to calculate and compile results for vault and waste flow, to serve as input to radionuclide transport calculations. Near-field simulations have been performed to sample four repository orientations and three cases of hydraulic properties of the concrete backfill. Models and results have been analysed with respect to the direction of the local flow system relative to the orientation of the rock vaults, the interaction of the vaults with the high permeability stochastic features, the interaction between vaults regarding mass transfer and the tracer mass released from the waste compartments. In addition, the time needed to reach full water saturation of the SFL vaults after repository closure has been evaluated by means of numerical simulation of flow in variably saturated porous media accounting for changes in hydraulic properties with water saturation.

Sammanfattning

Föreliggande arbete utgör en del av säkerhetsvärderingen för SFL (SE-SFL) och behandlar hydrologiska förhållanden i förvarets närzon. Med närzonen avses förvarssalarna, deras komponenter och barriärer, samt det omgivande berget i förvarets närhet.

Geologiska data från Laxemar-området har använts för att representera ett granitiskt berg i SFL:s omgivning. Området är väl karaktäriserat, med hög datatäthet, då det föreslagits som möjlig plats för ett slutförvar för använt kärnbränsle (SKB 2011). Preliminär modellering av hydrogeologin i SFL:s närzon utforskade påverkan av egenskaper hos berg och barriärer (Abarca et al. 2016). Simulering av närzonen omfattade två bergvolymer som vardera utvärderades vid tre djup (300 m, 500 m och 700 m djup). Arbetet som presenteras här fokuserar på bergpositionen kallad 500_1, som är vald som ett representativt granitiskt berg för SFL. Joyce et al. (2019) regionala hydrogeologimodell har använts som input för att tillhandahålla närzonsmodellen med randvillkor och initialvillkor.

Ett av detta arbetes huvudsyften har varit att beräkna flöden genom förvarssalar och avfall, som indata till radionuklidtransportberäkningar. Flödet genom SFL:s närzon har simulerats för fyra olika orienteringar av förvaret. Vidare har tre olika degraderingstillstånd antagits för betongåterfyllnaden i BHK. Modeller och resultat har analyserats med avseende på den lokala riktningen av flödesfältet relativt förvarssalarna och med hänsyn till påverkan från stokastiska sprickzoner med hög permeabilitet. Interaktion mellan förvarssalar har utvärderats med hjälp av beräkningar av masstransport kopplad till det lokala flödet. Vidare har tiden för att nå vattenmättnad i förvaret efter förslutning utvärderats med hjälp av flödessimuleringar i omättat poröst medium. Här har hänsyn tagits till att de hydrauliska egenskaperna förändras med mättnadsgraden.

Contents

1 Introduction

SKB plans to dispose of long-lived low and intermediate level waste in SFL. The waste comes from the operation and decommissioning of the Swedish nuclear power plants, legacy waste from the early research in the Swedish nuclear programmes, and smaller amounts of waste from hospitals, industry and research. The long-lived low and intermediate level waste from the nuclear power plants consists of neutron-irradiated components and control rods. The total quantity of long-lived waste planned for SFL is estimated to approximately 16 000 m^3, of which about one third originates from the nuclear power plants. The remainder comes from AB SVAFO, Studsvik Nuclear AB and Cyclife Sweden AB, who manage the legacy waste and the waste from hospitals, industry and research.

In the proposed concept (Elfwing et al. 2013), SFL is as a deep geological repository with two storage vaults:

- one vault for the metallic waste from the nuclear power plants, and
- one vault for legacy waste from AB SVAFO, Studsvik Nuclear AB and Cyclife Sweden AB.

The vault for the metallic waste (BHK) is designed with a concrete barrier. The waste is segmented, after which the parts are deposited in steel tanks and stabilised with grout. The steel tanks are emplaced in the repository. This section of the repository is backfilled with concrete, which acts as a barrier against groundwater flow and contributes to a low diffusion rate and high sorption of many radionuclides. The concrete in the barrier will create an alkaline environment in the repository section, reducing the corrosion rate of the steel and thus limiting the release rate of radionuclides.

The vault for the legacy waste (BHA) from AB SVAFO, Studsvik Nuclear AB and Cyclife Sweden AB is designed with a bentonite barrier. The waste is deposited in containers designed for SFL and stabilised with grout. These containers are emplaced in the repository. The section is backfilled with bentonite. The bentonite acts as a barrier by limiting the groundwater flow, thereby making diffusion the dominant transport mechanism for radionuclides through the bentonite. Bentonite clay also has the ability to efficiently filter colloids.

Figure 1-1 shows a schematic representation of the repository design, with the BHA vault in the foreground and the BHK vault in the background.

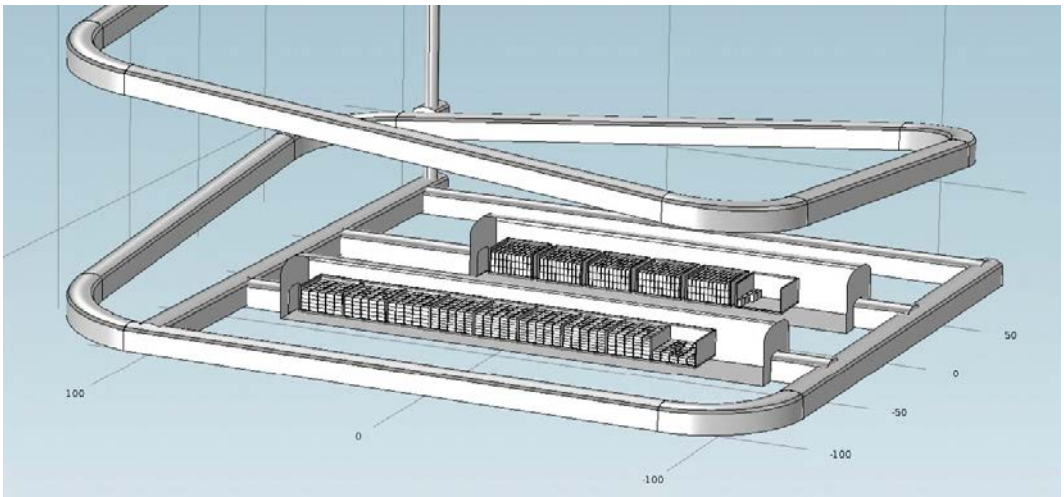

Figure 1-1. *SFL repository design with the BHA vault (front) and the BHK vault (back).*

Site data from the Laxemar area has been used to represent a granitic host rock around the SFL. The area is well characterised with high data density, having been considered as a potential site for the final repository for spent nuclear fuel (SKB 2011). Preliminary modelling work concerning the SFL near-field hydrogeology explored the influence of host rock characteristics and barrier properties (Abarca et al. 2016). These near-field simulations were conducted for two different locations at three different depths (300 m, 500 m, and 700 m depth). The simulations were analysed with respect to the permeability of the rock, the presence of fractures and deformation zones, the effect of groundwater salinity, and magnitude and direction of the Darcy flux relative to the orientation of the rock vaults. The present work focusses on groundwater flow in the near-field host rock at one location at the depth of 500 m.

1.1 Objective

The main objective of this work is to investigate the influence of the SFL repository on near-field hydrogeology under temperate climate conditions. The flow through the vaults and waste is calculated for a set of repository configurations, to serve as input to radionuclide transport calculations. The following aspects have been evaluated:

- Repository orientation and
- degradation of the concrete backfill in BHK.

Additional transport simulations are performed to deepen the understanding of solute transport in the near-field and to evaluate the interaction between vaults. A first evaluation of the time needed to reach full water saturation of the SFL vaults after the repository is also given.

1.2 Outline of the report

Chapter 2 gives an overview of the blocks of simulations that have been carried out. It explains the hierarchy of models, the processes that are considered, and the flow of information between models.

Chapter 3 describes the repository scale model used for the groundwater flow and transport simulations. It contains the equations describing the simulated processes and the numerical details of each model. The geometry and material properties of the engineered structures as well as the rock in the repository near-field are presented.

Chapter 4 provides an overview of the results and how they are calculated.

Chapter 5 presents an analysis of the results for the base case. It describes the groundwater flow around the repository, the interaction between the BHA and BHK vaults as well as the temporal evolution of a tracer released from the waste compartments.

Chapter 6 presents an analysis of the influence of the repository orientation relative to the direction of groundwater flow and how the flow through the vault and waste compartments is affected.

Chapter 7 presents an analysis of the effects of an increase in permeability due to the degradation of the concrete backfill in BHK.

Chapter 8 presents an analysis of the role of the backfill material with regard to the transport of a tracer released from the waste. The results of these simulations provide information about the total mass outflow from each vault to the rock.

Chapter 9 presents an estimate of the time needed to reach full water saturation of the SFL vaults after repository closure.

2 Methodology

The influence of the SFL repository on the near-field hydrogeology is evaluated by means of a repository scale model developed in COMSOL Multiphysics (COMSOL 2015).

In previous modelling work, the repository scale model of SFL was set up using a regional groundwater flow model of the Laxemar area implemented in DarcyTools (Abarca el at. 2016). The appropriate domain size of the near-field was estimated in such a way, that changes to hydraulic properties of materials in the repository tunnels and vaults would not influence the regional groundwater flow.

Here, the repository scale model is fed by a regional groundwater flow model set up and solved with the ConnectFlow software (Amec Foster Wheeler 2015). The regional model simulates the entire transient evolution of the temperate conditions (Joyce et al. 2019). The near-field flow analysis is carried out using time-slice simulations based on a snap-shot in time of the ConnectFlow model at 2000 AD. The repository is assumed to be closed and fully saturated. The regional flow model supplies the repository scale model with boundary and initial conditions. It also provides the hydraulic properties of the bedrock such as the anisotropic permeability tensor and the porosity. The groundwater salinity increases with depth and density variations need to be accounted for when calculating the flow. The groundwater density varies with the chloride mass fraction according to a linear relationship derived from the regional flow model (see Figure 3-10). The groundwater flow in the repository scale model is calculated using density dependent porous media flow coupled to chloride transport, to reproduce the flow in the repository near-filed. A comparison exercise is carried out to check that the regional and repository scale models have been consistently coupled (Appendix A).

In Simulation Block 1 (Figure 2-1), the repository scale model is used to study the groundwater flow through the repository, considering several vault orientation and backfill degradation scenarios. These density driven flow simulations form the core of this report and computed results serve as input to radionuclide transport calculations.

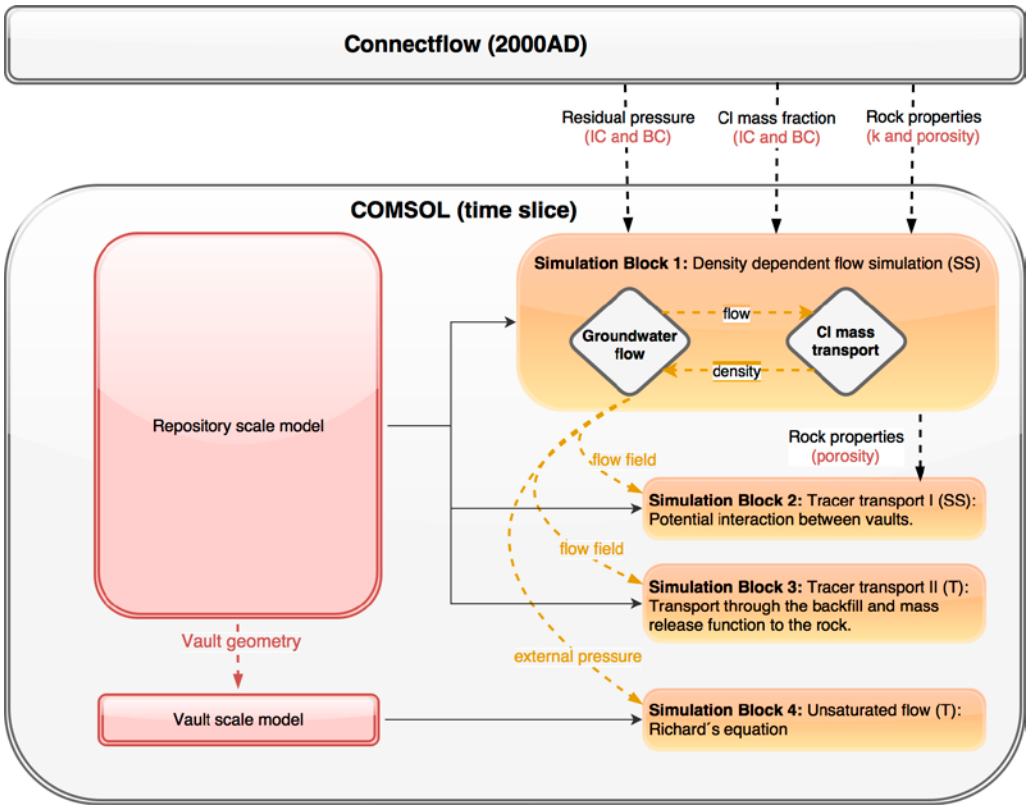

Figure 2-1. *Simulated processes and flow of information between the regional hydrogeology model in ConnectFlow and the repository and vault scale models in COMSOL. SS=Steady state simulation. T=Transient simulation.*

Simulation Block 2 (Figure 2-1) makes use of the flow fields calculated with the repository scale model to simulate the steady state transport of a tracer in the rock. The tracer concentrations are considered too low to affect the flow field. The modelling aims at estimating the extent of a solute plume generated by the leaching of backfills and to quantify the interaction between vaults.

Simulation Block 3 (Figure 2-1) again makes use of the stationary flow fields calculated with the repository scale in simulations of transient tracer transport through the backfill of BHA and BHK. A tracer is released from the waste domain and the time-dependent mass flux is evaluated at the backfill/rock interface of the vaults.

Simulation Block 4 (Figure 2-1) deals with transient unsaturated flow simulations to estimate of the time required to reach full saturation of the BHA and BHK. In this block, vault scale models are used. Boundary conditions are obtained from the saturated repository-scale flow simulation.

3 Model description

Nested numerical models have been developed to study the near-field hydrogeology of the SFL repository (Figure 3-1). A repository-scale model of dimensions $1\,000 \times 1\,000 \times 650$ m^3 has been used to study groundwater flow around the repository, for several vault orientation and backfill degradation scenarios. It has also been used to assess the interaction between the BHA and BHK vaults and to study the temporal evolution of a tracer released from the waste compartments. The repository vaults are situated at 500 m depth in granitic rock (see Section 3.2). The box defining the model domain is defined by the coordinates in Table 3-1.

Table 3-1. Coordinates of the corner coordinates of the model domain.

RT90 X	Y	Local coordinates X	Y	Depth Z
1546500	6366750	7500	6750	−250
1546500	6367750	7500	7750	−250
1547500	6367750	8500	7750	−250
1547500	6366750	8500	6750	−250
1546500	6366750	7500	6750	−900
1546500	6367750	7500	7750	−900
1547500	6367750	8500	7750	−900
1547500	6366750	8500	6750	−900

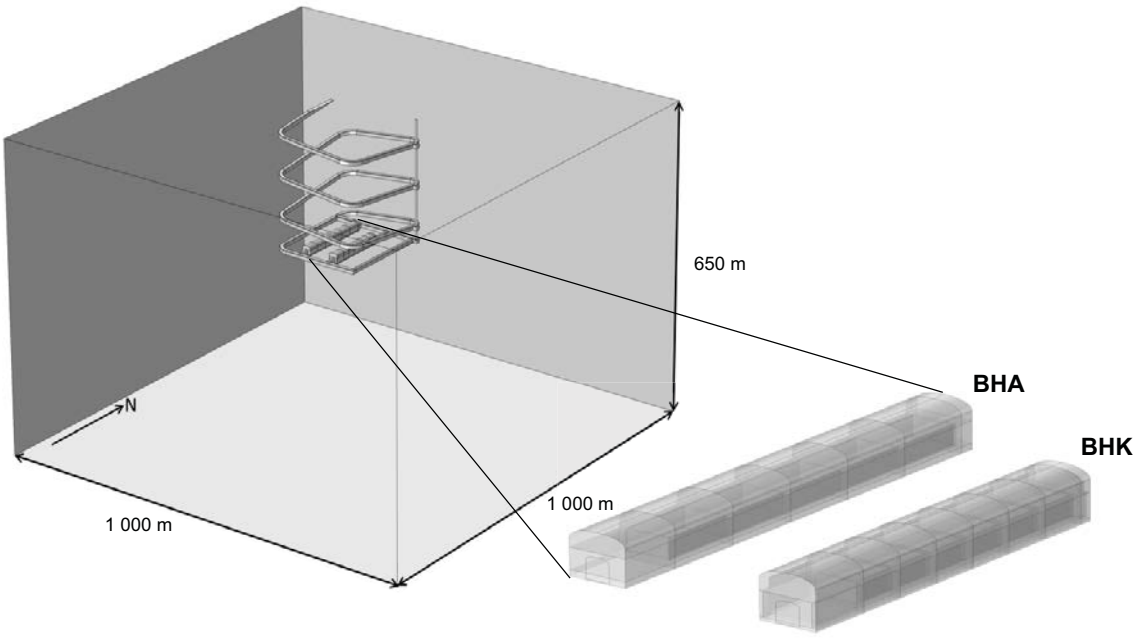

Figure 3-1. *Model domain and dimensions (m) of the repository scale model.*

3.1 Geometries and materials

Two storage vaults are planned for SFL; one vault for legacy waste (BHA), and one vault for the metallic waste from the nuclear power plants (BHK). Waste containers are to be emplaced in concrete structures that serve as radiation barriers during operation. Backfill materials will be installed upon repository closure. The BHA vault will be backfilled with bentonite and the BHK vault will be backfilled with concrete. Figure 3-2 and Figure 3-3 show schematic cross-sections of BHA and BHK, respectively.

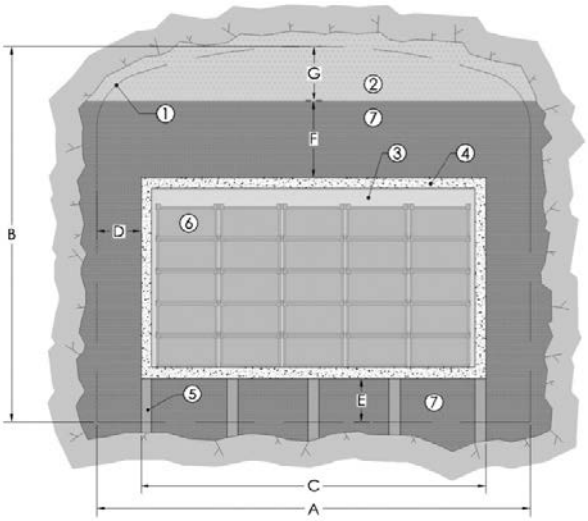

Figure 3-2. *Schematic cross-sectional layout of BHA (from Elfwing et al. 2013). Legend: 1.) Theoretical tunnel contour. 2) Bentonite pellets. 3) Grout. 4) Concrete structure (0.5 m). 5) Granite pillars. 6) Waste packages. 7) Bentonite blocks. The outermost grey area represents the rock. Approximate dimensions: A = 20.6 m, B = 18.5 m, C = 16 m, D = 2.3 m, E = 2.4 m, F = 4 m, G = 3.7 m.*

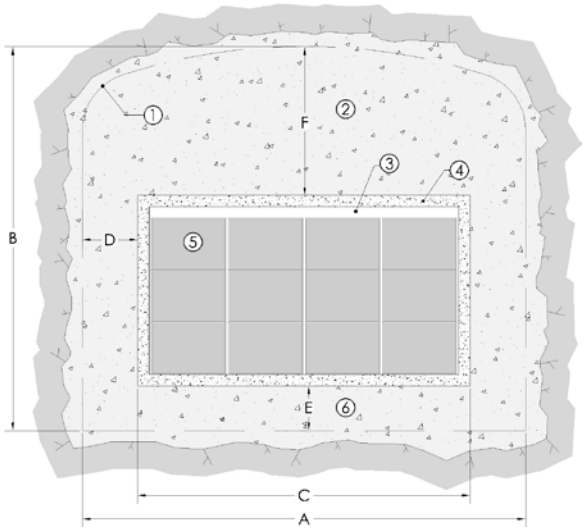

Figure 3-3. *Schematic cross-sectional layout of the BHK vault for metallic waste (from Elfwing et al. 2013). Legend: 1.) Theoretical tunnel contour. 2) Concrete backfill. 3) Grout. 4) Concrete structure. (0.5 m). 5) Steel tanks. 6) Concrete. The outermost grey area represents the rock. Approximate dimensions: A = 20.6 m, B = 19.6 m, C = 15 m, D = 2.8 m, E = 2.4 m, F = 8.8 m.*

The ramp and access tunnels will be filled with crushed rock or similar material. Bentonite plugs and seals will be placed in the tunnel sections connecting the vaults and access tunnels, in the vertical shaft and in the access ramp (Figure 3-4).

The geometries developed by Abarca et al. (2016) have been used also in this work. The values of the permeability, effective diffusivity and porosity of repository materials are given in Table 3-2. The assigned permeability values are illustrated in Figure 3-5. The waste domain is defined to include the waste containers, the waste compartment volume and the concrete structure. Properties of a single composite material are set to represent this domain.

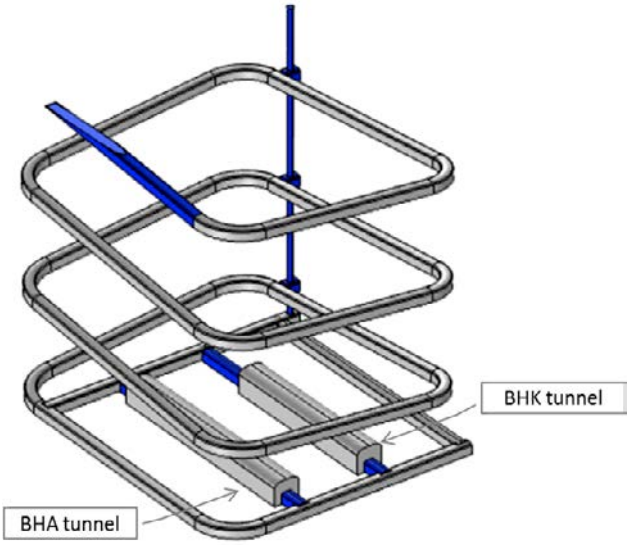

Figure 3-4. *Sealing sections (blue) installed at closure in the tunnel sections connecting the vaults and access tunnels, the vertical shaft and in the access ramp.*

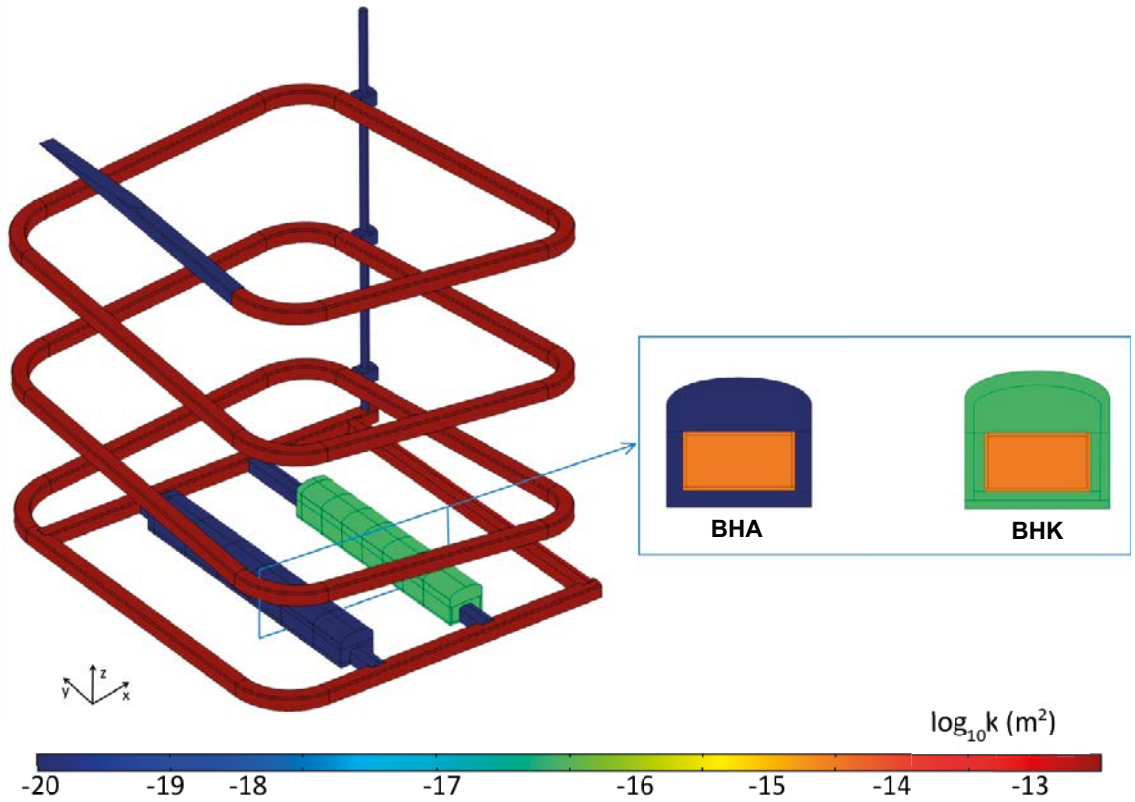

Figure 3-5. *Permeability values of the materials in the SFL repository.*

Table 3-2. Repository material properties for the base case calculation.

Description	Material	k (m^2)(*)	De (m^2/s)	ϕ	Reference
Access tunnels backfill	Crushed rock	2.0×10^{-12}	6.0×10^{-10}	0.30	SKB 2001
Waste domain	Homogenised	2.0×10^{-14}	3.5×10^{-10}	0.30	SKB 2014
Sealing sections	Bentonite	2.0×10^{-20}	1.4×10^{-10}	0.43	SKB 2010
BHK vault backfill	Concrete	1.7×10^{-16}	3.5×10^{-12}	0.11	SKB 2014
BHA vault backfill	Bentonite	2.0×10^{-20}	1.4×10^{-10}	0.43	SKB 2010

(*) Calculated assuming $\rho = 1\,000$ kg/m^3 and $\mu = 0.002$ Pa·s.

The BHK backfill domain has been divided into an inner and outer zone (Figure 3-6), to allow for simulations of a schematic degradation of the backfill. Three cases have been considered: a base case, a degraded case and a degraded zone case. The degraded zone case considers a preferential degradation of the outer part of the backfill. The calculation cases and the associated material properties applied to the BHK backfill are summarised in Table 3-3.

Table 3-3. BHK backfill material properties for different calculation cases.

Description	k (m^2)(*)	De (m^2/s)	ϕ	Reference
Base case	1.7×10^{-16}	3.5×10^{-12}	0.11	SKB 2014
Degraded case	2.0×10^{-14}	5.0×10^{-12}	0.14	SKB 2014
Degraded zone case (inner zone/outer zone)	1.7×10^{-16}/2.0×10^{-14}	3.5×10^{-12}/5.0×10^{-12}	0.11/0.14	SKB 2014

(*) Calculated assuming $\rho = 1\,000$ kg/m^3 and $\mu = 0.002$ Pa·s.

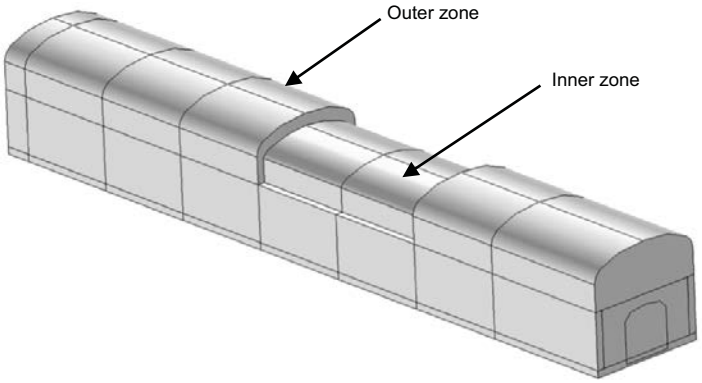

Figure 3-6. *BHK backfill geometry divided into an inner and outer zone.*

3.2 Properties of the host rock

Site data from the Laxemar area has been used to represent a granitic host rock for the SFL repository. The area, which has been considered a potential site for the final repository for spent nuclear fuel (SKB 2011), is well characterised with high data density. Figure 3-7 shows the focus area and a suggested layout of the final repository for spent nuclear fuel. Deformation zones delimit several rock domains. The present work assumes that SFL is located in the position marked as 1 in Figure 3-7, at a depth of 500 m. Other locations in the Laxemar area have been investigated in previous work (Abarca et al. 2016).

The anisotropic permeability field of the host rock was obtained from the regional hydrogeology model (Joyce et al. 2019). It was imported into COMSOL and interpolated over the finite element mesh. The resulting rock permeability field (k_{xx}) is displayed in a horizontal plane at repository depth (Figure 3-8 top) and three vertical planes traversing the BHA and BHK vaults (Figure 3-8 and Figure 3-9), with a common colour scale. The high permeability structures in contact with the repository are labelled as "STi", where *i* is a number. They correspond approximately to the ECPM representation in COMSOL of the stochastic fractures. Repository structures are intersected by stochastic features, with permeability values ranging from 10^{-14} to 10^{-15} m^2. ST7 has the highest permeability value (10^{-12} m^2) but it does not intersect with the repository tunnels.

The BHA is located below a high permeability zone (Figure 3-9). The vault is intersected by three vertical stochastic features, namely ST13, ST14 and ST15. The BHK vault is located between two areas with high permeability values ranging from 10^{-14} to 10^{-15} m^2 (Figure 3-9). The vault is intersected by two subvertical stochastic features labelled ST16 and ST14 (Figure 3-9).

The permeability values of the repository materials are also illustrated in Figure 3-8 and Figure 3-9. The crushed rock backfill in the access tunnels has the highest permeability value in the model domain whereas the bentonite is the least permeable material. The BHK concrete backfill has a higher permeability value than the surrounding rock.

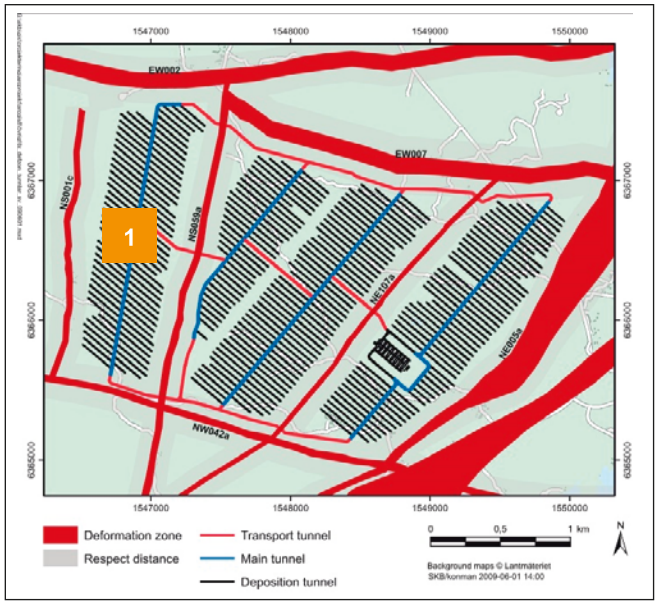

Figure 3-7. *Laxemar focus area (modified from SKB 2011). Rock domains delimited by deformation zones. SFL is assumed to be located at the position marked 1 at 500 m depth.*

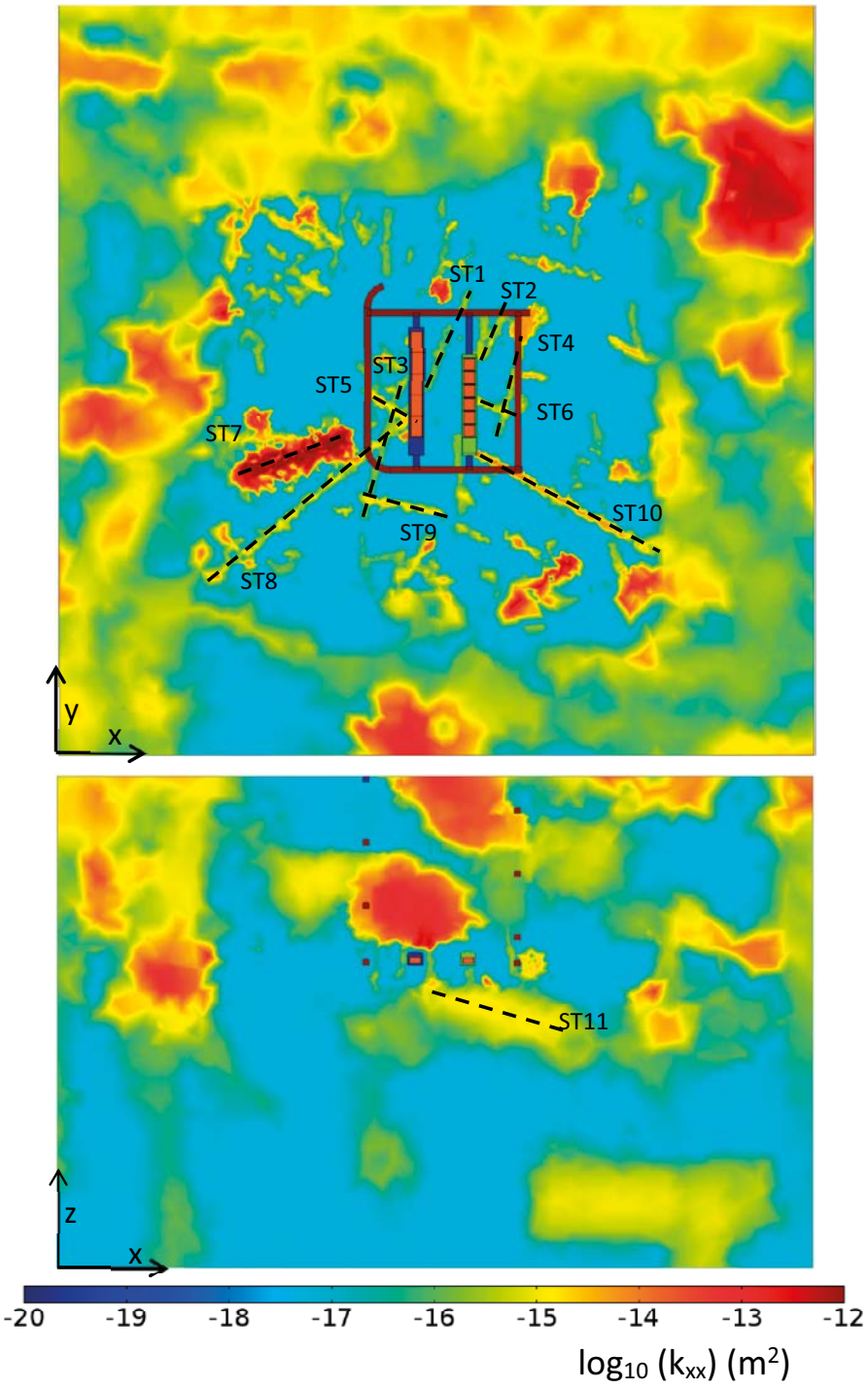

Figure 3-8. *Rock permeability field (k_{xx}) in a xy-plane (top) and xz-plane (bottom) intersecting the BHA and BHK vaults and permeability values of the repository materials for the base case. The dashed lines delineate approximately the ECPM representation in COMSOL of the stochastic fractures. North is oriented along the y-axis.*

3.3 Model equations

3.3.1 Density dependent flow

The model equations have been implemented using the Subsurface Flow Module of COMSOL Multiphysics (COMSOL 2015). Fluid salinity induces density gradients in the modelled domain (Abarca et al. 2016, Joyce et al. 2019). Therefore, the groundwater flow simulation is coupled to a mass transport simulation. The density of the fluid changes with the chloride mass fraction (see Figure 3-10). The *Darcy's law* interface in COMSOL solves for the water flow and the *Transport of diluted species in porous media* interface for the chloride transport.

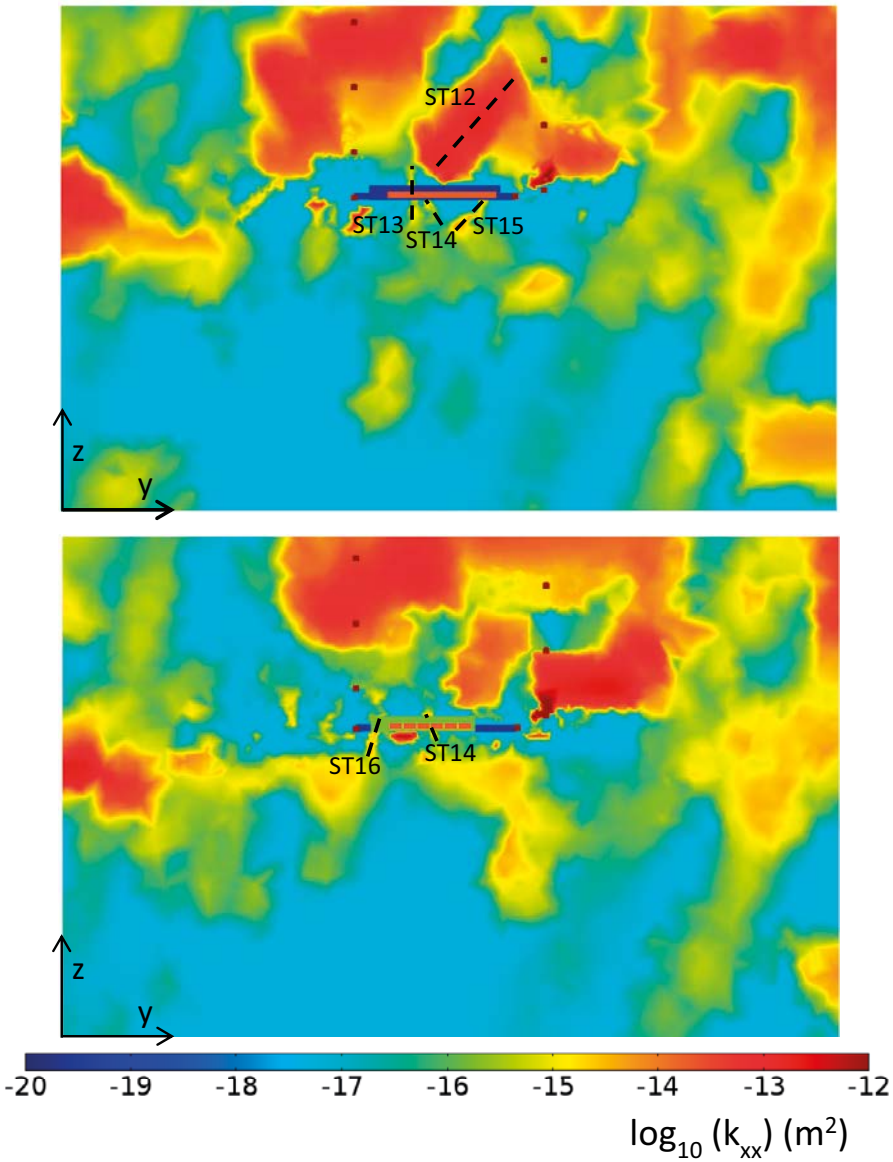

Figure 3-9. *Rock permeability field (k_{xx}) in a yz-plane intersecting the BHA vault (top) and a yz-plane intersecting the BHK vault (bottom) and permeability values of the repository materials for the base case. The dashed lines delineate approximately the ECPM representation in COMSOL of the stochastic fractures.*

Fluid mass conservation at steady state is given by:

$$\nabla \cdot (\rho \mathbf{u}) = 0$$

$$\boldsymbol{u} = -\frac{k}{\mu}(\nabla \mathrm{p} + \rho g \nabla E)$$

where ρ is the density (kg/m^3), μ the dynamic viscosity (Pa·s), $\mathbf{u}$ the Darcy velocity (m/s), k the permeability of the porous medium (m^2), p the absolute water pressure (Pa), g the acceleration of gravity (9.81 m/s^2) and E the elevation (m).

Mass is transported by three processes: advection, which describes the dragging of solute with the mean fluid velocity, diffusion, which describes the apparently random displacements of solute particles through Brownian motion, and dispersion, which describes the effect of velocity fluctuations with respect to the mean velocity (e.g. Bear 1972). This is captured by the steady state advection-dispersion equation, given by:

$$\nabla \cdot [-(\boldsymbol{D_D} + D_e)\nabla c] + \nabla \cdot (c\mathbf{u}) = 0$$

Above, c is the solute concentration (g/m^3), D_e the effective diffusivity (m^2/s) and **u** the Darcy velocity (m/s). The effective diffusivity values of the repository materials (Table 3-2) are used. However, chloride transport occurs mainly in the rock domain under the repository where the effective diffusion coefficient is calculated as:

$$D_e = \phi \tau D_F$$

Above, τ is the tortuosity and D_F is the species diffusion coefficient in water (m^2/s). The resulting effective diffusion coefficients in the rock range between 3.2×10^{-14} to 4.35×10^{-10} m^2/s.

The mechanical dispersion tensor D_D(m$^2 \cdot$ s^{-1}) is defined as:

$$\boldsymbol{D}_D = \alpha_L |\mathbf{u}| + (\alpha_L - \alpha_T) \frac{\mathbf{u}\,\mathbf{u}^t}{|\mathbf{u}|}$$

where α_L (m) and α_T (m) are the longitudinal and transversal dispersivity, respectively.

Dispersivity is a scale dependent parameter (Gelhar et al. 1992) and, in heterogeneous media, it depends on the correlation scale of heterogeneities (Gelhar and Axness 1983). In this highly heterogeneous model, the effective dispersivity has been chosen to be a combination of a local dispersivity term plus a term that depends on the element size. This implies that the Peclet number is nearly constant throughout the model domain. The dispersivity is defined as $\alpha_L = 15 + 3$h and $\alpha_T = 15 + 1.5$h, where h is the element size (m). The resulting values of the dispersivity range between 15 to 170 m. In the present system the velocity-dependent dispersion is small compared to diffusion. Nevertheless, given the uncertainty related to the dispersivity values, a sensitivity analysis has been carried out in previous work (Abarca el at. 2016). The calculated groundwater flows showed little sensitivity to the dispersivity values.

A linear equation of state relates fluid density with salinity:

$$\rho = \rho_0 (1 + \varepsilon \omega)$$

where ω is the chloride mass fraction (kg of solute per kg of solution) and ρ_0 the reference density.

Data on residual pressure, fluid density and chloride mass fraction were exported from the ConnectFlow regional model (Joyce et al. 2019) as explained in Appendix A. The exported fluid density shows a linear relationship with the chloride mass fraction, as illustrated in Figure 3-10.

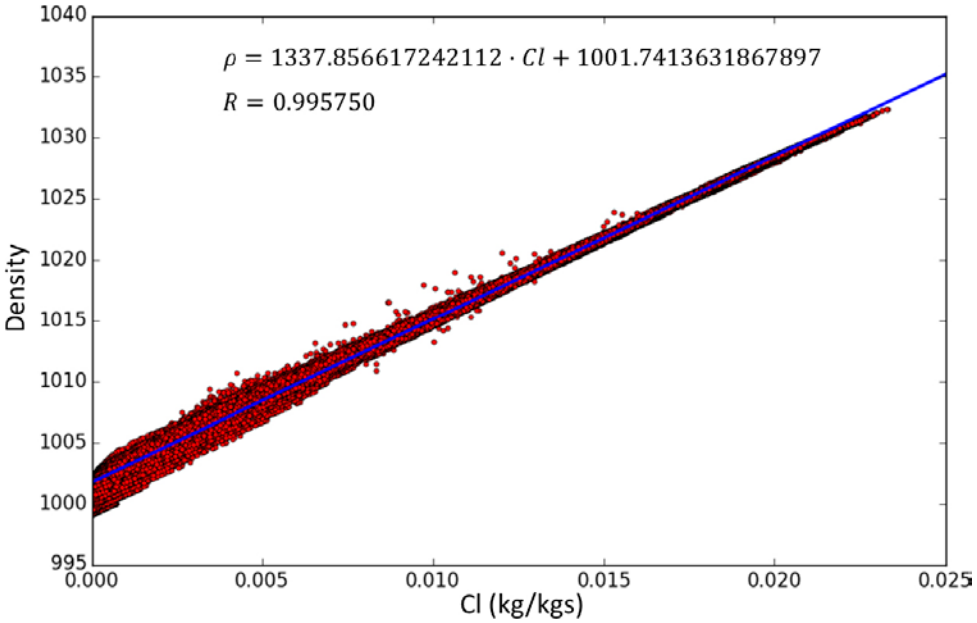

Figure 3-10. *Relationship between the chloride mass fraction (kg of solute per kg of solution) and the density of water (kg/m^3). The red dots refer to the regional model results (Joyce et al. 2019) and the blue shows a linear regression fit to the points.*

The linear regression that best reproduces that relationship (Figure 3-10) is used to define the values of ρ_0 (1 001.74 kg/m^3) and ε (*1.3355)* to be used in the density correlation. The water density in the near-field SFL model ranges from 1 001.74 to 1 027.71 kg/m^3.

The imported residual pressure, P (Pa), is converted into absolute pressure by adding the gravitational term, assuming ρ_0 = 1 001.74 kg/m^3:

$$p_{CF} = P_{CF} - \rho_0 g z$$

Note that z, the vertical coordinate, is negative in the modelled area.

The system of flow and transport equations is solved with a fully coupled solution approach that uses a damped version of the Newton´s method to handle parameters.

3.3.2 Tracer transport

Tracer transport simulations are carried out using groundwater flow fields at steady state. The tracer transport does not affect the flow. The simulations are carried out using the *Transport of diluted species in porous media* interface (COMSOL 2015). The mass conservation equation reads:

$$\phi \frac{\partial c}{\partial t} + \nabla \cdot [-(\boldsymbol{D_D} + D_e)\nabla c] + \nabla \cdot (c\mathbf{u}) = 0$$

Above, ϕ is the porosity (-), c the concentration (g/m^3), **u** the Darcy velocity field (m/s), D_e the effective diffusivity (m^2/s) and D_D the mechanical dispersion (m^2/s).

Two blocks of transport simulations are carried out to understand solute transport in the near-field (see Chapter 2):

Tracer transport I (Figure 2-1) makes use of the flow fields calculated with the repository scale model to simulate the steady state transport of a tracer in the rock ($\partial c/\partial t = 0$). The tracer concentrations are considered too low to affect the flow field. The modelling aims at estimating the extent of a solute plume generated by the leaching of backfills and to quantify the interaction between vaults.

Tracer transport II (Figure 2-1) again makes use of the stationary flow fields calculated with the repository scale in simulations of transient tracer transport through the backfill of BHA and BHK. A tracer is released from the waste domain and the time-dependent mass flux is evaluated at the backfill/rock interface of the vaults.

3.4 Initial and boundary conditions

3.4.1 Density dependent flow

Input data for the near-field hydrology models have been obtained from the regional hydrogeological simulations (Joyce et al. 2019). The residual pressure field and the chloride mass fraction distribution have been imported into COMSOL. The fields are interpolated over the finite element mesh using a linear interpolation method and imposed as initial and boundary conditions in the repository scale model. A check that the calculated flow in the repository scale model is consistent with the regional flow is presented in Appendix A.

The imported residual pressure, P_{CF} (Pa), is converted into absolute pressure by adding the gravitational term, assuming a freshwater density of ρ_0 = 1 001.74 kg/m^3.

$$p_{CF} = P_{CF} - \rho_0 g z$$

The vertical coordinate, z, is negative in the model. The pressure P_{CF} is used to define the initial pressure in the model domain and to prescribe pressure at the model boundaries.

The ramp and shaft are sealed with bentonite of low permeability at the intersection with the top model boundary (Figure 3-4), and a zero flux boundary condition is specified here. This intersection is not included in the regional model.

For the solute transport equation, the chloride mass fraction distribution obtained from the regional model was used as initial condition and to prescribe the chloride concentration (Dirichlet type) in all model boundaries.

3.4.2 Tracer transport I: Potential interaction between vaults

The tracer transport is simulated using the repository scale model. One tracer is released at the BHK backfill/rock and another from the BHA backfill/rock interface (see Figure 3-11). A unit concentration of tracer is prescribed (Dirichlet type) at the source boundary. At the outer boundaries of the model domain the following boundary condition is applied:

$$-\mathbf{n}\cdot(\boldsymbol{D_D}+D_e)\nabla c_i = 0 \quad if \quad \mathbf{n}\cdot\mathbf{u}\geq 0$$
$$c_i = c_{ext,i} \quad if \quad \mathbf{n}\cdot\mathbf{u}<0$$

This boundary condition switches between a prescribed concentration (c_{ext}=0) when groundwater enters the model domain, and a mass flux boundary condition (Neumann type) when water leaves the model domain. The water leaving the model domain has the computed concentration of the resident water.

The initial concentration of both tracers is set to c_i = 0 for the entire model domain.

3.4.3 Tracer transport II: Transport through the backfill

Transient tracer transport simulations are performed to evaluate the role of the backfill in the transport of a solute released from the waste. Two simulations have been performed to simulate the release at the waste of each vault. In both simulations, a unit concentration of tracer has been prescribed at the waste/backfill interface (Figure 3-12). At the outer boundaries of the model domain the following boundary condition is applied:

$$-\mathbf{n}\cdot(\boldsymbol{D_D}+D_e)\nabla c_i = 0 \quad if \quad \mathbf{n}\cdot\mathbf{u}\geq 0$$
$$c_i = c_{ext,i} \quad if \quad \mathbf{n}\cdot\mathbf{u}<0$$

This boundary condition switches between a prescribed concentration (c_{ext}=0) when groundwater enters the model domain, and a mass flux boundary condition (Neumann type) when water leaves the model domain.

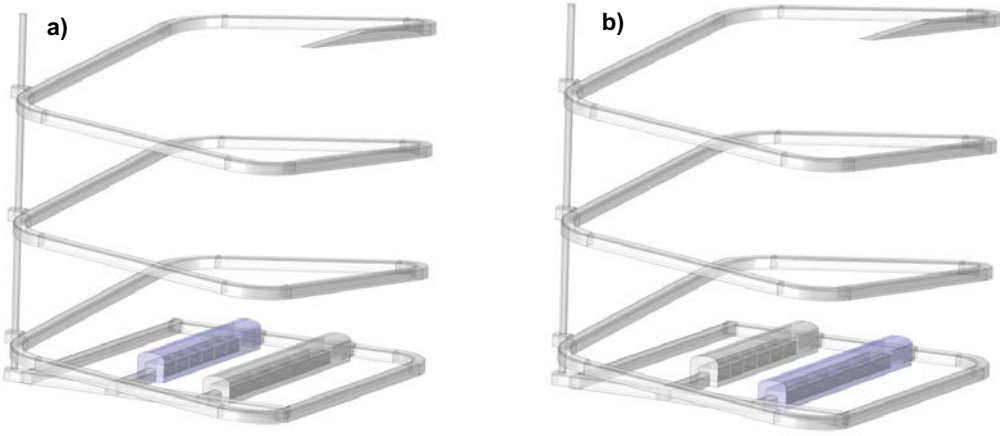

Figure 3-11. *a) Interface at the BHK backfill/rock (blue) where the concentration of the BHK tracer is prescribed and b) interface at the BHA backfill/rock (blue) where the concentration of the BHA tracer is prescribed.*

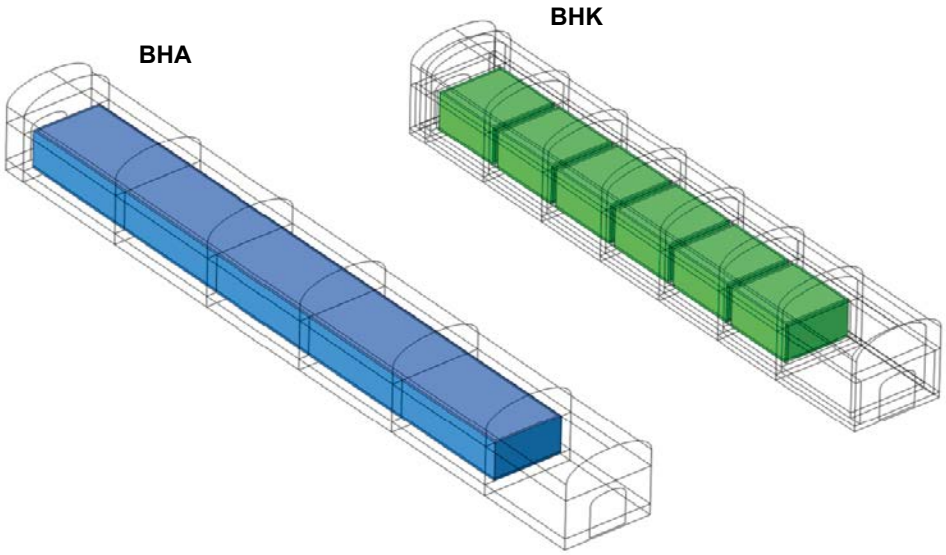

Figure 3-12. *Interface waste/backfill where the unit concentration is prescribed in the BHA waste (blue) and BHK waste (green).*

3.5 Mesh discretization

The model geometry is discretised with an unstructured finite element mesh of 3.14×10^6 tetrahedral elements (Figure 3-13). The mesh is refined in an inner box around the repository vaults (Figure 3-14) to match the mesh resolution of the model by Joyce et al. (2019).

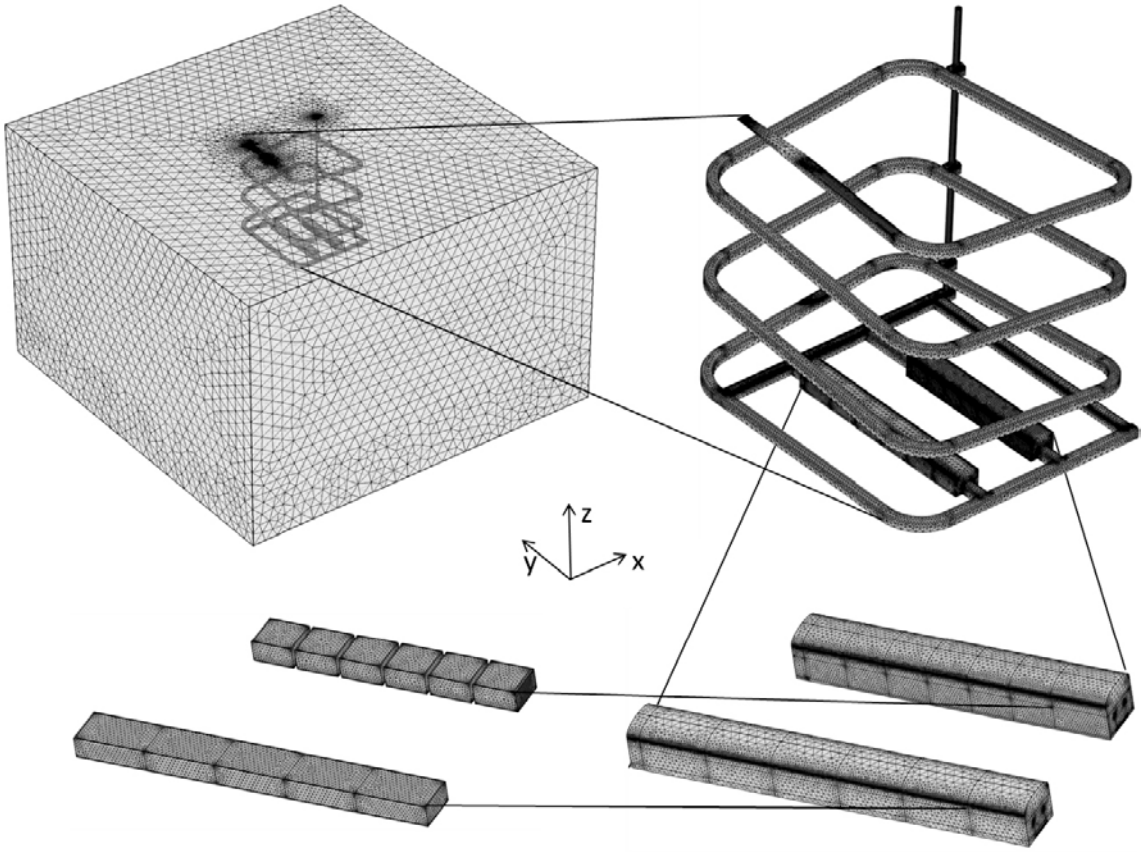

Figure 3-13. *Finite element mesh of the repository scale model composed of 3.14×10^6 tetrahedral elements.*

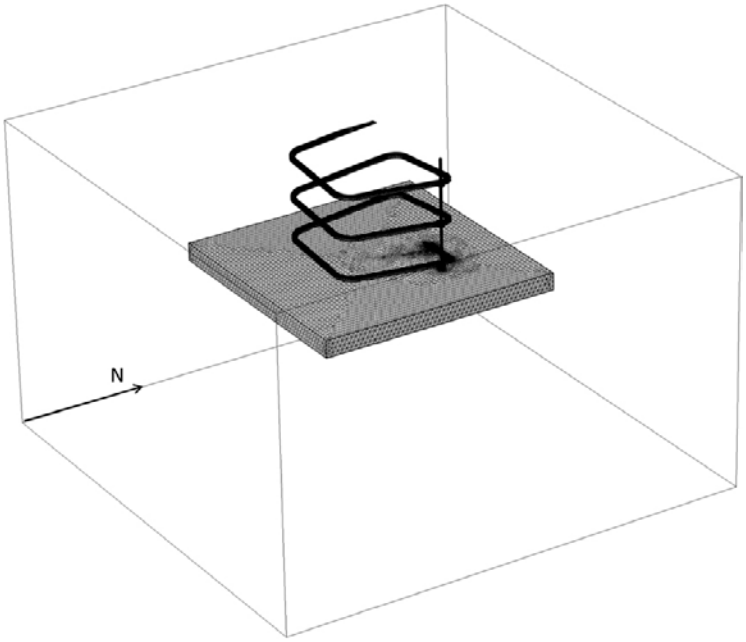

Figure 3-14. *Refined mesh in a volume close to the vaults.*

3.6 Observables

3.6.1 Flow through the tunnels and compartments

Total flow through the vaults and waste

The flow through the repository is described by the total flow through the BHA and BHK vaults and waste. These global indicators provide a convenient way to compare the results of various conditions tested in different calculation cases. These indicators are not passed on to the radionuclide transport calculations. For this purpose detailed flows are evaluated, for each surface of each waste compartment (see Appendix C).

The vault flow, Q_{Vault} (m^3/yr) has been defined as the total inflow through the backfill/rock interface and has been calculated by integrating the positive values of the normal Darcy flux over the backfill/rock surface. The waste flow, Q_{Waste} (m^3/yr) has been defined as the total inflow through the waste/backfill interface and has been calculated by integrating the positive values of the normal Darcy flux over waste/backfill interface.

$$Q_{Vault} = \sum \iint_{(\vec{q}\cdot\vec{n})>0} \vec{q} \cdot \vec{n}$$

$$Q_{Waste} = \sum \iint_{(\vec{q}\cdot\vec{n})>0} \vec{q} \cdot \vec{n}$$

Note that the BHA has one waste/backfill interface enclosing the entire waste. However, the BHK waste is divided into six individual compartments, embedded in the concrete backfill (Figure 3-15). The reported flow Q_{Waste} through the BHK waste is the average over the 6 compartments. The averaged flow has been calculated as the sum of the flow through all compartments divided by the number of compartments. That the average flow times the number of compartments can become greater than the vault flow is a sign that the direction of flow is along the vault, and that water can pass from compartment to compartment.

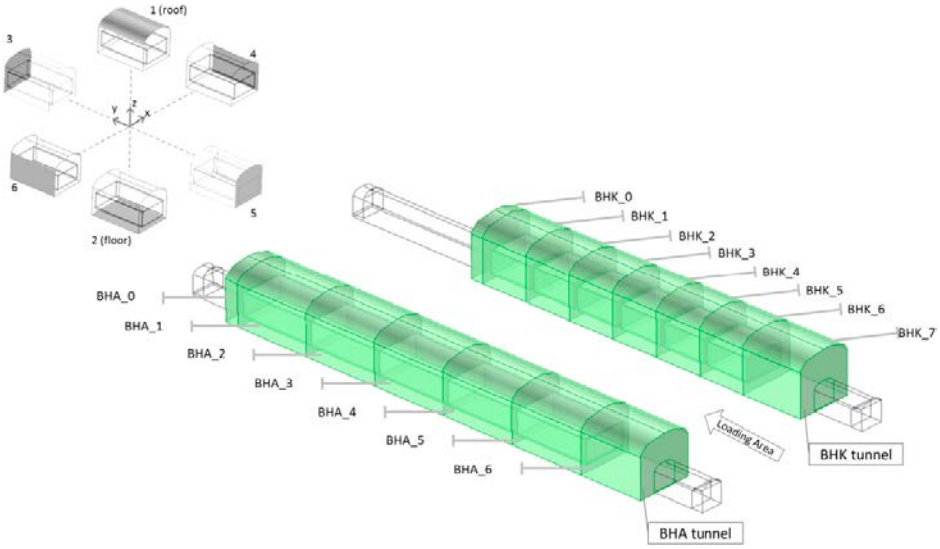

Figure 3-15. *Longitudinal sections along the BHA and BHK vaults and labelling of the volume faces.*

Flow through backfill and waste compartments

Each vault is divided into a set of sections along its longitudinal axis (Figure 3-15). These divisions provide information on the spatial distribution of the flow through the backfill and waste. For each section, the groundwater flow has been calculated with surface integrals over each of the six faces of the volume ($Q_{C,face}$ (m^3/yr)). The faces of each section have been labelled as shown in Figure 3-15. Positive values have been added up representing the groundwater flow crossing the control volume ($Q_{C,section,in}$ u(m^3/yr)):

$$Q_{C,face} = \iint \vec{q} \cdot \vec{n}$$

$$Q_{C,section,in} = \sum_{Q_{face}<0} Q_{face}$$

$$Q_{C,section,out} = \sum_{Q_{face}>0} Q_{face}$$

Above, C refers to the type of compartment in the section. It can be either waste (C=W) or backfill (C=B).

3.6.2 Tracer transport I: Potential interaction between vaults

Non-reactive tracer transport simulations have been performed to quantify the potential interaction between repository vaults. A tracer has been released from the backfill/rock interface of each vault. Under steady state conditions, the mass flux released is equal to the surface integral of the mass flow over a closed domain. In this case, the amount of tracer released from the vaults (m_r (g/yr)) has been computed by integrating the mass flux leaving the surfaces of the model domain (positive values):

$$m_r = \sum_{J>0} \iint_{A_{rock}} (-(\boldsymbol{D_D} + D_e)\nabla c + \mathbf{u}c) \cdot \mathbf{n} \cdot dS$$

Above, A_{rock} is the outer surface of the model domain, $\boldsymbol{D_D}$ is the dispersion tensor coefficient (m^2/s), D_e the effective diffusivity (m^2/s), c is the solute concentration (g/m^3), **u** is the Darcy velocity (m/s) and **n** is the normal vector of the surface S.

The mass flux of tracer released from a vault that reaches the neighbouring vault (m_v (g/yr)) has been calculated by integrating the total mass flux of tracer over the rock/backfill surface of the receiving vault:

$$m_v = \sum_{J>0} \iint_{A_{vault}} (-(\boldsymbol{D_D} + D_e)\nabla c + \mathbf{u}c) \cdot \mathbf{n} \cdot dS$$

where A_{vault} is the surface of the rock/vault interface.

The interaction between the BHK and BHA vaults has been evaluated with the following ratio:

$$Ratio = \frac{m_v}{m_r}$$

The extension of the tracer plume is represented in figures by the isosurface delineating 20 % of the released concentration.

3.6.3 Tracer transport II: Transport through the backfill

Non-reactive tracer transport simulations have been performed to quantify the tracer release from waste to the rock. The mass flux of tracer crossing the different vault/rock boundaries has been calculated by integrating the mass fluxes over the rock/backfill surfaces of the vault. The first component of the total mass flux is the advective term:

$$m_c = \sum_{J>0} \iint_{Avault} \mathbf{u}c \cdot n \cdot dS$$

The diffusive term is calculated as:

$$m_{diff} = \sum_{J>0} \iint_{Avault} -D_e \nabla c \cdot n \cdot dS$$

where D_e is the effective diffusivity (m^2/s) of the material. The dispersive term of the outflow flux is calculated as:

$$m_{dis} = \sum_{J>0} \iint_{Avault} -\boldsymbol{D_D} \nabla c \cdot n \cdot dS$$

where $\boldsymbol{D_D}$ is the dispersion coefficient (m^2/s).

The total flow is the summation of the three terms:

$$m_{rtotal} = m_c + m_{diff} + m_{dis}$$

4 Base case

This chapter describes the main features of groundwater flow in the base case simulation, with focus on the

- stratification of groundwater salinity,
- direction of the local flow system relative to the orientation of the rock vaults,
- interaction between vaults based on non-reactive tracer transport,
- temporal evolution of the mass released from the waste.

4.1 Salinity

Groundwater salinity increases with depth, affecting the groundwater density. The salinity stratification is mainly horizontal (Figure 4-1). The density in the model domain ranges from 1 000 kg/m^3 at the top of the model domain up to 1 025 kg/m^3 at the bottom (Figure 4-1).

4.2 Groundwater flow field

The calculated total groundwater flow entering the model domain is 4.28×10^3 m^3/year. The local groundwater flow around the repository is illustrated by streamlines in Figure 4-2 (top). Streamlines are calculated in COMSOL by selecting a surface as origin of the streamlines and a number of initial points (400 points at each surface). The algorithm finds the Darcy velocity field at these points by interpolation and integrates the points along the direction of the Darcy velocity using a second-order Runge-Kutta algorithm. Light blue streamlines are followed by water entering the model domain through the top boundary and dark blue streamlines are followed by water entering from the bottom boundary. This way of representing the streamlines highlights the interaction between the groundwater flow and the salinity interface (Figure 4-2, bottom). Light blue streamlines show vertical inflow from the top boundary down to the freshwater/saltwater interface (Figure 4-2).

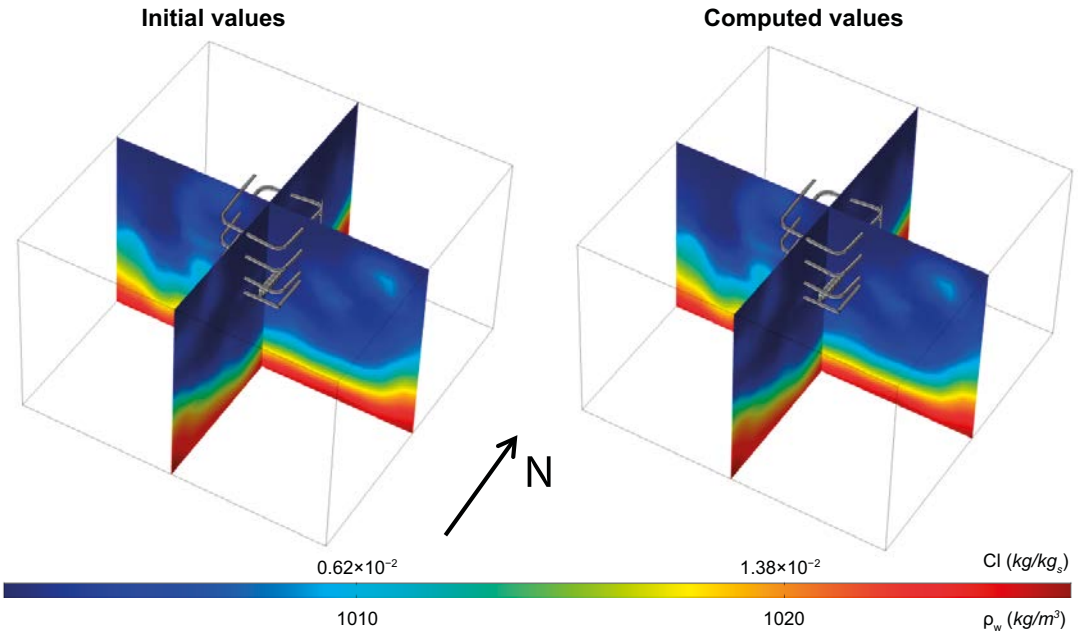

Figure 4-1. *Salinity and density at the repository location, with initial values (left) and computed values (right).*

The streamlines become parallel to the freshwater/saltwater interface below the repository (Figure 4-2). These streamlines reflect freshwater recharge from the surface. Dark blue streamlines illustrate the paths of saline water entering the domain from the bottom boundary. Saline water moves up towards the salinity interface where it deflects and moves sideward under the saline interface. The low density of streamlines below the repository indicates low flow at the interface. This is typical for a stable saline interface. The interface acts as a boundary between the freshwater and the saltwater systems. The presence of stochastic fractures and deformation zones affects the position of the saline interface (Figure 4-2, bottom). A higher elevation of the saline water locally (upconing) is associated with the presence of deformation zones.

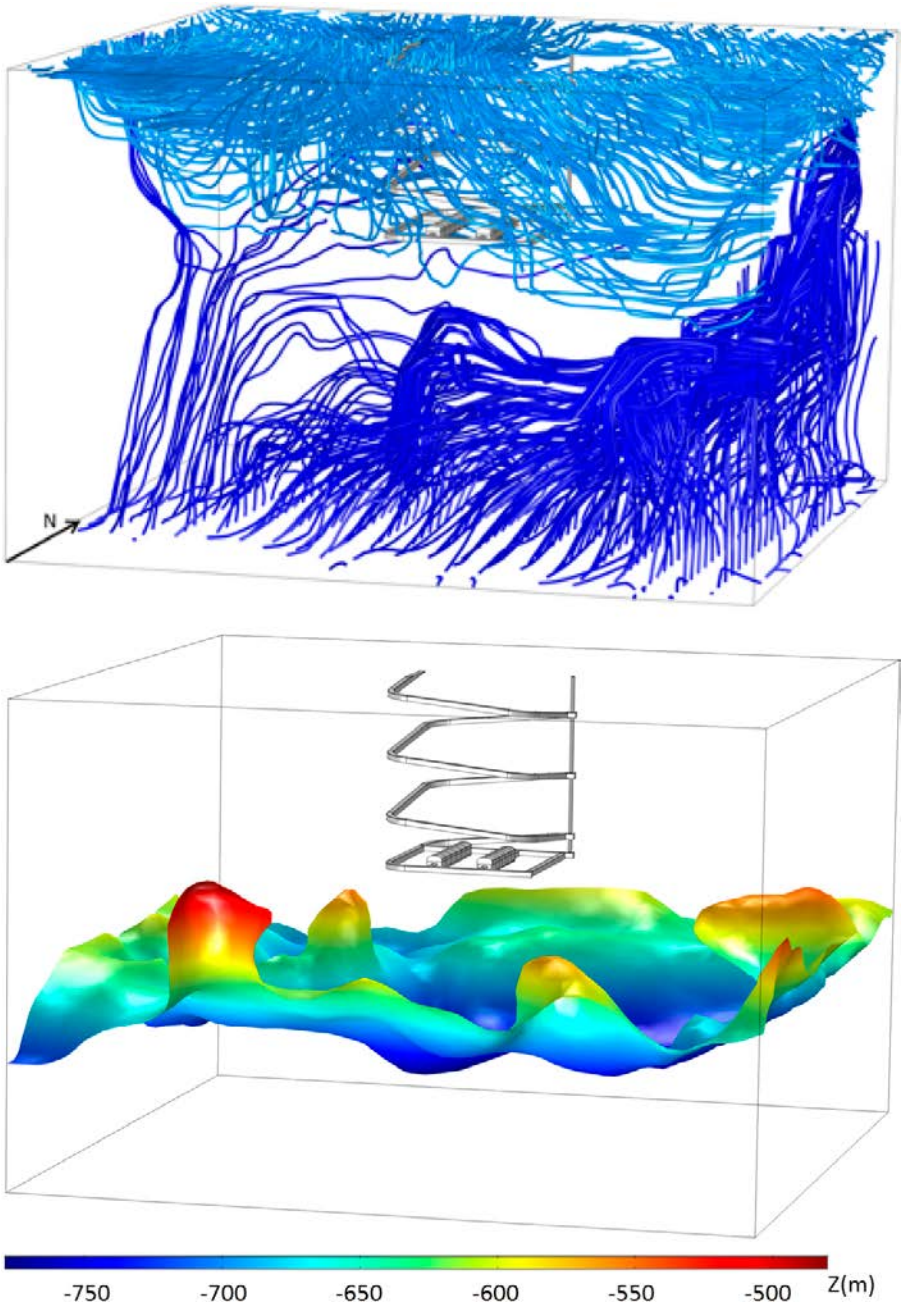

Figure 4-2. *Groundwater streamlines illustrating the flow direction in the repository scale model (top). Light blue streamlines and dark blue streamlines illustrate water entering through the top and from the bottom boundary, respectively. The isosurface of salinity equal to 0.006 kg/kgs (bottom) indicates the location of the saline interface. It is coloured according to its elevation to illustrate local upconing associated to deformation zones.*

4.3 Flow through the vaults and waste

Table 4-1 and Figure 4-3 show the calculated groundwater flow per waste control volume and the total flow per vault. The calculated flow through the BHA vault (2×10^{-2} m^3/yr) is two orders of magnitude lower than the flow through the BHK (1.1 m^3/yr). This reduced through flow is due to the lower permeability of the bentonite with respect to the surrounding rock. 1–2 % of the BHA vault flow enters a waste domain (Table 4-1). The longitudinal distribution of flow through the BHA backfill compartments is presented in Appendix B, Table B-1. 22–27 % of groundwater flow through the BHK vault enters the central BHK waste compartments. However, this proportion is reduced to 4–9 % in the waste compartments located at both ends of the vault. The longitudinal distribution of flow through the BHK backfill compartments is presented in Appendix B, Table B-2.

Figure 4-4 shows the direction of the Darcy velocity field (vectors) and the permeability of the rock together with the magnitude of the Darcy flow inside the waste control volumes. The BHA waste is affected by flow through stochastic features ST1, ST3, ST5 and ST8. As the waste compartments are connected the flow is homogenised. ST6 intersects BHK at waste compartments 3 and 4, which receive most of the vault flow (Table 4-1).

Figure 4-5 shows streamlines reaching and leaving the waste control volumes. The streamlines illustrate the vertical inflow. Water reaches the vaults from the top and moves downwards until reaching the saline water. Then, it becomes horizontal and flows eastward.

Table 4-1. Computed flow through waste control volumes and through the BHA and BHK vaults for the base case. Waste IDs refer to the vault section containing the control volume.

			Total flow (m^3/year)
BHA	Waste	1	3.33E-04
		2	2.71E-04
		3	5.11E-04
		4	2.69E-04
		5	1.66E-04
	Vault	**BHA**	**2.18E-02**
BHK	Waste	1	4.47E-02
		2	5.47E-02
		3	2.42E-01
		4	3.03E-01
		5	1.79E-01
		6	9.82E-02
	Vault	**BHK**	**1.09E+00**

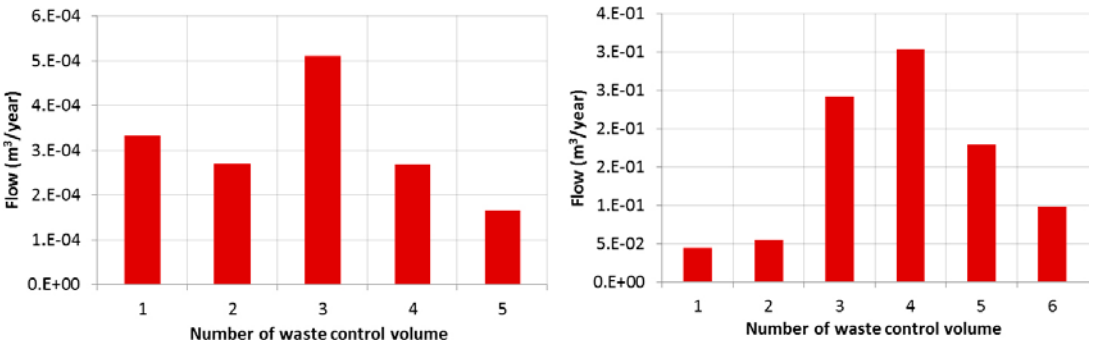

Figure 4-3. *Calculated flow through the waste control volumes of BHA (left) and BHK (right). Numbers refer to the vault axial section containing the control volume (Figure 3-15).*

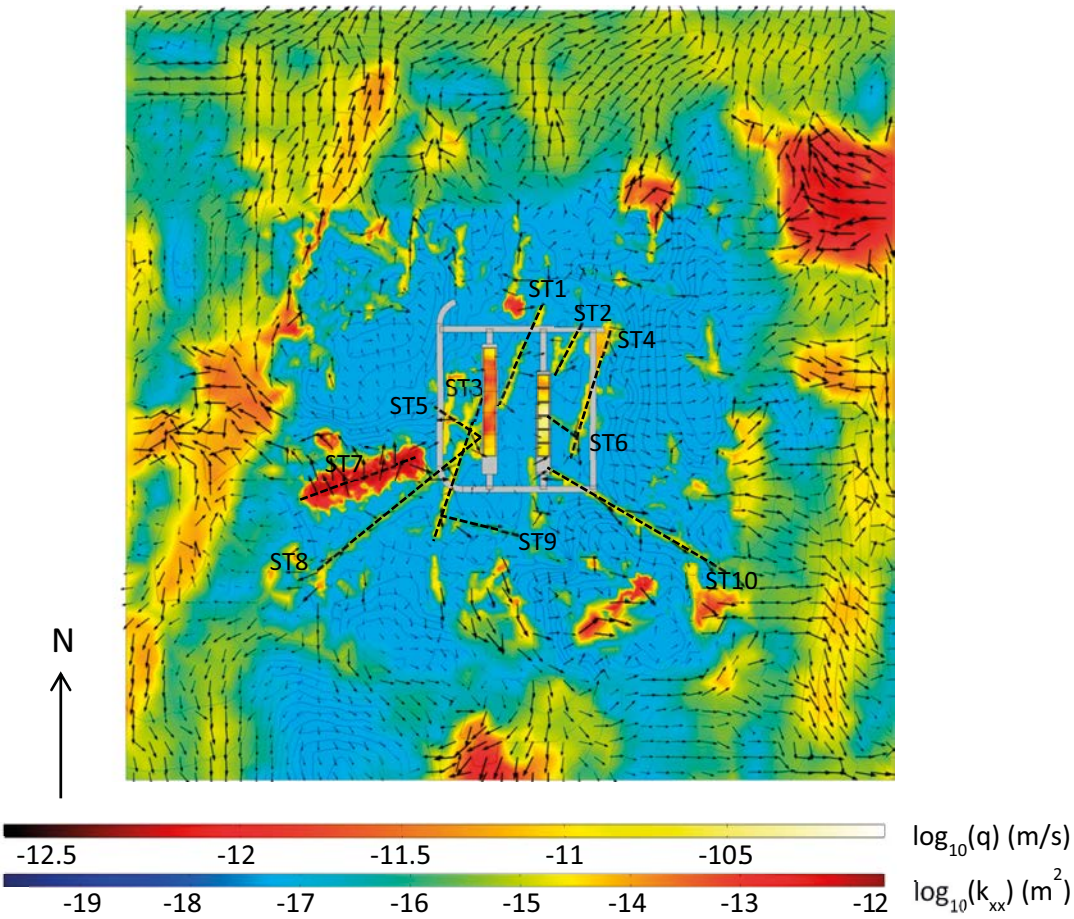

Figure 4-4. *Magnitude of the Darcy velocity through the waste control volumes, permeability values of the rock and flow vectors in a horizontal plane at repository depth. The dash lines delineate approximately the ECPM representation in COMSOL of the stochastic fractures.*

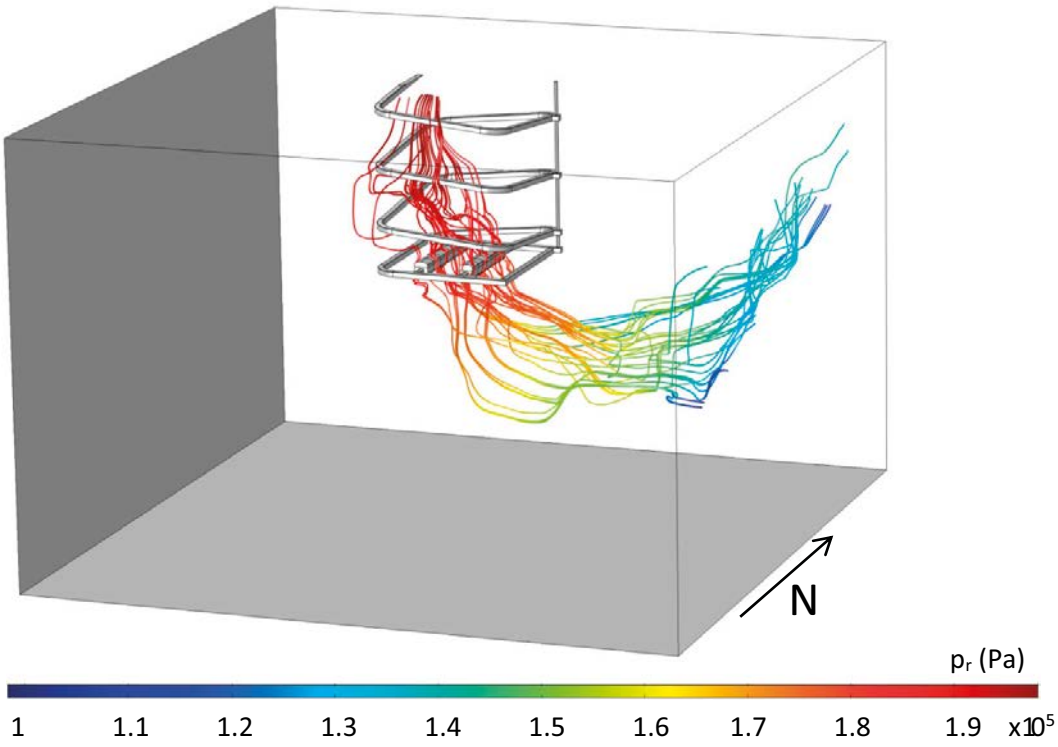

Figure 4-5. *Groundwater flow streamlines passing through the waste control volumes of the BHA and BHK vaults.*

4.4 Interaction between vaults

The interaction between vaults is analysed based on the results of two simulations of non-reactive tracer transport, carried out with the repository scale model. Figure 4-6 shows the extent of two tracer plumes originating from the vault/rock interface. They are delineated by the isosurface representing 20 % of the released concentration (c_r). The tracer plume from BHK (green plume in Figure 4-6) is driven downwards by the vertical groundwater flow. The extent of the plume from the BHA (blue plume in Figure 4-6) occupies a relatively small volume. This limited extent is related to the low mass of tracer released from the BHA vault (m_r in Table 4-2) due to the low permeability of the bentonite backfill.

The fraction of tracer mass released from each vault (m_r) reaching the neighbouring vault (m_v) is presented in Table 4-2. Less than 1 ‰ of the tracer released from the BHA vault is detected at the BHK vault, located downstream. The tracer released from the BHK vault is not detected at the BHA vault, located upstream. This result indicates that spreading by diffusion and upstream velocity-dependent dispersion do not induce interaction between vaults.

Table 4-2. Calculated tracer interaction for the base case.

	BHA to BHK	BHK to BHA
mr(g/yr)	5.69E-01	2.50E+00
mv(g/yr)	3.28E-04	0.0000
Ratio	0.0006	0.0000

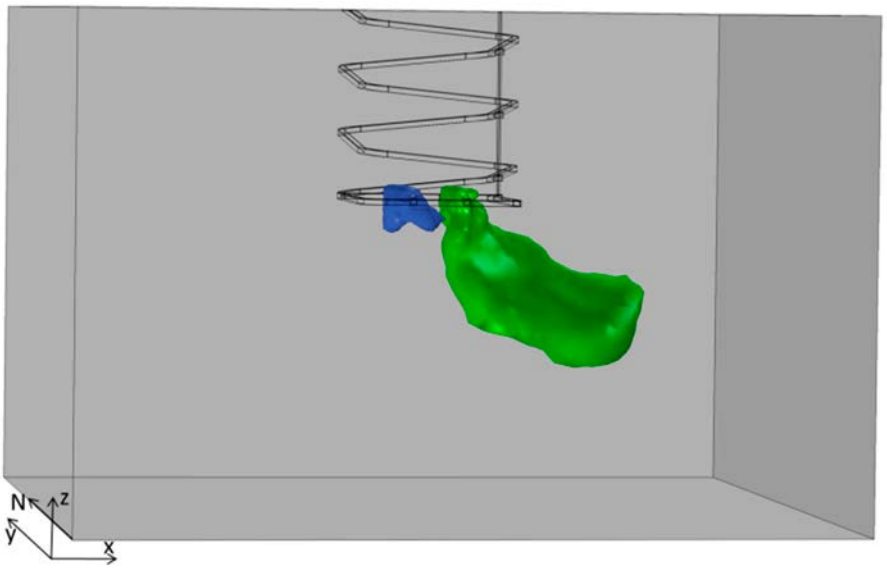

Figure 4-6. *Extent of tracer plumes illustrated by the 20 % isosurface of the released concentration (c_r) for the base case. The tracer plume released from BHK is shown in green and the tracer plume from BHA in blue.*

5 Sensitivity to repository orientation

The orientation of the repository with respect to the flow field can affect the flow through the vaults and waste as well as the interaction between the vaults. The sensitivity to the repository orientation has been investigated with the repository scale model by rotating the repository geometry around a vertical axis at the centre of the modelling domain. Figure 5-1 through Figure 5-4 illustrate the different repository orientations.

Two cases have been considered for the BHK backfill structure. The first case assumes homogeneous properties for the concrete backfill with values of the base case (see Table 3-2). The second case assumes that the concrete backfill has been degraded in an outer zone, at the backfill/rock interface. The geometrical representation of the degraded outer zone is shown in Figure 3-6 and the associated material properties are listed in Table 3-3.

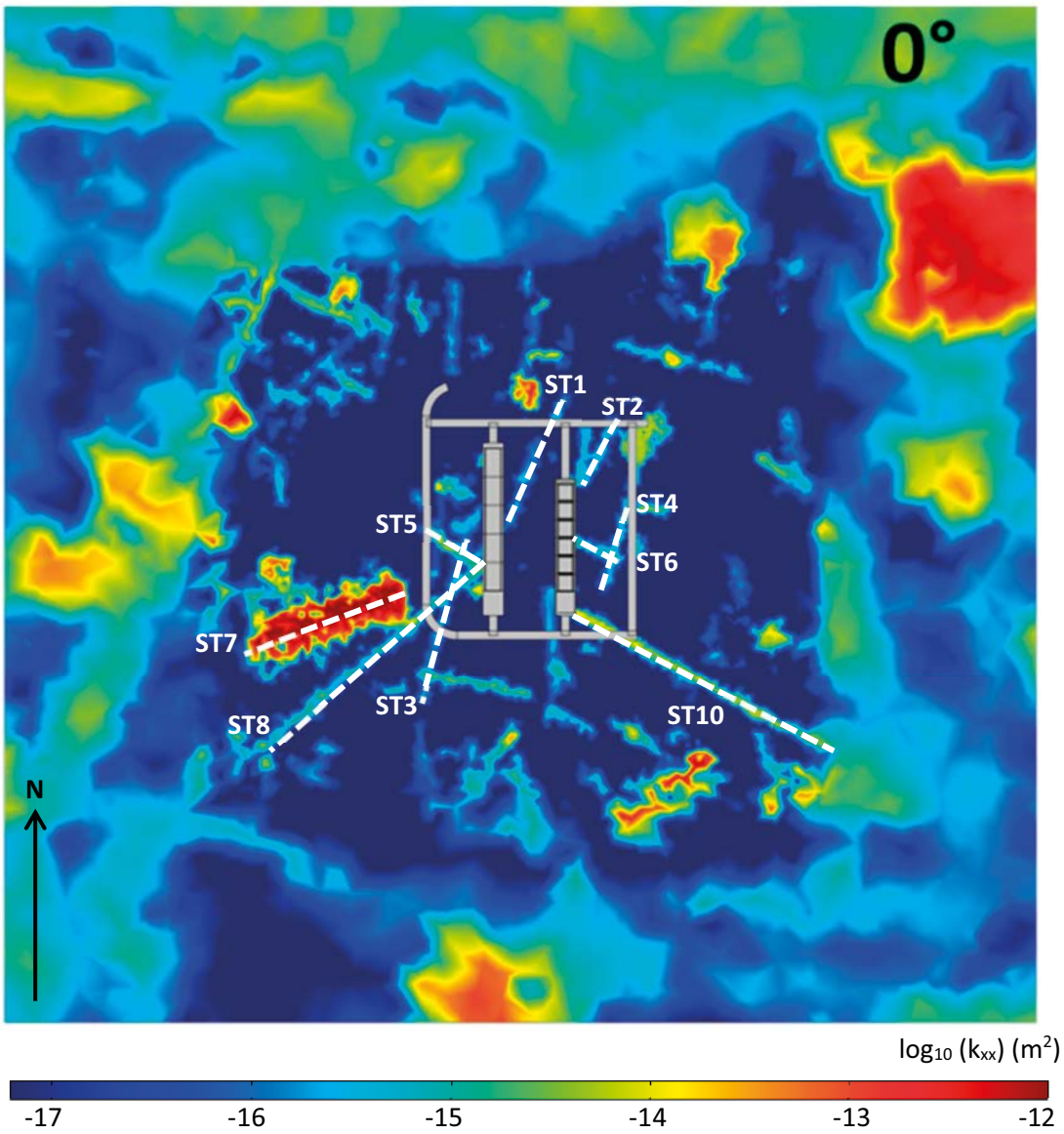

Figure 5-1. *Repository orientation 0° (base case). The colour scale indicates the horizontal rock permeability values on log scale at a xy cross-section at 500 m depth. The dash lines delineate approximately the ECPM representation in COMSOL of the stochastic fractures.*

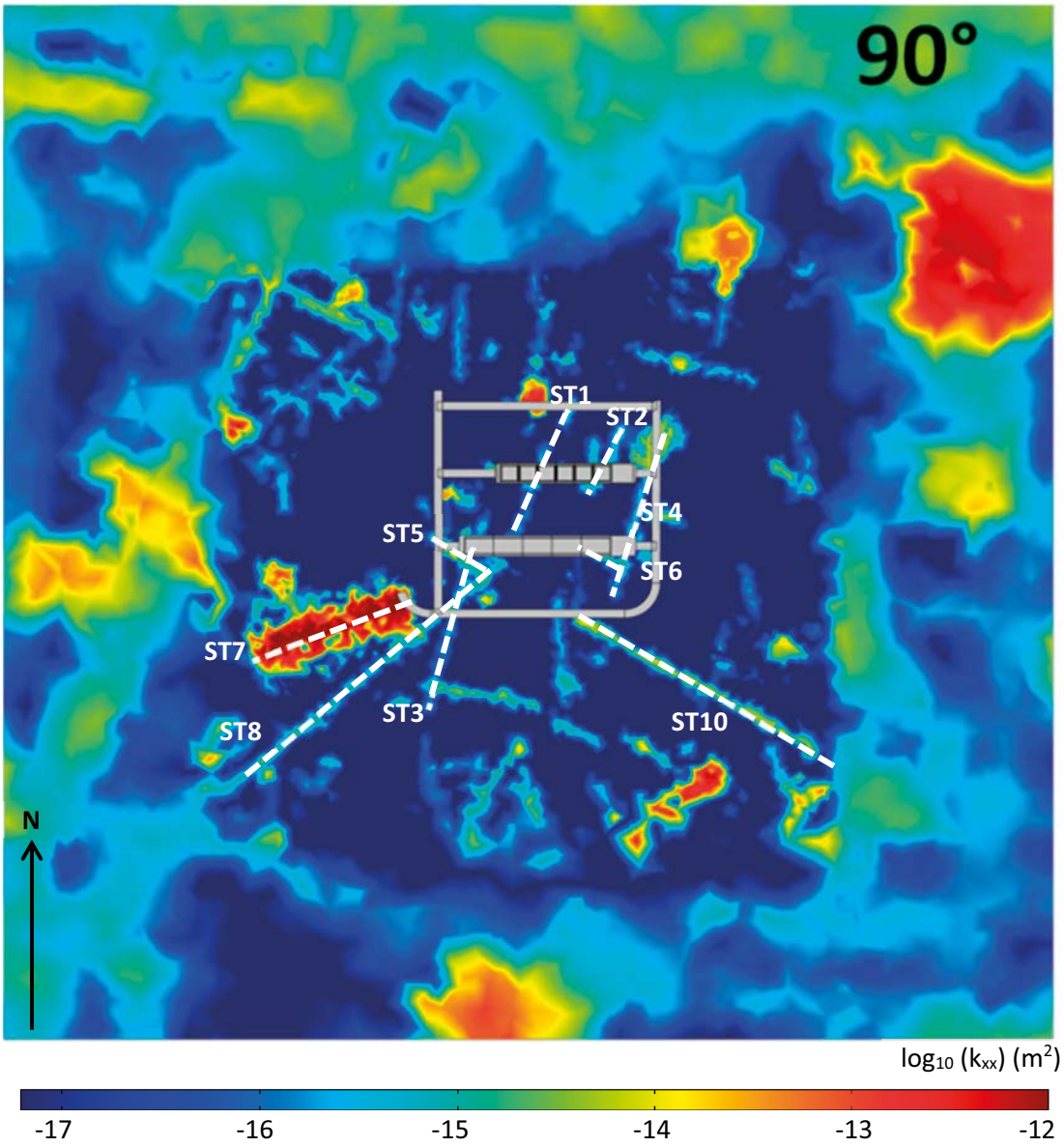

Figure 5-2. *Repository orientation 90° (rotation compared to the base case). The colour scale indicates the horizontal rock permeability values on log scale at a xy cross-section at 500 m depth. The dash lines delineate approximately the ECPM representation in COMSOL of the stochastic fractures.*

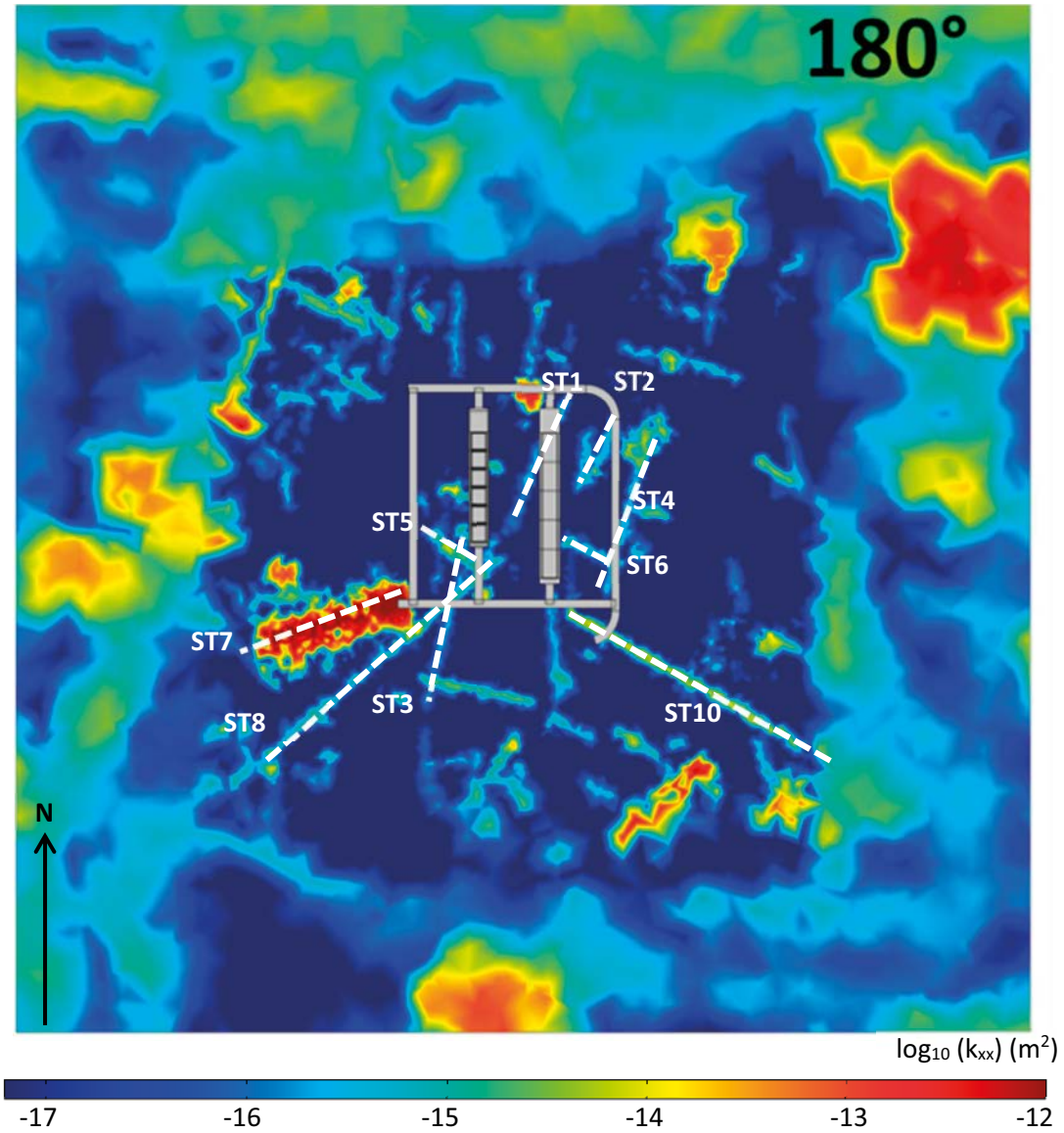

Figure 5-3. *Repository orientation 180° (rotation compared to the base case).. The colour scale indicates the horizontal rock permeability values on log scale at a xy cross-section at 500 m depth. The dash lines delineate approximately the ECPM representation in COMSOL of the stochastic fractures.*

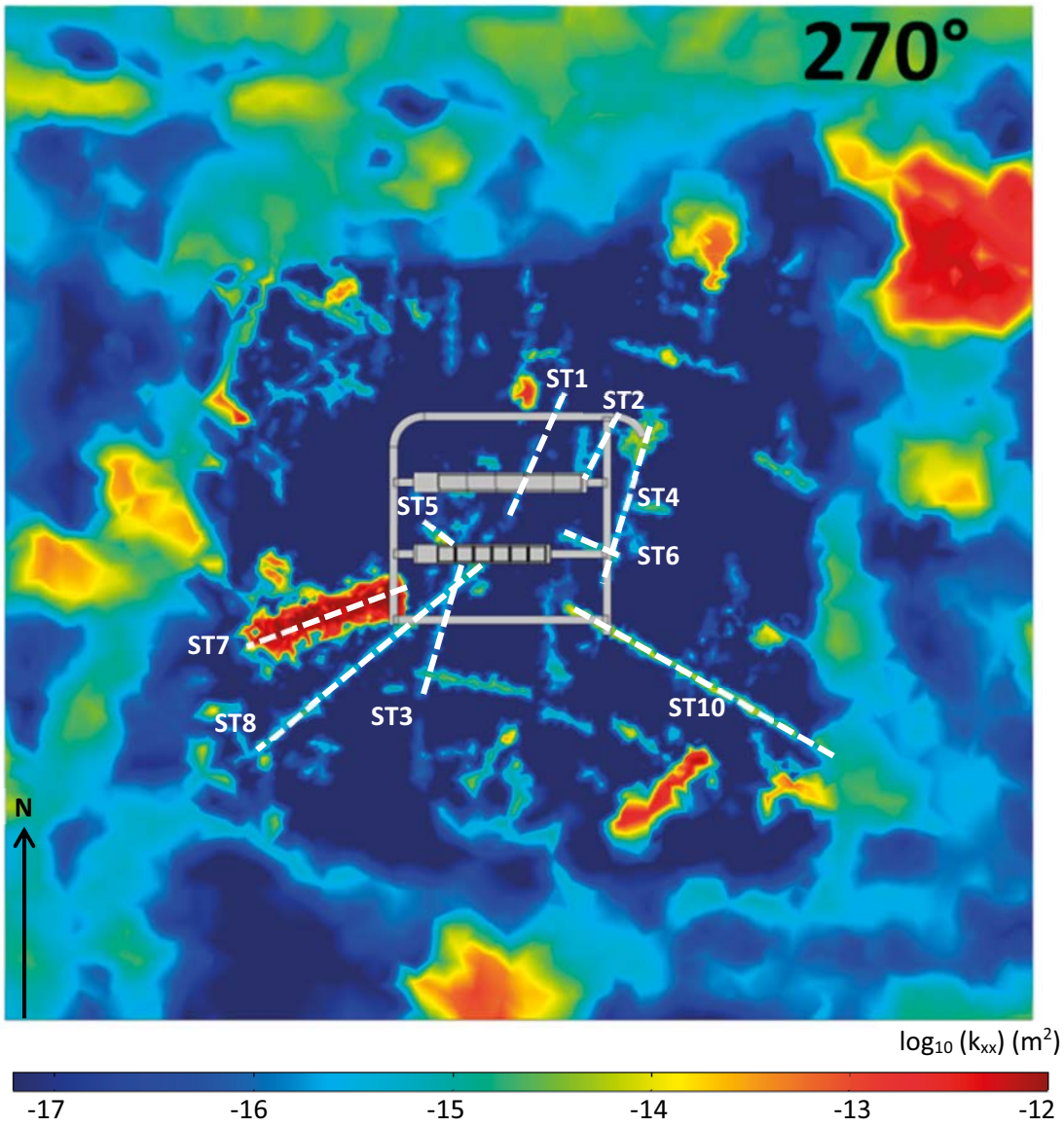

Figure 5-4. *Repository orientation 270° (rotation compared to the base case). The colour scale indicates the horizontal rock permeability values on log scale at a xy cross-section at 500 m depth. The dash lines delineate approximately the ECPM representation in COMSOL of the stochastic fractures.*

5.1 BHK backfill at initial state

5.1.1 Groundwater flow

Table 5-1 gives the computed ratio of groundwater flow through the vaults and waste compartments for all orientation cases to the flow at the base case (Table 4-1). In general, differences are small for the vault flows. For BHA, higher flows are computed when the vault is oriented in an east-west direction. For the 90° rotation the vault flow is approximately four times that of the base case. For BHK, the vault flow decreases to half the flow at the base case for a rotation of 180°.

The flow through the backfill control volumes indicates the spatial distribution of the inflow to the vaults and the role of the stochastic features. Tabulated results are presented in Table B-1 through Table B-8 in Appendix B. The results are presented graphically in bar plots in Figure 5-5 for BHA and Figure 5-7 for BHK. In general, the sections in contact with higher fractures experience higher flows.

Table 5-1. Flow ratio between the different repository orientations and the base case (0°) for the waste control volumes and vaults. Waste IDs refer to the vault section containing the control volume.

			Ratio 90°/0°	Ratio 180°/0°	Ratio 270°/0°
BHA	Waste	1	1.00	0.28	2.18
		2	2.66	0.39	1.43
		3	1.82	0.30	1.10
		4	2.28	0.51	0.89
		5	3.14	0.28	3.31
	Vault	**BHA**	**3.64**	**0.35**	**1.79**
BHK	Waste	1	1.48	1.06	0.32
		2	3.09	0.41	0.23
		3	0.82	0.57	0.40
		4	0.54	0.80	0.77
		5	1.21	0.45	1.24
		6	2.90	0.09	2.84
	Vault	**BHK**	**0.98**	**0.45**	**0.89**

BHA backfill

Figure 5-5 shows the groundwater flow entering different sections of the BHA vault for the different rotation cases. Waste compartments experience different flow due to the existence of fractures in connection to its location. Thus, for the 0° rotation (base case) the highest flows are observed for Sections 1 and 5 (2.5×10^{-3} and 3.96×10^{-3} m^3/year respectively). Section 1 is intersected by the vertical stochastic feature ST15 (Figure 3-9) while Section 5 is intersected by ST8 and ST5 (Figure 5-1).

For the 90° rotation, the highest flow through the BHA backfill (1.54×10^{-2} m^3/year) is located in Section 6, which corresponds to the loading area and is affected by the presence of ST4. Sections 2 and 1, with flow values of 2.28×10^{-3} and 4.59×10^{-2} m^3/year, respectively, are also affected by zones ST5 and ST8 (Figure 5-2).

For the 180° rotation, groundwater flow enters the BHA backfill mainly through Section 5 (7.50×10^{-3} m^3/year) due to the intersection with the zone ST1 (Figure 5-3).

Finally, for the 270° rotation, the highest flow enters the BHA through Section 3 (7.51×10^{-3} m^3/year). This section intersects with the stochastic feature ST1 (Figure 5-4).

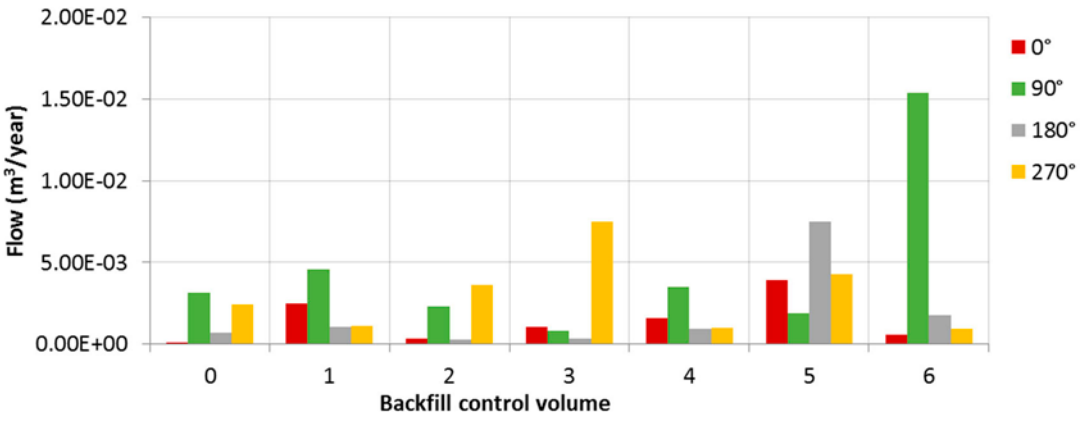

Figure 5-5. *Calculated flow through the BHA backfill control volumes for each rotation case. Numbers refer to the vault axial section containing the control volume* (Figure 3-15*).*

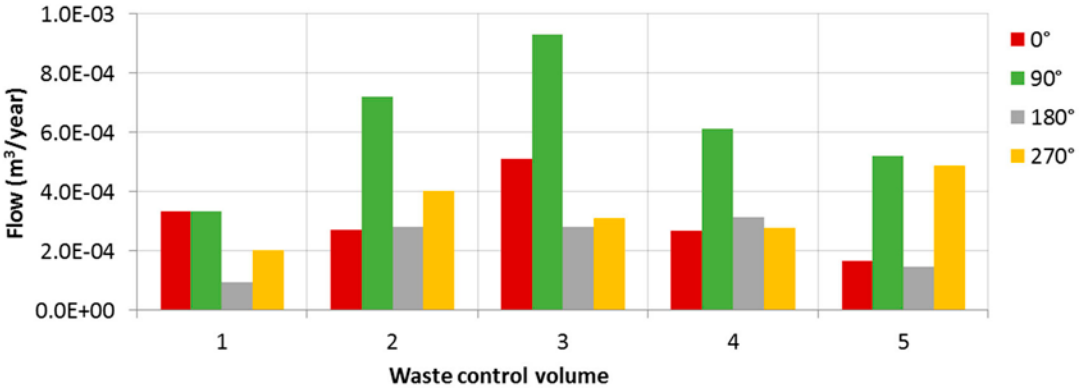

Figure 5-6. *Calculated flow through the BHA waste control volumes for each rotation case. Numbers refer to the vault axial section containing the control volume (Figure 3-15).*

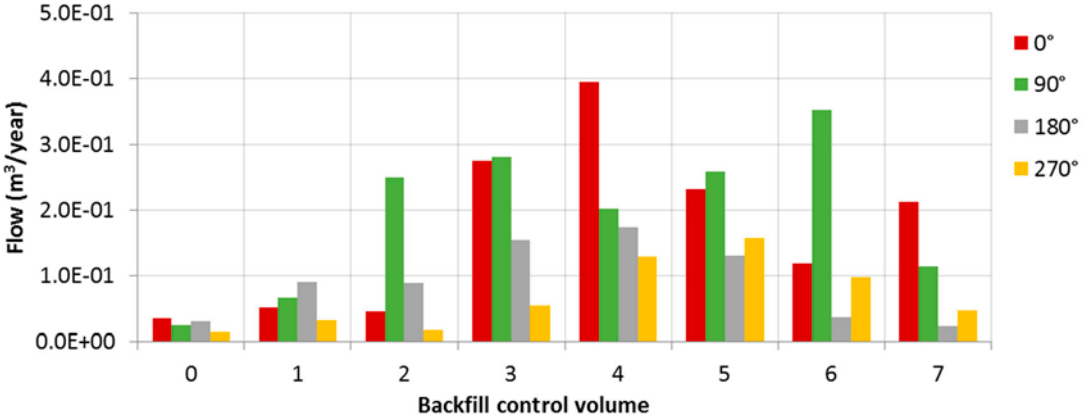

Figure 5-7. *Calculated flow through the BHK backfill control volumes for each rotation case. Numbers refer to the vault axial section containing the control volume (Figure 3-15).*

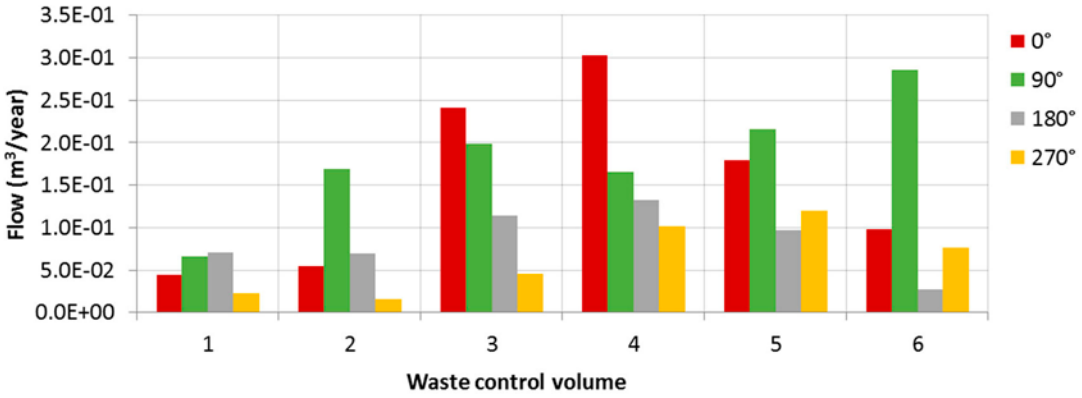

Figure 5-8. *Calculated flow through the BHK waste control volumes for each rotation case. Numbers refer to the vault axial section containing the control volume (Figure 3-15).*

BHA waste

Figure 5-6 shows the groundwater flow reaching BHA waste sections. The maximum flow is found for the 90° rotation. This correlates with the highest computed vault flow. The lowest flow occurs for the 180° rotation.

In general, the distribution of the waste flow is rather homogeneous. This is explained by the modelling assumption treating the BHA waste domain as a homogeneous block of relatively high permeability. Water that crosses over the bentonite backfill can move along the entire waste volume. Therefore, the correlation between waste section flow and the presence of fractures is not as pronounced.

BHK backfill

Figure 5-7 shows the groundwater flow entering the BHK backfill control volumes for the different rotation cases. For the 0° rotation, the highest flows are observed in the central sections (3, 4 and 5). The groundwater flow values amount 2.76×10^{-1}, 3.94×10^{-1} and 2.33×10^{-1} m^3/year, respectively, influenced by the intersection with ST6 (Figure 5-1).

For the 90° rotation, the highest values of groundwater flow are computed in Sections 3 and 6. The flows reaching Sections 6, 5 and 4 (3.53×10^{-1}, 2.59×10^{-1} and 2.03×10^{-1} m^3/year, respectively) are influenced by stochastic feature ST2 see (Figure 5-2), while flows entering compartments 3 and 2 (2.82×10^{-1} and 2.50×10^{-1} m^3/year respectively) are influenced by stochastic feature ST1.

For the 180° rotation, higher flows are observed for the sections BHK_BF_3, 4 and 5 with flow values of 1.54×10^{-1}, 1.74×10^{-1} and 1.31×10^{-1} m^3/year respectively. Higher flows are caused by intersection of the vault with zones ST13 and ST14 (Figure 3-9).

Finally, for the 270° rotation, the sections BHK_BF_4, 5 and 6 experience the highest flows (1.28×10^{-1}, 1.57×10^{-1} and 9.77×10^{-2} m^3/year, respectively), due to the presence of zones ST5, ST8 and ST3.

BHK waste

Figure 5-8 shows the spatial distribution of groundwater flow reaching the BHK waste. The waste in BHK is stored in individual structures separated by concrete backfill. The distribution of the waste flow is therefore expected to follow the trend observed for the flow entering the backfill sections.

The relation between the amount of water that reaches each waste compartment and the amount of water that enters each backfill compartment is very similar for the different rotation cases. In summary, the average of flow reaching the waste compartments is approximately 80 % of the average flow entering in the backfill sections.

5.1.2 Interaction between vaults

The interaction between vaults is analysed by means of non-reactive tracer transport simulations, using the repository-scale model. The mass flow of tracer released (m_r) from each vault and rotation case is given in Table 5-2. The results correlate with the computed vault flows (Table 5-1). The largest tracer release rates are seen for the 90° rotation for BHA and for the 0° rotation for BHK.

Table 5-2. Calculated tracer mass flow (m_r (g/yr)) released from the BHA and BHK backfill/rock interface for different repository orientations.

Rotation angle	m_r (g/yr) BHA	BHK
0	5.69E-01	2.50E+00
90	1.53E+00	1.79E+00
180	9.79E-01	4.34E-01
270	5.13E-01	7.14E-01

The mass flow of tracer that reaches the neighbouring vault (m_v) has also been calculated. The ratio m_v/m_r serves as indicator of the mass transfer interaction between the two vaults. The interaction is lower than 1 ‰ in all cases (Table 5-3). The limited interaction is due to the prevailing vertical downward component of the local flow (Figure 4-5). The minor horizontal flow component from west to east in the regional flow leads to a slight mass transfer from the upstream vault to the downstream vault when the vaults are oriented along a north-south direction (0° and 180° rotation cases). The interaction is negligible when the vaults are parallel to the horizontal flow component.

Table 5-3. Interaction (m_r/m_v) between vaults for the base case affected by repository rotation.

Rotation angle	BHA to BHK (-)	BHK to BHA (-)
0	0.0006	0.0000
90	0.0003	0.0000
180	0.0000	0.0005
270	0.0001	0.0001

5.2 Degraded zone case

5.2.1 Groundwater flow

Here it is assumed that the concrete backfill has been degraded in an outer zone, at the backfill/rock interface. Table 5-4 presents the computed flows through the vault and waste control volumes for different repository orientations. The ratio between the computed flows for the degraded zone case and the base case is used to analyse the impact of an outer degraded zone in the BHK backfill (Table 5-5).

Table 5-4. Computed flow through waste control volumes and through the BHA and BHK vaults for the degraded zone case. Waste IDs refer to the vault section containing the control volume. Flow ratio between the different repository orientations and the base case (0°).

			0° Total flow (m^3/yr)	90° Ratio 90°/0°	180° Ratio 180°/0°	270° Ratio 270°/0°
BHA	Waste	1	3.25E-04	0.97	0.30	2.17
		2	2.44E-04	2.85	0.41	1.42
		3	4.93E-04	1.82	0.31	1.10
		4	2.60E-04	2.25	0.54	0.88
		5	1.57E-04	3.22	0.29	3.30
	Vault	**BHA**	**2.11E-02**	**3.55**	**0.36**	**1.77**
BHK	Waste	1	1.97E-02	1.84	0.75	0.73
		2	3.62E-02	2.93	0.29	0.53
		3	1.14E-01	1.20	0.37	0.52
		4	1.41E-01	0.89	0.44	1.01
		5	1.14E-01	1.43	0.24	1.87
		6	5.83E-02	3.48	0.09	2.92
	Vault	**BHK**	**3.40E+00**	**1.13**	**0.30**	**1.38**

The degraded zone has a permeability value of 2.0×10^{-14} m^2. This leads to an increase in the vault flow by a factor 2.5–3.8, depending on the repository orientation (Table 5-5). However, the groundwater flow that reaches the BHK waste compartments is reduced to half of the base case (Table 5-5).

The flow through the BHA vault and waste is reduced up to 5 % by the change in the BHK backfill properties. The capture zone of the BHK vault increases, detracting flow from the BHA vault and waste compartments. This effect is maximised for the 90° rotation.

Table 5-5. Ratio between the flows at the base case and degraded zone case for BHA and BHK waste compartments and vaults under four repository orientations. Waste IDs refer to the vault section containing the control volume.

			Rotation angle			
		Ratio DZC/BC	0°	90°	180°	270°
BHA	Waste	1	0.97	0.94	1.00	1.00
		2	0.90	0.97	1.00	1.00
		3	0.97	0.97	1.00	1.00
		4	0.97	0.96	1.00	1.00
		5	0.95	0.97	1.00	1.00
	Vault	**BHA**	**0.97**	**0.95**	**0.99**	**0.98**
BHK	Waste	1	0.44	0.55	0.39	0.87
		2	0.66	0.63	0.45	1.05
		3	0.47	0.69	0.45	0.58
		4	0.46	0.76	0.42	0.55
		5	0.64	0.75	0.41	0.62
		6	0.59	0.71	0.69	0.71
	Vault	**BHK**	**3.12**	**3.59**	**2.42**	**3.75**

5.2.2 Interaction between vaults

A degraded concrete zone in the BHK backfill results in higher tracer release rates (m_r) as compared to the base case (Table 5-6). The release rate increases by a factor of 2.5 with respect to the base case for all orientations. This increase correlates with the increment in flow through the vault (Table 5-5) indicating that advection controls mass release from the vault to the rock. The results from the BHA tracer also show this correlation. The small decrease in release rate from the BHA (Table 5-6) is of the same order than the decrease of flow through the vault (Table 5-5).

Table 5-6. Calculated m_r for the degraded zone case at different rotation angle simulations of a conservative tracer released from the BHA/rock interface and the conservative tracer released from the BHK/rock interface.

Rotation angle	BHA	BHK
0	5.41E-01	6.00E+00
90	1.46E+00	4.47E+00
180	9.80E-01	9.70E-01
270	5.03E-01	1.71E+00

Even if the interaction between the tracer released from the BHA and the BHK is still small, it increases for the 0° and 90° rotation cases. The maximum ratio is 2.6 ‰ for the 90° rotation (Table 5-7). The increase in interaction between vaults with respect to the base case is related to the flow increase in the BHK (Table 5-5) and the flow reduction in the BHA. The capture zone of the BHK increases capturing water from the surrounding rock and from the BHA capture zone. As a result, part of the tracer from the BHA moves towards the BHK capture zone. The interaction between the tracer released from the BHK and the BHA is not affected by the degraded outer backfill in the BHK.

Table 5-7. Interaction (m_r/m_v) between vaults for the degraded zone case affected by repository rotation.

Rotation angle	BHA to BHK (-)	BHK to BHA (-)
0	0.0018	0.0000
90	0.0026	0.0000
180	0.0000	0.0004
270	0.0001	0.0000

5.3 Summary

An intact concrete backfill in BHK has been compared to a partially degraded backfill, considering four repository orientations. The flow results for the vault and waste flow are summarised in Figure 5-9 and Figure 5-10, respectively. The lowest groundwater inflow to the BHA vault is observed for the 0° rotation (0.022 m^3/year) and the highest flow a 90° rotation (Figure 5-9). The flows at the BHA are not significantly affected by the degradation of the outer zone of the BHK concrete backfill (Figure 5-9).

For an intact concrete backfill, the smallest flows through the BHK vault are found to be 0.4 and 0.5 m^3/year for the 270° and 180° repository rotations, respectively (Figure 5-9). A degraded outer zone in the BHK backfill increases the vault flow by a factor of four, as compared to the base case. A degraded outer concrete backfill leads to a small reduction (<5 %) of the groundwater flow entering BHA. The higher permeability of the degraded zone drives groundwater towards the BHK, even capturing some of the flow towards the BHA.

The lowest flows for the BHA waste occur for the 90 and 270° rotation cases (Figure 5-10), when the vaults are oriented parallel to the horizontal flow component (Figure 4-5). The BHK backfill degradation does not affect the BHA waste flow.

In the case of an intact concrete backfill, the lowest flows in the BHK waste (Figure 5-10) are seen for the 270° rotation case (0.07 m^3/year). The degraded backfill acts as a by-pass for groundwater reducing the flow reaching the waste compartments (Figure 5-10).

Tracer simulations show a limited interaction between the vaults, due to the prevailing vertical downward component of the local flow. The largest interaction is observed for the case of a degraded backfill and a rotation of 90°. Here, 2.7 ‰ of the mass leaving BHA reached BHK. When the vaults are oriented perpendicular to the horizontal flow component (0° and 180° rotation cases) the maximum interaction is 1 ‰ for the downstream vault.

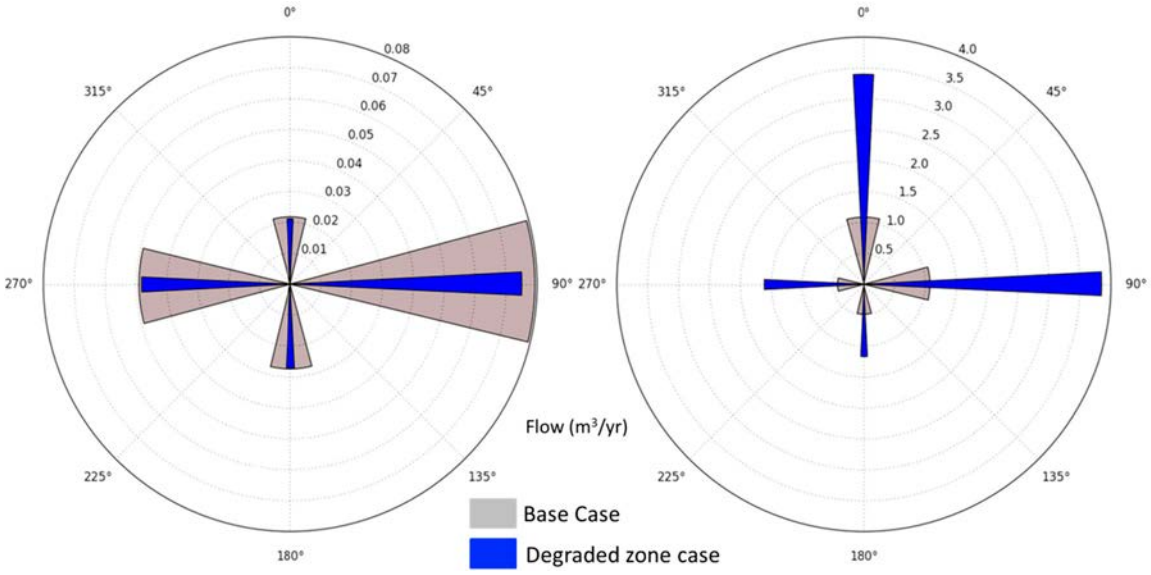

Figure 5-9. *Groundwater flow entering BHA (left) and BHK (right) for each repository rotation angle (0, 90, 180 and 270) for the base case and the degraded zone case.*

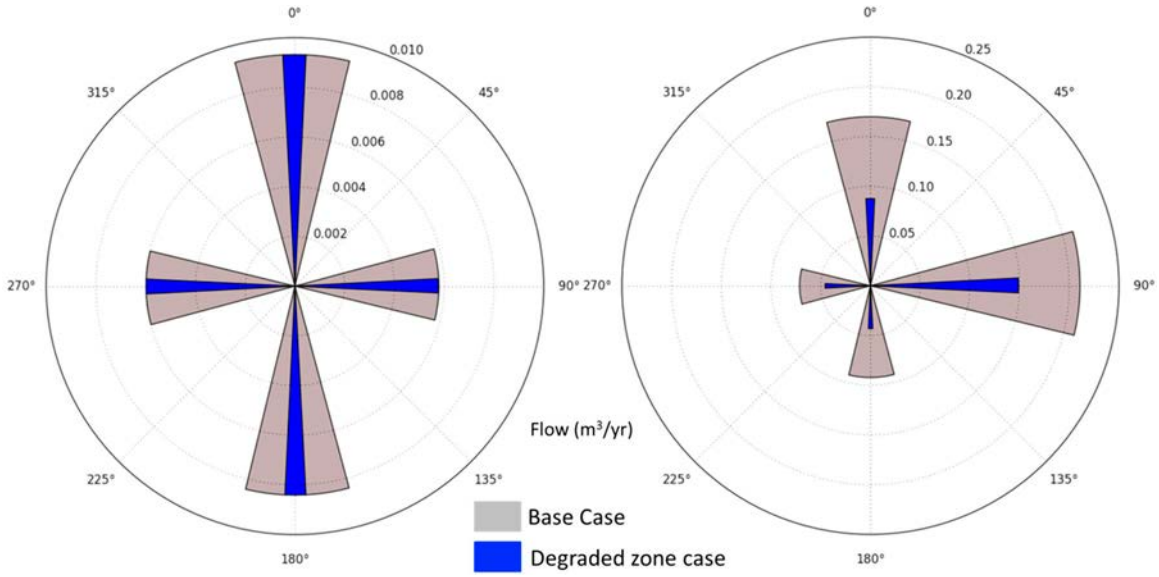

Figure 5-10. *Groundwater flow entering the BHA (left) and BHK (right) waste for each repository rotation angle (0, 90, 180 and 270) for the base case and the degraded zone case.*

6 Influence of the concrete barrier degradation

A simulation with a completely degraded backfill completes the set of simulations that assume an increasing permeability of the BHK concrete backfill. The three cases considered are the base case, the degraded zone case and a degraded case. The repository orientation is 0° degrees. The simulation cases and the associated material properties applied to the BHK backfill are summarised in Table 3-3. The density dependent flow is computed with the repository scale model. A comprehensive set of tables detailing the groundwater flows through vaults and waste is presented in Appendix B.

The material properties of the bentonite backfill in BHA are assumed to be constant over time. The influence of a degrading bentonite backfill on the flow though the BHA vault and waste has been investigated in previous work (Abarca et al. 2016).

6.1 Groundwater flow

As detailed in Chapter 4, the groundwater flow near the repository is mainly directed vertically downwards but it becomes quasi-horizontal at greater depths.

BHK

Table 6-1 shows the calculated flows for the different concrete backfill degradation cases. Table 6-2 shows that degradation of the BHK backfill results in a general increase in the groundwater flow entering the vault. Figure 6-1 shows the spatial distribution of the flow through the backfill, which increases with increasing degradation at Sections 3, 4 and 5. However, there is a decrease in flow going from the degraded zone case to the degraded case in Sections 0, 1 and 2. This reduction in flow, affecting the northernmost sections, indicate that flow is driven preferentially towards the south of the BHK between fractures ST6 and ST10.

Table 6-1. Groundwater flow through BHK waste and backfill sections. IDs refer to the vault section containing the control volume. The flow ratio is calculated with respect to the base case.

		Base case	Degraded zone case		Degraded case	
Flow Control Volume		Total flow (m^3/yr)	Total flow (m^3/yr)	Ratio	Total flow (m^3/yr)	Ratio
Waste	1	4.47E-02	1.97E-02	0.44	1.01E-01	2.27
	2	5.47E-02	3.62E-02	0.66	1.03E-01	1.88
	3	2.42E-01	1.14E-01	0.47	5.16E-01	2.14
	4	3.03E-01	1.41E-01	0.46	7.91E-01	2.61
	5	1.79E-01	1.14E-01	0.64	6.65E-01	3.71
	6	9.82E-02	5.83E-02	0.59	3.31E-01	3.38
Backfill	0	3.46E-02	1.93E-01	5.58	1.68E-01	4.85
	1	5.13E-02	1.40E-01	2.73	9.93E-02	1.94
	2	4.59E-02	9.68E-02	2.11	4.76E-02	1.04
	3	2.76E-01	7.11E-01	2.58	8.43E-01	3.06
	4	3.94E-01	1.37E+00	3.48	1.80E+00	4.56
	5	2.33E-01	1.02E+00	4.37	1.44E+00	6.18
	6	1.18E-01	3.82E-01	3.23	6.76E-01	5.71
	7	2.13E-01	1.09E+00	5.13	1.50E+00	7.04

The BHK waste flow decreases by approximately 50–60 % comparing the base case to the degraded zone case (Table 6-3). However, there is an increase by a factor of 2 to 4 going from the base case to the degraded case (Table 6-3). The spatial distribution of the flow through the BHK waste is illustrated in Figure 6-2. In all waste compartments, the highest flows occur when the concrete backfill is completely

degraded. The lowest waste flows are calculated for the degraded zone case. Here, groundwater is being redirected through the degraded outer zone reducing the flow reaching the waste.

Groundwater flow is displayed in longitudinal cut planes through the vaults to analyse local changes in the flow direction around the vaults. The different planes are labelled with the vault name and the Y coordinate of the plane (Figure 6-3).

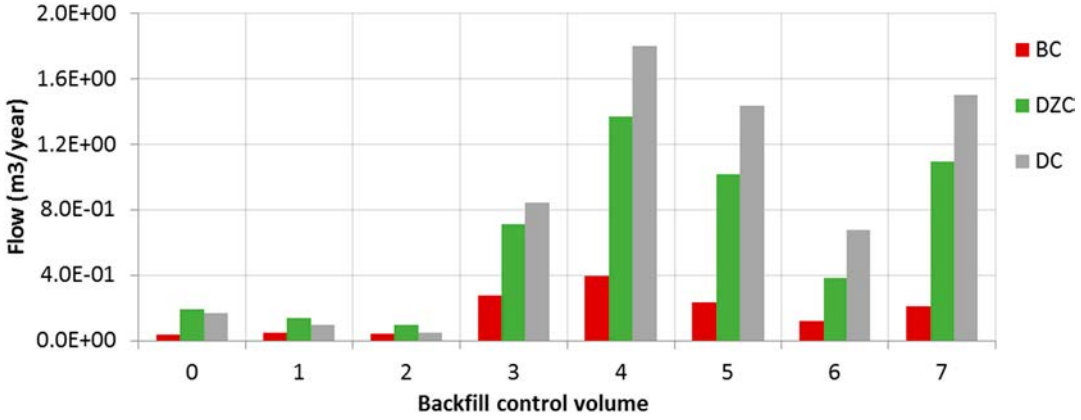

Figure 6-1. *Groundwater flow through the BHK backfill sections. BC = base case, DZC = Degraded zone case and DC = Degraded case. Numbers refer to the vault axial section containing the control volume (Figure 3-15).*

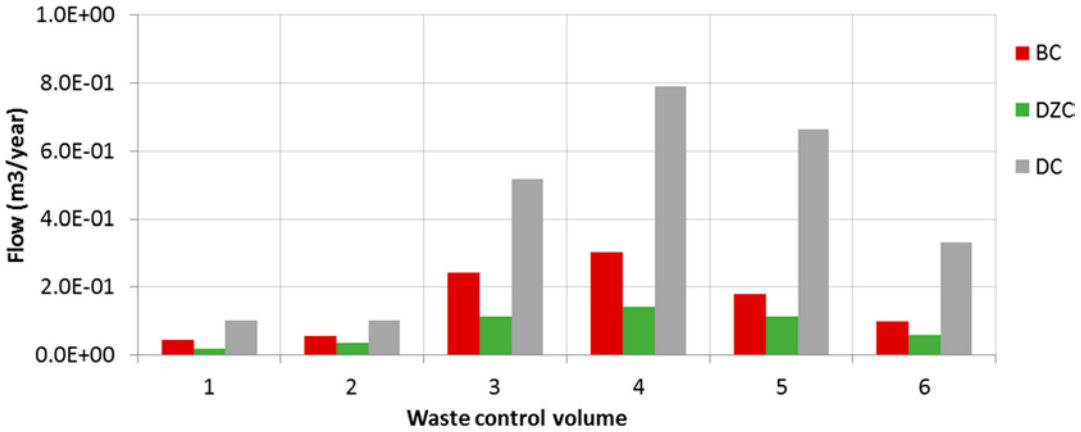

Figure 6-2. *Groundwater flow through the BHK waste sections. BC = base case, DZC = Degraded zone case and DC = Degraded case. Numbers refer to the vault axial section containing the control volume (Figure 3-15).*

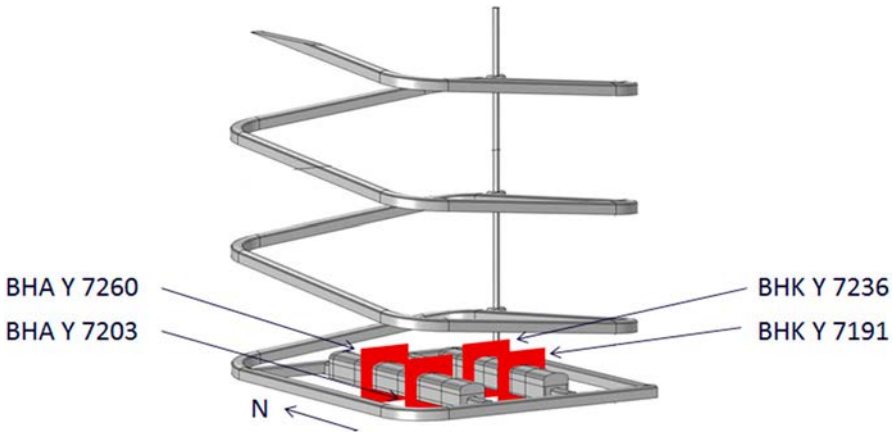

Figure 6-3. *Vertical plot planes cutting the BHA (left) and BHK (right) vaults.*

Figure 6-4 shows the groundwater flow direction and the Darcy velocities near the BHK vault. The groundwater flow in the BHK Y 7236 section is affected by the presence of ST14 crossing the vault. The highest magnitude of the Darcy velocity is calculated at that stochastic feature for all three cases. For the base case, higher flow velocities are observed in the waste than in the backfill. The higher Darcy flow inside the waste results of the combination of a high permeability of the waste, the 3D flow field and the density-driven flow that can cause rotational flow with closed streamlines. The resulting 3D flow field cannot be accurately depicted in a 2D plane. When concrete degradation is considered in the outer parts of the backfill, most of the flow that enters the vault flows around the intact part of the backfill through the degraded zone. The Darcy velocity values in the waste are reduced compared to the base case. When the concrete backfill is completely degraded, the Darcy velocities inside BHK are uniform and similar to the velocities observed in the stochastic features in the rock.

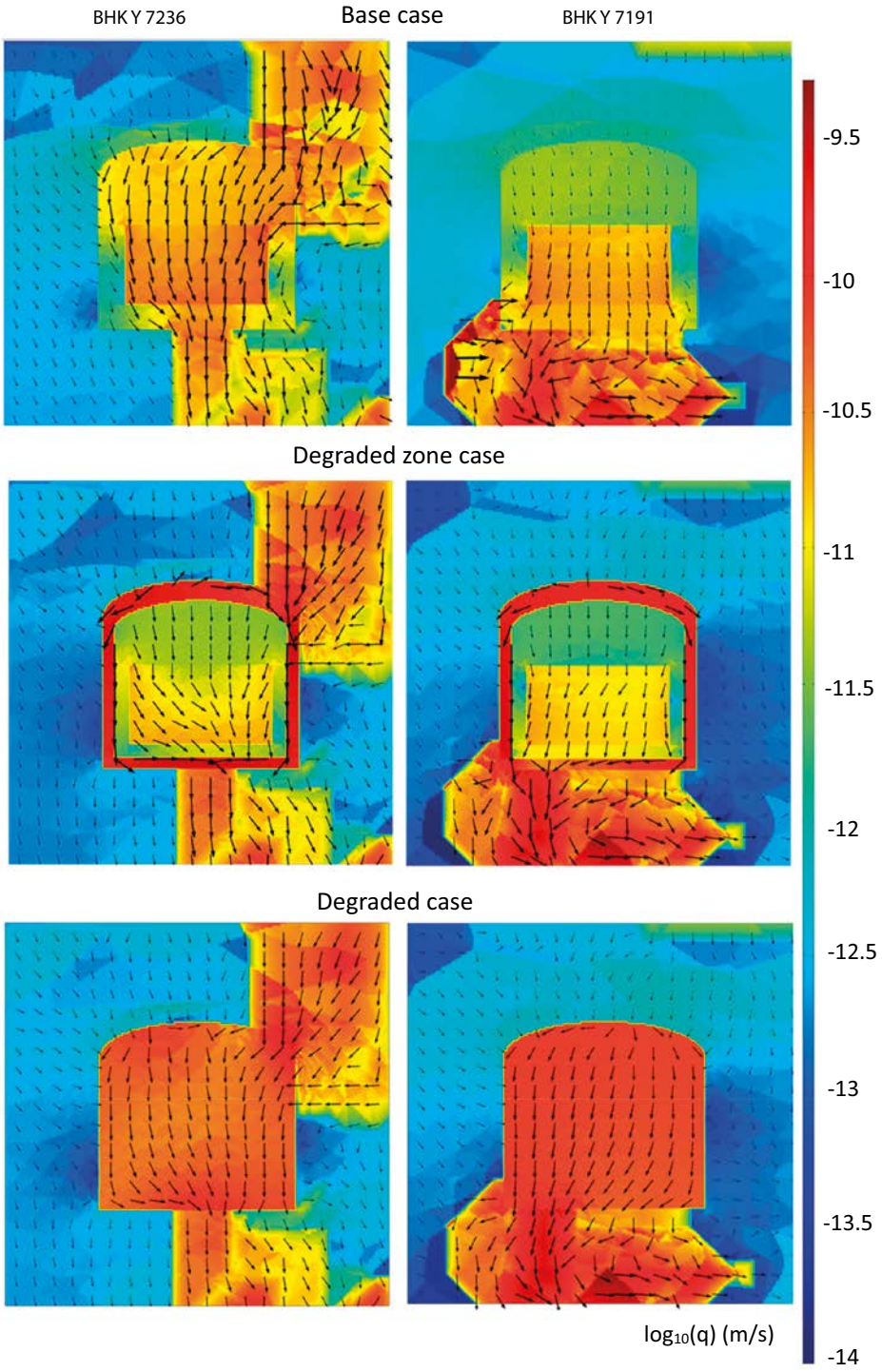

Figure 6-4. *Flow vectors showing the groundwater flow direction superimposed on Darcy velocity magnitude trough the BHK vault.*

BHA

Table 6-2 shows the calculated flow values through the BHA for the different concrete backfill degradation cases. The degraded zone case and the degraded case have a similar effect on the BHA flow. In general, a decrease in the flow through the BHA is observed for the degraded cases. This is caused by flow being driven towards the BHK vault as the backfill degrades. The largest decrease in flow in a given backfill section is 30 %.

Table 6-2. Groundwater flow through BHA waste and backfill sections. IDs refer to the vault section containing the control volume. The flow ratio is calculated with respect to the base case.

		Base case	Degraded zone case		Degraded case	
Flow control volume		Total flow (m^3/yr)	Total flow (m^3/yr)	Ratio	Total flow (m^3/yr)	Ratio
Waste	1	3.33E-04	3.25E-04	0.98	3.24E-04	0.97
	2	2.71E-04	2.44E-04	0.90	2.44E-04	0.90
	3	5.11E-04	4.93E-04	0.97	4.93E-04	0.96
	4	2.69E-04	2.60E-04	0.97	2.59E-04	0.96
	5	1.66E-04	1.57E-04	0.95	1.57E-04	0.94
Backfill	0	7.15E-05	6.84E-05	0.96	6.81E-05	0.95
	1	2.50E-03	2.88E-03	1.15	2.86E-03	1.14
	2	3.50E-04	3.25E-04	0.93	3.23E-04	0.92
	3	1.07E-03	7.49E-04	0.70	7.43E-04	0.69
	4	1.59E-03	1.15E-03	0.72	1.15E-03	0.72
	5	3.93E-03	3.77E-03	0.96	3.75E-03	0.95
	6	5.97E-04	5.66E-04	0.95	5.64E-04	0.95

Figure 6-5 shows the spatial distribution of the flow in the BHA backfill sections. Except for section 1, the flow decreases for both concrete backfill degradation cases. A degraded BHK backfill drains groundwater from the surrounding repository areas. Figure 6-6 shows the spatial distribution of the calculated flows through the BHA waste sections. The waste flow follows the same trend observed in the flow through the backfill sections.

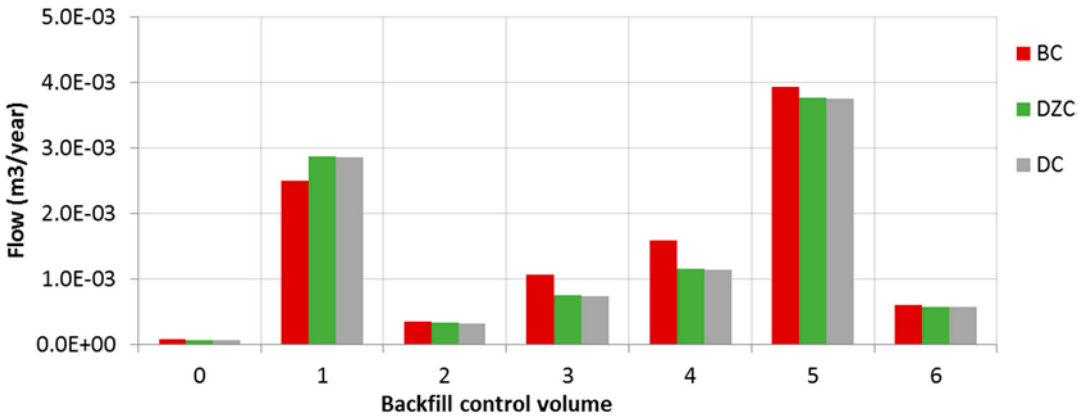

Figure 6-5. *Groundwater flow through the BHA backfill sections. BC = base case, DZC = Degraded zone case and DC = Degraded case. Numbers refer to the vault axial section containing the control volume (Figure 3-15).*

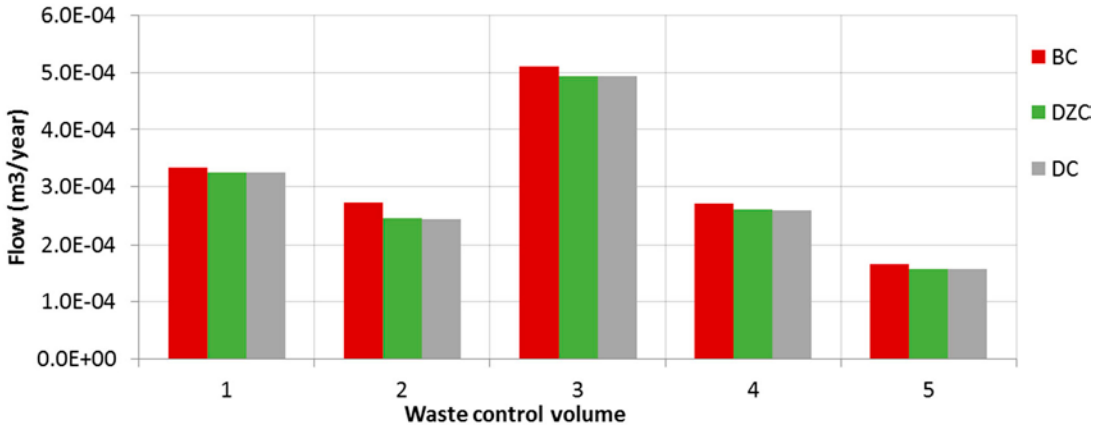

Figure 6-6. *Groundwater flow through the BHA waste sections. BC = base case, DZC = Degraded zone case and DC = Degraded case. Numbers refer to the vault axial section containing the control volume (Figure 3-15).*

Figure 6-7 shows the groundwater flow direction and the Darcy velocity magnitude of two cross-sections of the BHA vault (Figure 6-3) for the three different concrete degradation cases. Degradation of the concrete backfill in BHK has no clear effect on the groundwater flow pattern near BHA.

6.2 Interaction between vaults

Tracer transport simulations have been performed with the repository scale model to quantify the steady state extent of a plume of tracer leaking from each of the vaults. The results have been used to assess the interaction between vaults for the three cases of concrete backfill degradation.

Figure 6-8 shows the extent of the tracer plumes delineated by the isosurface representing 20 % of the released concentration. The shape of the BHA plume (blue) is slightly modified by the degradation state of the BHK backfill. The BHK tracer plumes (green) are more extended for the degraded cases. The extent is similar for the degraded zone case and the degraded case. The larger extent relates with the increase in mass released from the rock in these cases. The mass flux of tracer released from a vault (m_r) and the mass flux reaching the neighbouring vault (m_v) is presented in Table 6-3. The mass released from the BHK vault for the degraded zone case doubles the m_r for the base case but it is similar to m_r for the degraded case. The increase in m_r responds to the increase in vault flow when the backfill degrades (see Table 5-5 and Table 6-1).

The ratio m_v/m_r serves as an indicator of the interaction between vaults. For a tracer released from BHA, the ratio increases to approximately 2 ‰ when the concrete backfill degrades. This is caused by the increase in the groundwater flow entering the BHK vault. For a tracer released from BHK the effects due to degradation is negligible.

Table 6-3. Calculated tracer interaction for each BHK backfill degradation case.

	Base case		Degraded zone case		Degraded case	
	BHA to BHK	BHK to BHA	BHA to BHK	BHK to BHA	BHA to BHK	BHK to BHA
m_r(g/yr)	5.69E-01	2.50E+00	5.36E-01	6.02E+00	5.31E-01	6.82E+00
m_v(g/yr)	3.28E-04	5.02E-08	8.25E-04	1.32E-07	1.03E-03	1.36E-07
Ratio	0.0006	0.0000	0.0015	0.0000	0.0019	0.0000

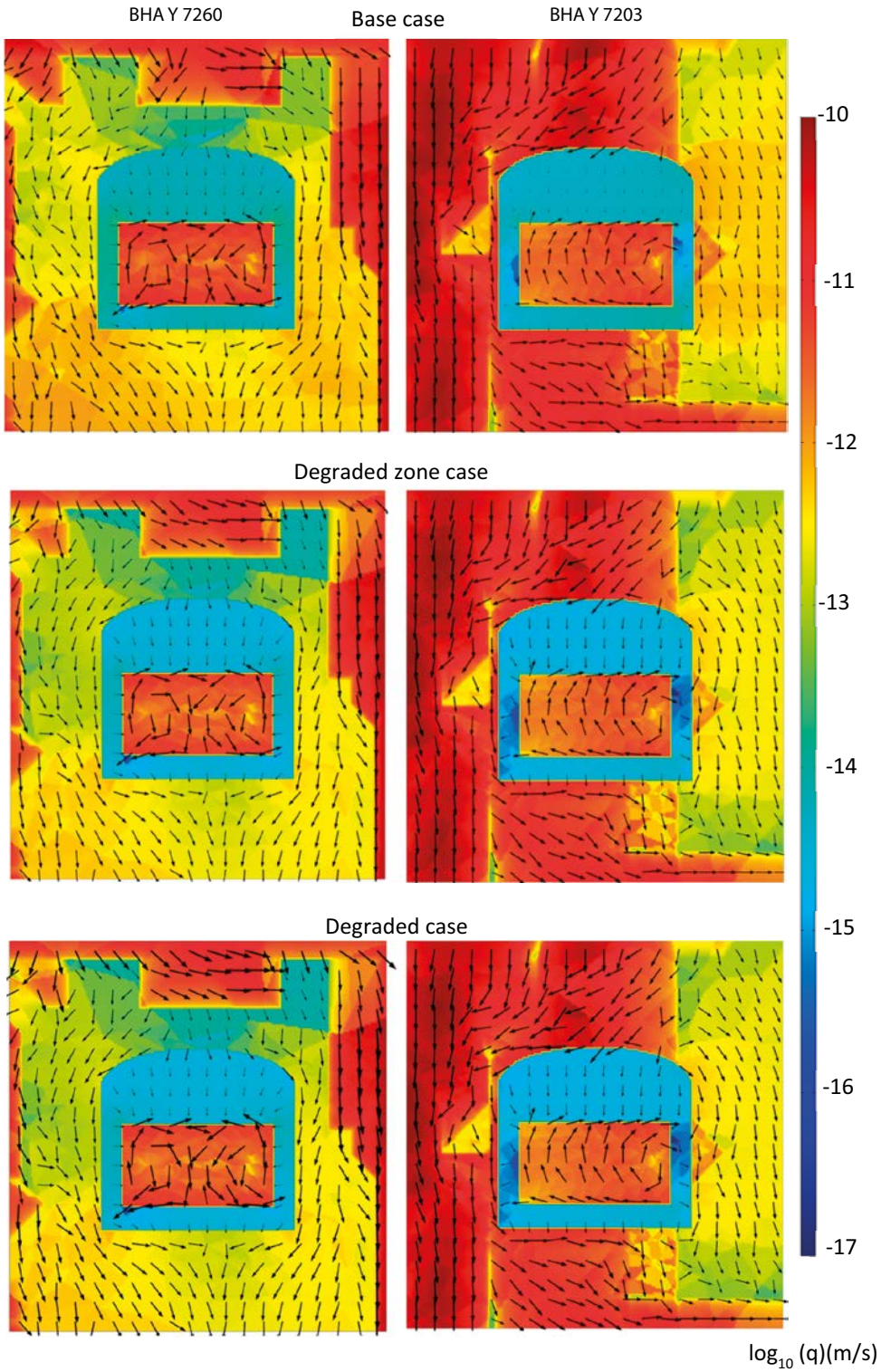

Figure 6-7. *Darcy velocity field through two cross-sections of the BHA vault. The colour scale illustrates the logarithm of the magnitude of the Darcy velocity (m/s).*

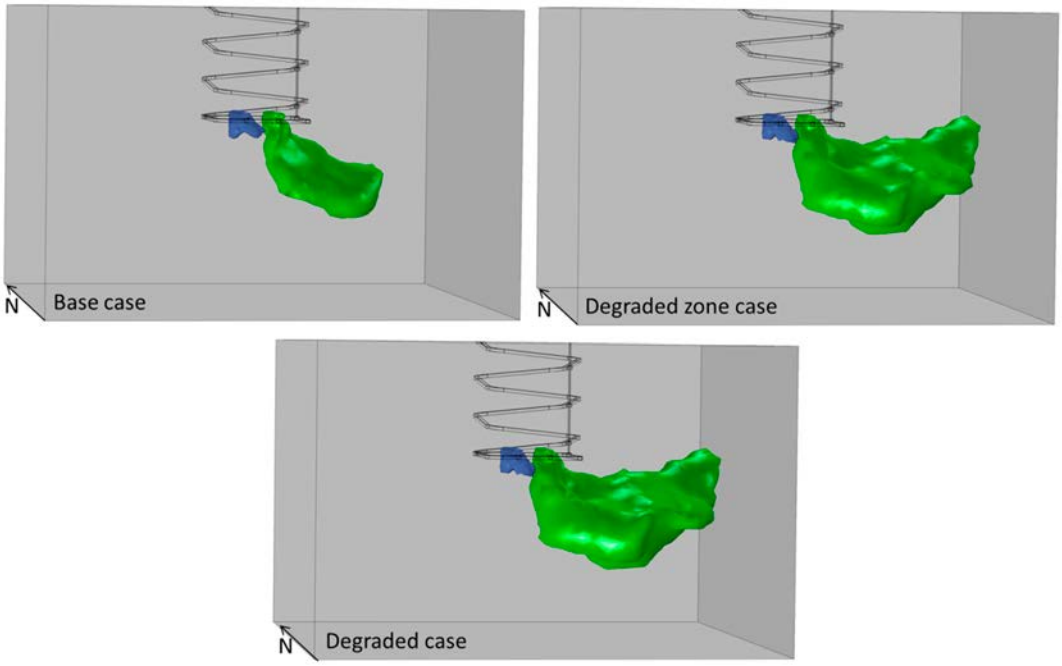

Figure 6-8. *Extension of tracer plumes illustrated by the 20 % isosurface of the released concentration (c_r) the three cases of concrete backfill degradation. The tracer plume released from the BHK vault is shown in green and the tracer plume from the BHA vault in blue.*

The inflow and the outflow areas of the BHA and BHK waste for the different degradation cases are further illustrated in Figure 6-9. The calculated streamlines illustrate the vertical downward flow towards the waste at the base case. Inflow occurs mostly at the top of the waste and the outflow at the bottom. The waste sides are both inflow and outflow areas. The streamlines reaching the BHK waste change as the BHK backfill degrades. For the degraded zone case, streamlines follow the degraded zone and inflow to the waste occurs through the waste sides. The homogenously distributed vertical flow of the base case becomes more heterogeneous for the degraded case with streamlines concentrating at the transmissive fractures.

6.3 Summary

An outer zone of degraded concrete backfill in BHK has a hydraulic cage effect. It acts as a by-pass for water redirecting water from the waste (see Figure 6-10). When the entire BHK backfill is degraded, the same permeability is assumed for the entire vault, including the waste. In this case, the vault becomes more permeable than the surrounding rock. This leads to a hydraulic connection between stochastic fractures and an increase in vault and waste flows. The effect of the BHK degradation on the groundwater flow entering the BHA vault and waste is minimal (Figure 6-10).

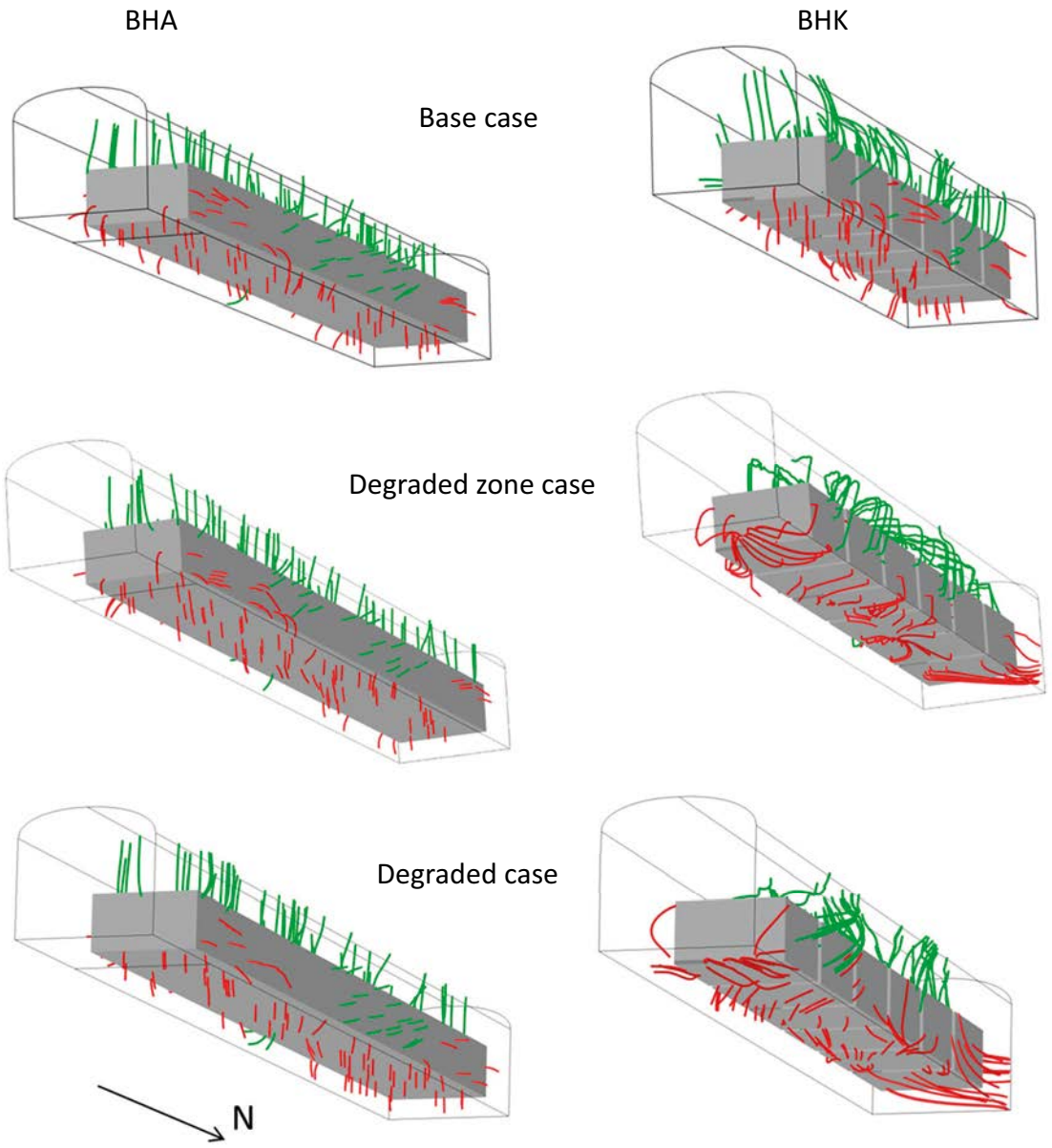

Figure 6-9. *Groundwater flow streamlines entering waste (green) and groundwater flow streamlines leaving the waste (red). The BHA vault is located at the left of the screens and the BHK vault at the right.*

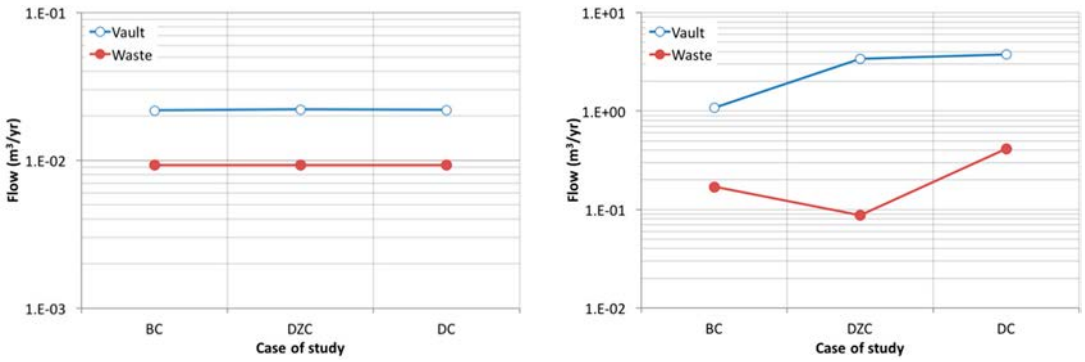

Figure 6-10. *Average flows through the BHA (left) and BHK (right) vault and waste considering different degradation states of the concrete backfill, for the Base case (BC), the Degraded zone case (DZC) and the Degraded case (DC).*

7 Transient tracer release

The release of a tracer plume leaking from the waste to the rock is analysed based on the results of two simulations of non-reactive tracer transport through the backfill and rock. These transient mass transport simulations are carried out using the repository scale model, assuming that the groundwater flow is at steady state. A fixed tracer concentration is set at the waste/backfill interface (Figure 3-12). The tracer is transported through the backfill and rock by advection, diffusion and dispersion. The total mass released from the waste and the breakthrough curve of tracer at the interface backfill/rock is computed at each vault.

Three cases with different descriptions of the BHK backfill have been considered: a base case, a degraded case and a degraded zone case. The simulation cases and the associated material properties applied to the BHK backfill are summarised in Table 3-3. The hydraulic properties of the BHA backfill remain constant over time.

The relevance of advection, diffusion and dispersion processes has been evaluated for each vault and for each concrete degradation case. Tracer release has been simulated for 2 000 years.

7.1 Base case

This simulation assumes that the concrete backfill keeps the hydraulic properties of the base case during the 2 000 years of simulation.

Figure 7-1 shows the mass of the tracer released from the waste over time. The initial mass release from the BHA is 45 g/yr. The release declines to 1.8 g/yr after 2 000 years due to the decreasing concentration gradient. The mass release from the BHK waste is substantially lower. It ranges from 1 g/yr at early times to 0.8 g/yr after 2 000 years. The difference in the waste volume and surface area between the vaults (Table 7-1) is not enough to explain the large difference between the released mass. Rather, the reason is the effective diffusion coefficient of the bentonite (Table 3-2) which is two orders of magnitude larger than that of the concrete.

Table 7-1. Surface area of the waste/backfill interface and waste volume of the SFL vaults.

	Area waste/backfill (m^2)	Waste volume (m^3)
BHA	7 100.8	18 816
BHK	6 030	12 247

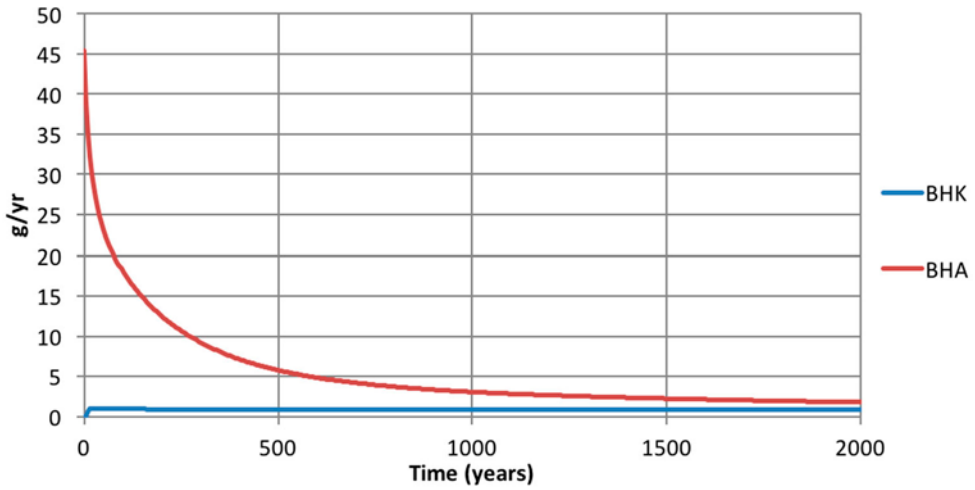

Figure 7-1. *Mass of tracer released over time from the BHA and BHK waste for the base case.*

The mass flow that reaches the rock is evaluated at the backfill/rock interface. Figure 7-2 shows the breakthrough curve at the backfill/rock interface of the tracer released from the BHA waste. The mass flow rate reaches a maximum release to the rock of 2.65 g/yr after 55 years. Then, the release decreases until reaching a rate of 0.27 g/yr after 2 000 years. The curve for the total mass flow rate overlaps with that for release by diffusion during the first 300 years. BHA is backfilled with bentonite of low permeability value ($2.0 \times 10{-}20$ m^2) resulting in low flows through the vault and waste. As a consequence, diffusion dominates the mass transport. The tracer distribution in the backfill after 2 000 simulation years illustrates the control of diffusion in the tracer transport through the bentonite backfill (Figure 7-3). The tracer concentration at the backfill/rock interface is a function of the backfill thickness. The highest tracer concentrations reach the rock through the bottom and lateral walls of the vault where the backfill is thinner. Due to the negligible role of advection, this tracer distribution does not reflect the computed streamlines leaving the waste compartments (Figure 6-9).

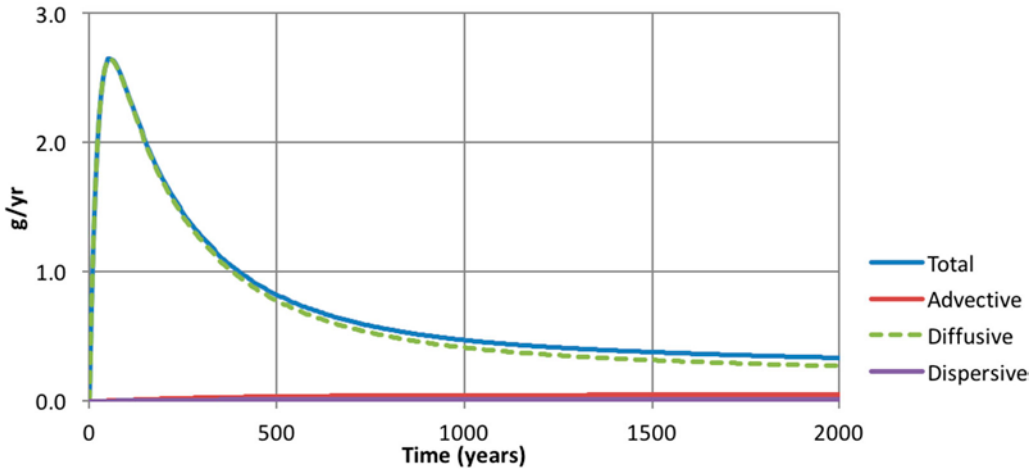

Figure 7-2. *Breakthrough curve at the backfill/rock interface of a tracer released from the BHA waste for the base case.*

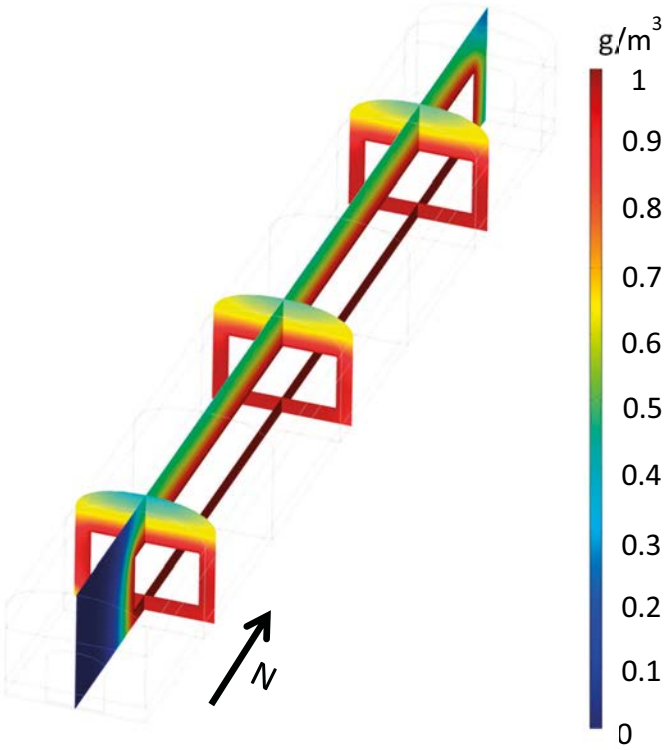

Figure 7-3. *Tracer concentration in the BHA backfill after 2 000 years for the base case.*

Figure 7-4 shows the breakthrough curve at the backfill/rock interface of a tracer released from the BHK waste. In this case, the main mass transport process is advection. This is not surprising as the permeability of the concrete backfill is assumed to be nearly four orders of magnitude higher than that of bentonite. The diffusion and dispersion contribution are one and three orders of magnitude lower than that of advection, respectively. The dispersion term depends on the Darcy velocity and the concentration gradient. In general, dispersion is the least important process. The total release is approximately 0.76 g/yr after 2 000 years.

The spatial distribution of tracer in the BHK is shown in Figure 7-5 for the different backfill degradation cases. For the base case, the main outflow areas are located at the central part of the vault. Most of the tracer exits through the bottom and the east lateral wall.

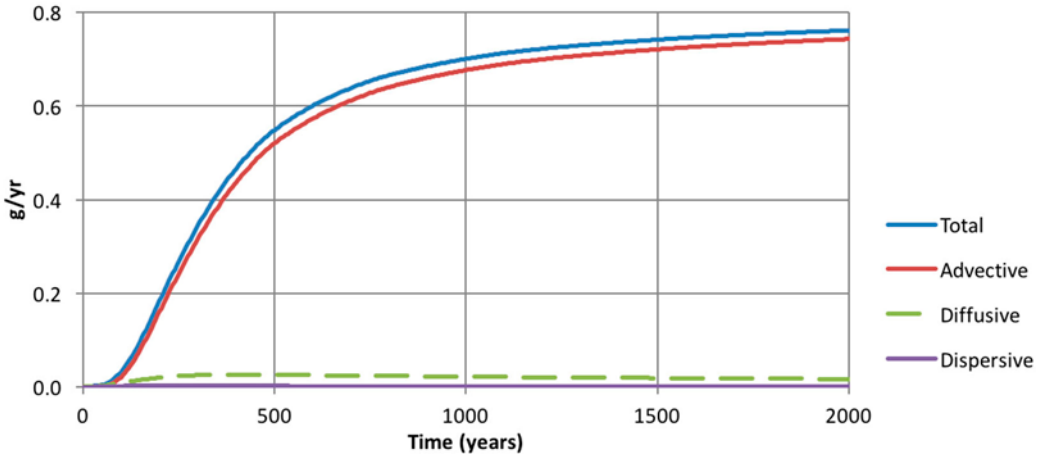

Figure 7-4. *Breakthrough curve at the backfill/rock interface of a tracer released from the BHK waste for the base case.*

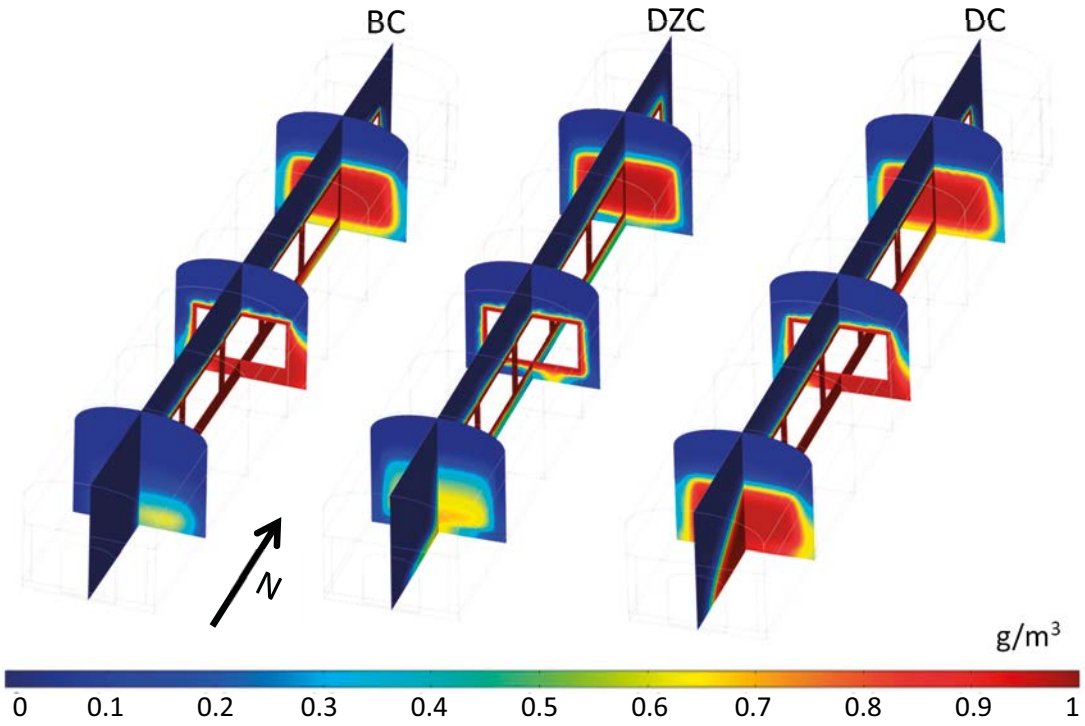

Figure 7-5. *Tracer concentration in the BHK after 2000 years, for the Base case (BC), the Degraded zone case (DZC) and the Degraded case (DC).*

7.2 Degraded zone case

This simulation assumes that the outer part of the concrete backfill in contact with the rock has been degraded. In this case, the mass release from the BHK waste is reduced with respect to the base case (Figure 7-6). The mass release reaches a maximum of 0.75 g/yr after approximately 20 years. The release then decreases with time reaching 0.46 g/yr after 2 000 years. The release from the BHA is not affected by the degradation of the BHK.

Figure 7-7 shows the breakthrough curve at the backfill/rock interface of a tracer released from the BHK waste. Advection dominates the mass transport. The dispersive component contributes 8 % to the total mass released from the BHK after 2 000 years. The diffusion term amounts to a 3 % of the total release. The contribution of diffusion is small (2 %) and comparable to the contribution for the base case.

The total mass released in the degraded zone case is lower than for the base case (Figure 7-4). This is due to the decrease in the advective term, which is consistent with the reduction of the flow through the waste in this case (Table 6-2). The increase in the groundwater flow through the degraded backfill dilutes the tracer concentration. Pathways of higher tracer concentration are observed at the bottom of the vault, revealing release areas (Figure 7-5).

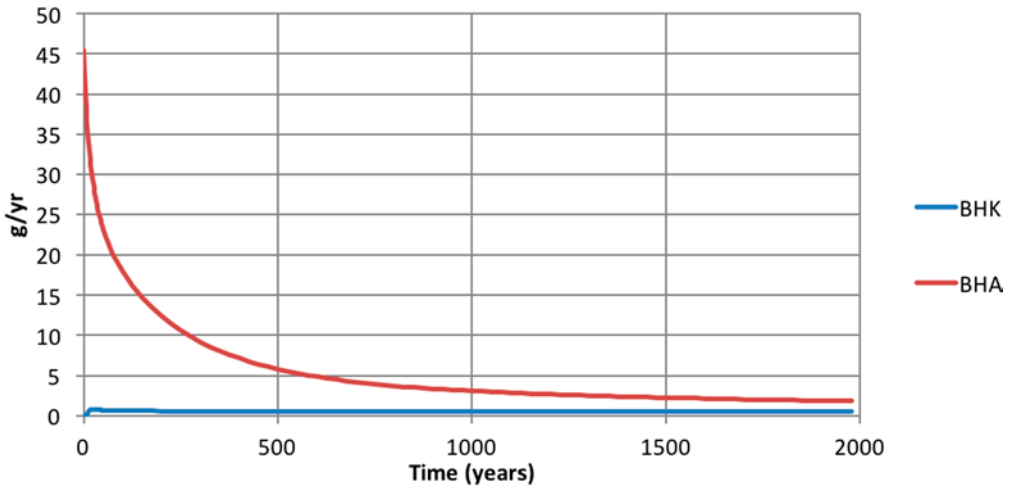

Figure 7-6. *Tracer mass released over time from the BHA and BHK waste for the degraded zone case.*

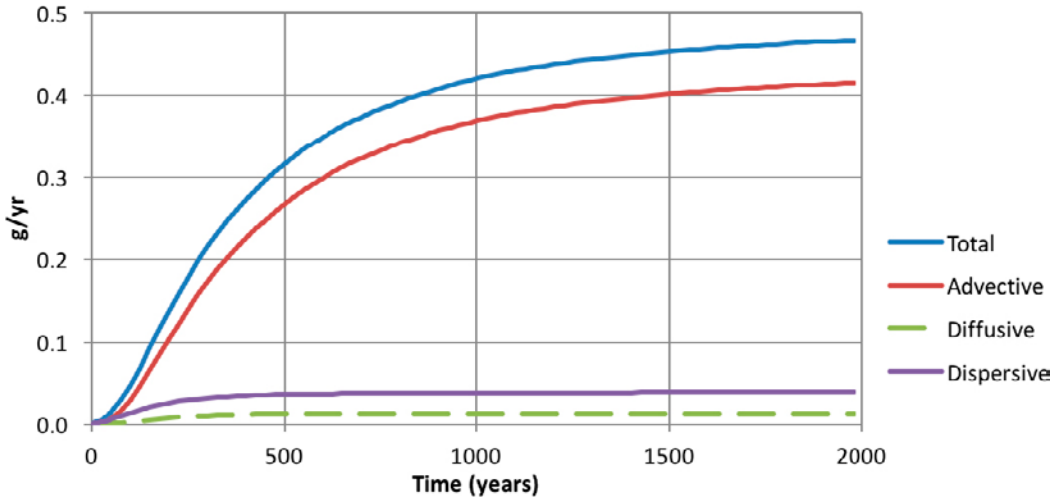

Figure 7-7. *Breakthrough curve at the backfill/rock interface of a tracer released from the BHK waste for the degraded zone case.*

The increase in the dispersive component can be explained by the combination of the flow field in the outer degraded backfill (Figure 6-4) and the tracer concentration distribution (Figure 7-5). Concentration in the inner part of the backfill is higher than in the base case and in the outer part the concentration is low. The high velocities in the degraded zone are mostly parallel to the waste/backfill interface (Figure 6-4) and the concentration gradient is perpendicular to the Darcy flow in this zone (Figure 7-5). In that configuration, transverse dispersion is an important transport mechanism.

7.3 Degraded case

The degraded case assumes that the entire BHK backfill is degraded. In this situation the mass release from waste increases compared to the base case (Figure 7-8). It reaches a maximum of 2.9 g/yr after approximately 20 years and then decreases to 2.10 g/yr after 2 000 years. The release from the BHA is not affected by the BHK degradation. The degraded case yields very similar mass releases from the BHA and BHK vaults after 1 500 years.

Advection dominates the release of mass from BHK (Figure 7-9). Dispersion and diffusion play a minor role and outflow rates are one order of magnitude lower than for advection. The calculated concentrations in the vault are the lowest of all the calculation cases (Figure 7-5). The tracer distribution resembles that of the bease case. However, the increase in groundwater flow though the degraded backfill increases the tracer concentration in the downstream backfill area (Figure 7-5).

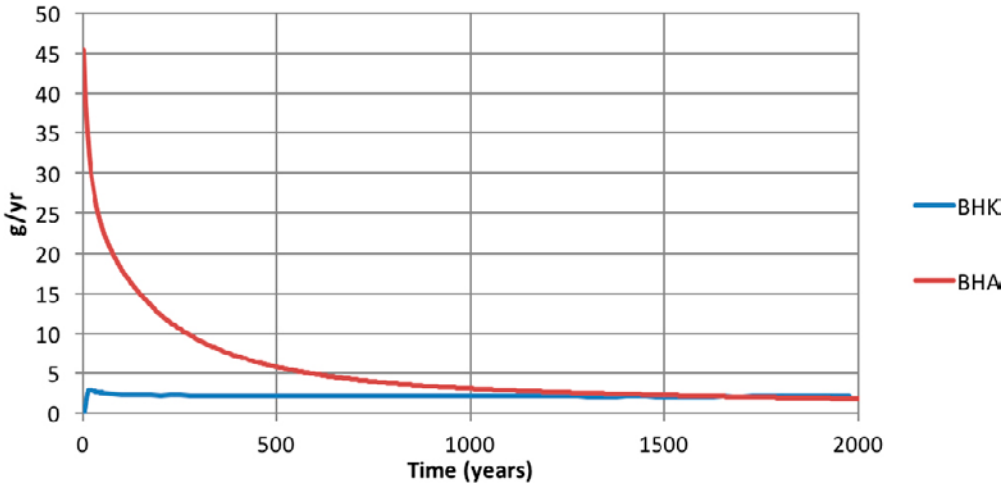

Figure 7-8. *Tracer mass released over time from the BHA and BHK waste for the degraded case.*

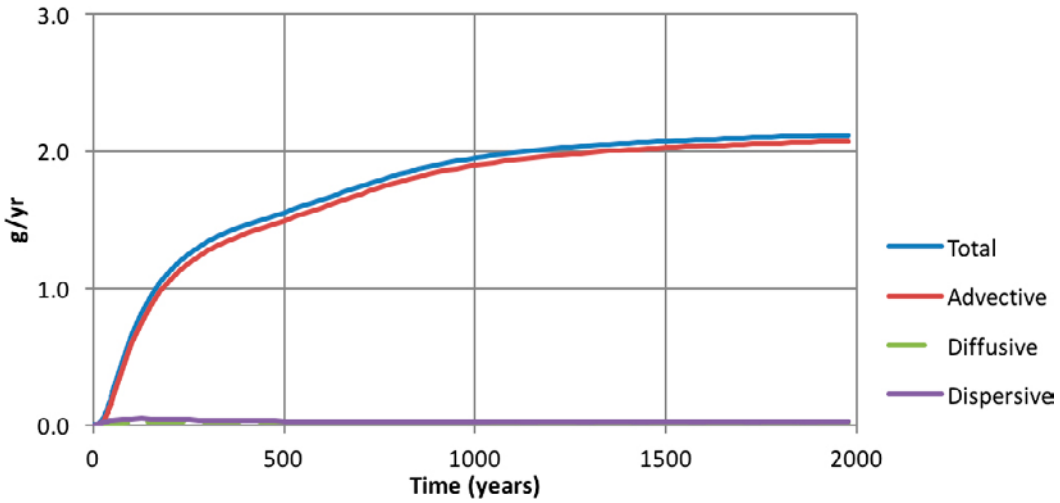

Figure 7-9. *Breakthrough curve at the backfill/rock interface of a tracer released from the BHK waste for the degraded case.*

7.4 Summary

Advection is the main transport process governing the mass transport through the BHK backfill. The maximum release from the waste is a function of the amount of water crossing the waste control volumes (Figure 7-10). The lowest mass release is calculated for the degraded zone case and the highest release for the completely degraded bakfill. Figure 7-11 shows the total mass outflow rates to the rock for the three degradation states of the BHK backfill. The breakthough curves reach a maximum release rate equal to the mass released from the waste after 1 500 years for the degraded zone case and the degraded case. In these cases, the mass transport has reached steady state and the backfill material does not have capacity to store more tracer. For the base case however, the mass released to the rock is 95 % of the mass released from the waste after 2 000 years for the base case and the system is still approaching steady state.

The transport through the BHA backfill is dominated by diffusion and remains the same regardless of the BHK backfill degradation state.

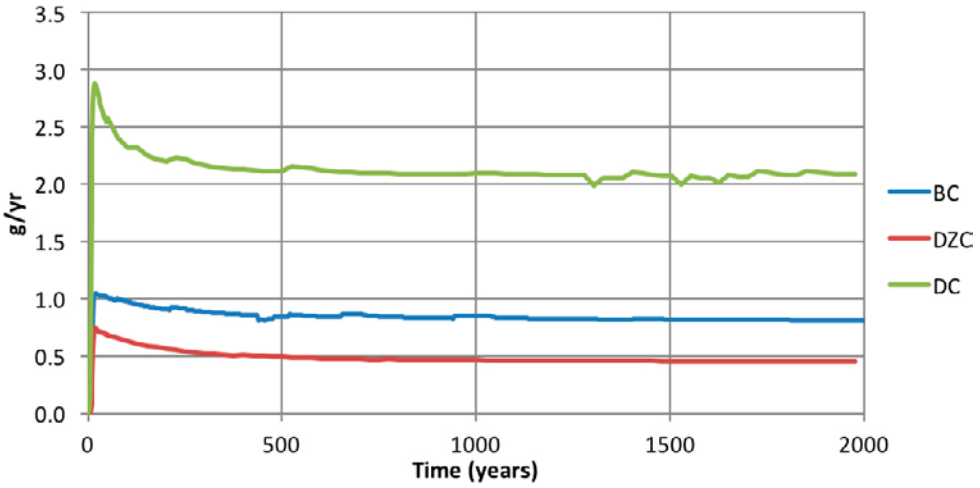

Figure 7-10. *Mass outflow release from the BHK waste for the three concrete backfill degradation cases, the Base case (BC), the Degraded zone case (DZC) and the Degraded case (DC).*

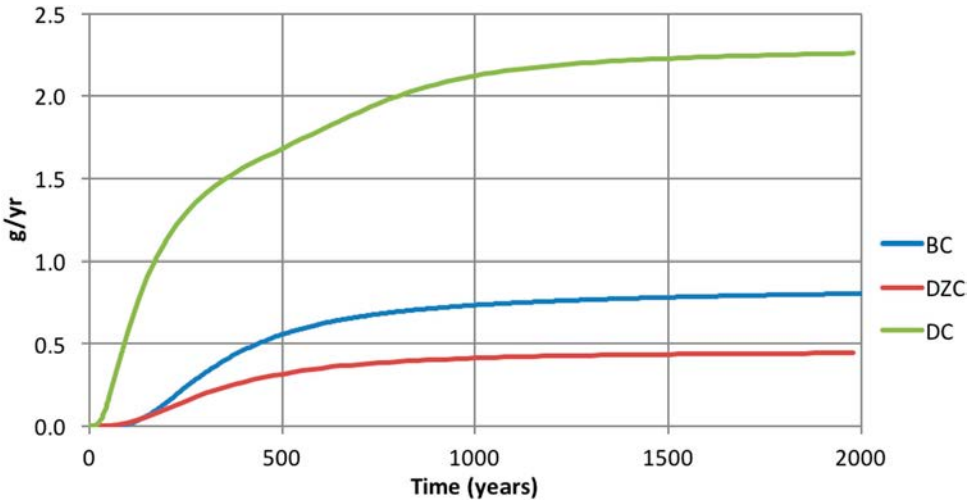

Figure 7-11. *Total mass outflow to the rock from the BHK for the three concrete backfill degradation cases, the Base case (BC), the Degraded zone case (DZC) and the Degraded case (DC).*

8 Groundwater saturation of the SFL vaults

This chapter describes simulations performed to determine the time required to saturate the SFL vaults. These simulations belong to the simulation block 4 described in Chapter 2 (Figure 2-1).

8.1 Model equations

Richards' equation describes flow in a variably saturated porous medium accounting for changes in hydraulic properties with water saturation. The pore space not filled with liquid is assumed to hold a stationary gas phase (air) at atmospheric pressure. The Richards' equation modelling interface of COMSOL Multiphysics (COMSOL 2015) has been used to set up and solve the following equation:

$$\rho\left(\frac{C_m}{\rho g}+S_eS\right)\frac{\partial p}{\partial t}+\nabla\cdot\rho\left(-\frac{\boldsymbol{\kappa_s}}{\mu}k_r(\nabla p+\rho g\nabla E)\right)=Q_m$$

Above, p is the pressure (Pa), C_m represents the specific moisture capacity, S_e denotes the effective saturation (-), S is the storage coefficient (-), $\boldsymbol{\kappa}_s$ is the permeability tensor (m^2), μ is the fluid dynamic viscosity (Pa·s), k_r denotes the relative permeability (-), ρ is the fluid density (kg/m^3), g is the acceleration of gravity (9.81 m/s^2), E represents the elevation (m), and Q_m is a fluid source/sink term.

The Darcy flow is given by:

$$\mathbf{u}=-\frac{\boldsymbol{\kappa_s}}{\mu}k_r(\nabla p+\rho g\nabla E)$$

where **u** is the flux vector (m/s). The storage coefficient (S) is expressed by:

$$S=\theta_sX_f+(1-\theta_s)X_P$$

where X_f is the fluid compressibility (4×10^{-10} Pa^{-1}) and X_p (Pa^{-1}) is the effective compressibility of the matrix.

The van Genuchten retention model has been used (van Genuchten 1980). The analytic expressions of this model require data for the saturated water content θ_s, the residual water content θ_r, the fluid volume fractions, as well as the constants α, n, m and l that are specific to the porous medium. The van Genuchten equations define the saturation at atmospheric fluid pressures ($H_p = 0$).

$$\theta=\begin{cases}\theta_r+S_e(\theta_s-\theta_r) & H_p<0\\ \theta_s & 0\le H_p\end{cases}$$

$$S_e=\begin{cases}\dfrac{1}{[1+|\alpha H_p|^n]^m} & H_p<0\\ 1 & 0\le H_p\end{cases}$$

$$C_m=\begin{cases}\dfrac{\alpha m}{1-m}(\theta_s-\theta_r)S_e^{\frac{1}{m}}\left(1-S_e^{\frac{1}{m}}\right)^m & H_p<0\\ 0 & 0\le H_p\end{cases}$$

Above, the constitutive parameter m is equal to $1-(1/n)$. The volume of liquid per porous medium volume is θ and ranges from a small residual value θ_r to the total porosity θ_s. S_e is the effective saturation, that is, the water content divided by the porosity. C_m is the specific moisture capacity.

The dependence of the relative permeability on the degree of saturation has been calculated with a cubic exponential law (Åkesson et al. 2010, Liu et al. 2013, Villar et al. 2012, Pintado et al. 2001, Saaltink et al. 2005):

$$k_r=\begin{cases}{S_e}^3 & H_p<0\\ 1 & 0\le H_p\end{cases}$$

8.2 Model description

Individual vault scale models for BHA and BHK have been set up. These models encompass the waste and backfill materials. The reduced model domains allow for more refined finite element meshes beneficial when solving this non-linear process. The vault scale models have been used to simulate the water saturation after repository closure. The flow boundary conditions of the vault scale models are based on the results from the saturated density-dependent flow simulation performed with the repository scale model. The actual system should have properties somewhere in between fully saturated and an open repository system (Börgesson et al. 2015). Here only properties from a fully saturated model have been used. Therefore, only one end of the spectrum has been evaluated.

8.3 Mesh discretisation

The mesh of the BHA vault consists of 603217 tetrahedral elements and the mesh of the BHK vault 898161 has tetrahedral elements.

8.4 Initial and boundary conditions

The initial degree of saturation is assumed to be 0.70 for the concrete backfill and waste domains (Höglund 2014) and 0.61 for the bentonite backfill (SKB 2006). The initial pressure head, $H_{p,}$ is calculated according to the van Genuchten expression for the parameters in Table 8-1 and the initial saturation of each material. The calculated initial pressure heads are −2 152.25 m and −2 369.25 m for the concrete and bentonite domains, respectively.

A commonly used boundary condition for unsaturated flow is to prescribe a saturated pressure. However, this boundary condition has several drawbacks. First the nodes at this interface are saturated initially. Furthermore, the thickness of the initially saturated periphery depends on the mesh. The resulting large pressure gradient between the boundary and the inner domain leads unrealistically large inflow of water during the first time steps of the simulation. This can in turn lead to saturation artefacts and affect the estimation of the saturation time.

For these reasons, a mixed-type (Cauchy) boundary condition is implemented at the backfill/rock interface. This boundary condition specifies that the mass flow (q_b) through that boundary is proportional to the pressure difference between the calculated pressure (p) and a prescribed external pressure (p'). The external pressure at the boundaries is taken from the repository scale model that assumes closed conditions (Figure 2-1).

$$q_b = \alpha \Delta p = \alpha(p' - p)$$

Above, q_b is the mass flow (kg/m^3/s), p is the dependent pressure variable (Pa) of the unsaturated problem and *p' is* the external pressure (Pa) at the backfill/rock boundary. The external pressure is obtained from the pressure field calculated with the repository scale model under saturated conditions (the base case described in Chapter 5). By doing so, it is assumed that the rock around the vault is fully saturated.

The physical meaning of the proportionality coefficient, α, can be understood from the form of the Darcy flow, u.

$$q_b = \rho \mathrm{u} = \rho \frac{k_x}{\mu}\frac{\Delta p}{L} = \rho \frac{k_x}{\mu}\frac{\Delta p}{L} = \frac{\overbrace{\rho}^{\beta}}{\mu L} k_x (p' - p) = \overbrace{\beta k_x}^{\alpha} (p' - p)$$

α is proportional to k_x which is the permeability of the rock at the backfill/rock boundaries (m^2). Hence, boundary fluxes will have higher values in areas where the vault intersects with stochastic features. The parameter β (s/m^3) is a leakage coefficient or conductance. By changing the value of the conductance β, the Cauchy boundary condition can cover the range between a prescribed pressure boundary condition ($\beta=\infty$) and a no flow boundary condition ($\beta=0$).

The maximum flow towards the vault will always be limited by the groundwater flowing through the rock domain. Therefore, a set of preliminary simulations were carried out to constrain the values of β that yield realistic groundwater flows from the rock to the vaults. The average Darcy velocity in the rock domain (Figure 8-1) shows a vertical variability ranging from 3.5×10^{-11} to 2.8×10^{-13} m/s. A realistic boundary condition should generate inflow values within that range.

Nine values of β between 0.1 and 2 000 were tested. The average flow that enters the model domain at the first calculation step grows linearly with β for the analysed range of β values (Figure 8-2). The rock flow is bounded by values of β between 2 and 200. Therefore, three values of β (2, 20 and 200) have been selected to estimate the saturation time. At the first time step they give the maximum, the average and the minimum Darcy velocities observed in the rock, respectively.

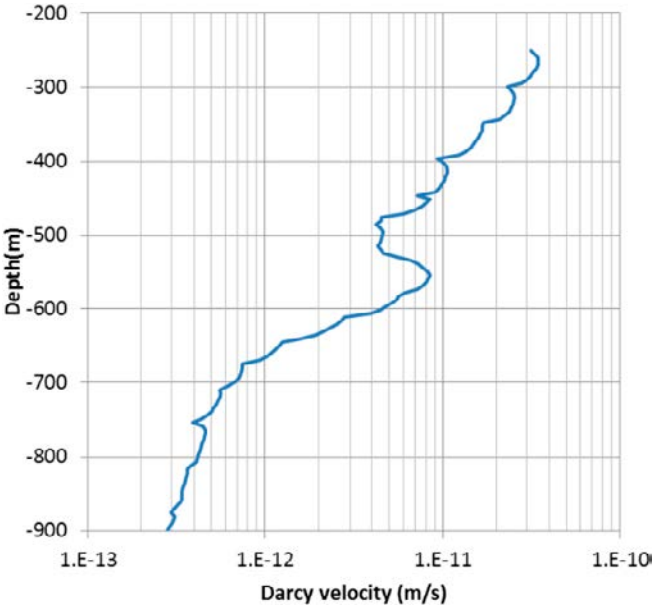

Figure 8-1. *Average value of Darcy velocity in the rock vs depth.*

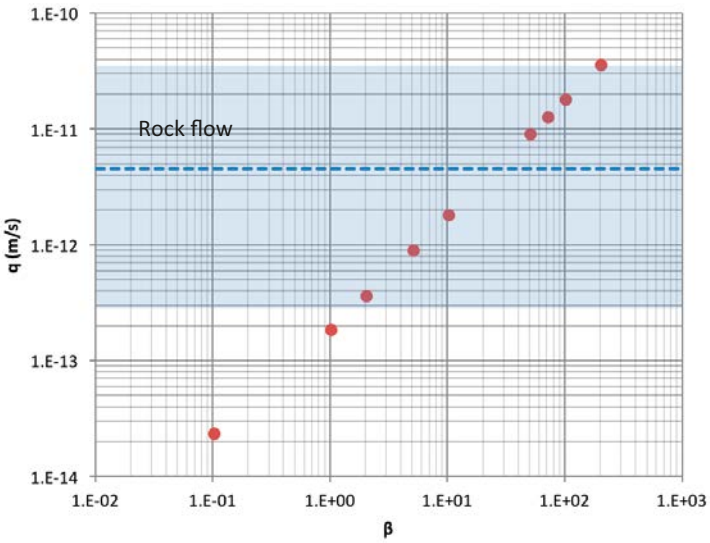

Figure 8-2. *Darcy flow entering the BHA vault at the first calculation time for different β values (s/m^3). The blue area delimits the range of Darcy flow in the rock domain. The dashed blue line shows the average Darcy flow in the rock at repository depth.*

8.5 Unsaturated parameters for concrete and bentonite

The saturated parameters for the base case (Table 3-2) are used for the simulations. The unsaturated parameters for bentonite and concrete are presented in Table 8-1 and the resulting van Genuchten retention curves are shown in Figure 8-3. The unsaturated properties of concrete are assumed for the waste domain.

Table 8-1. Bentonite and concrete unsaturated parameters.

Parameters	Bentonite	Reference	Concrete	Reference
α (m^{-1})	2.84E-03	Åkesson et al. 2010	5.26E-04	Baroghel-Bouny et al. 1999
n	1.25	Åkesson et al. 2010	1.784437	Baroghel-Bouny et al. 1999
m	0.20	Åkesson et al. 2010	0.44	Baroghel-Bouny et al. 1999
l	0.50	Åkesson et al. 2010	0.50	Baroghel-Bouny et al. 1999
X_p (Pa^{-1})	3.58E-09	Senger et al. 2008	9.00E-11	Bager 2013

The relative permeability function does not depend on the material properties but on the cube of the effective saturation (Figure 8-4).

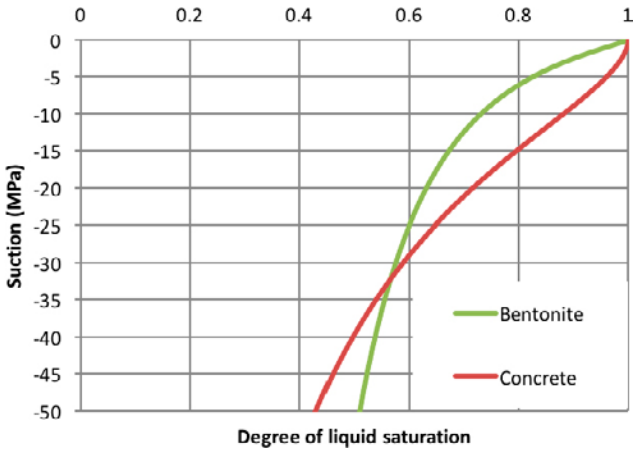

Figure 8-3. *Retention curves for bentonite and concrete.*

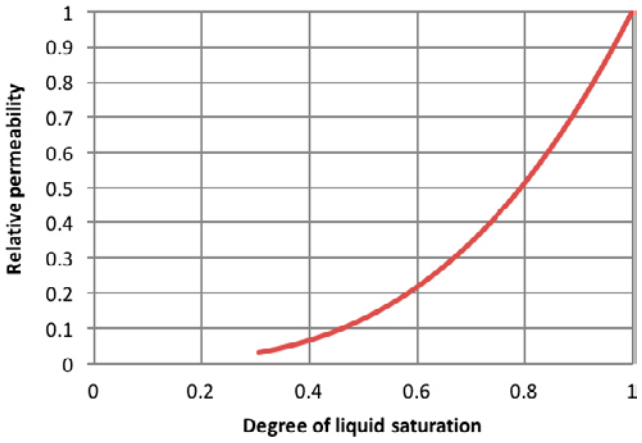

Figure 8-4. *Relative permeability as a function of the effective saturation ($Kr = Se^3$).*

8.6 Results

The time evolution of the average saturation in BHA is presented in Figure 8-5. The bentonite backfill has an initial degree of saturation of 61 % and the waste domain an initial degree of saturation of 70 %. The saturation time depends on the value of the conductance β and ranges between 1 600 and 15 000 years. The highest conductance (β = 200) leads to a higher flow from the rock to the vault and decreases the time to reach full saturation.

The distribution of saturation before full saturation is shown in Figure 8-6. Results show that most of the water enters the vault through areas in contact with stochastic features. Inflow areas are located at the intersection with stochastic features ST8, ST5 and ST3 (see Figure 3-8). Inflow at the vault floor are related to stochastic features ST13, ST14 (Figure 3-9) and ST8 (Figure 3-8). The loading area, completely filled with bentonite, takes the longest time to saturate. Waste saturation is faster than bentonite saturation (Figure 8-6) due to the lower porosity of the waste.

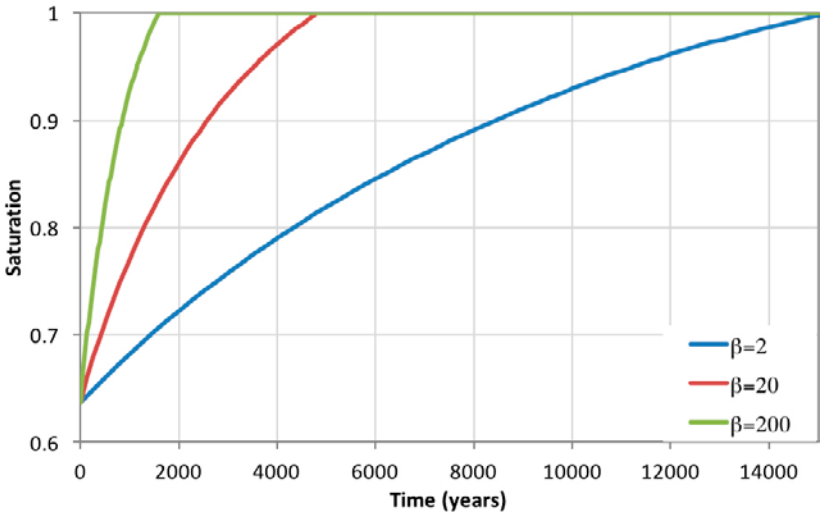

Figure 8-5. *Temporal evolution of the volume averaged effective saturation in the BHA for β = 2, 20 and 200.*

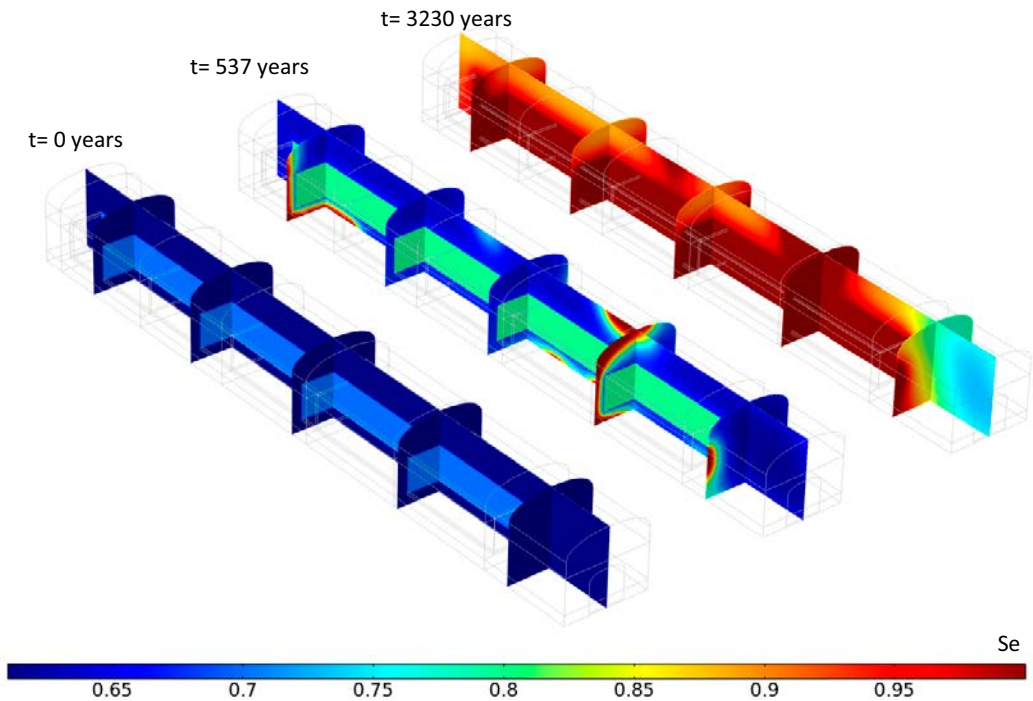

Figure 8-6. *Initial saturation in the BHA vault and saturation distribution at t = 537 and 3 230 years for β = 20 s/m³.*

The BHK vault has a concrete backfill and grouted waste domain, both with an initial saturation of 0.7. The time evolution of the averaged saturation in BHK is shown in Figure 8-7. Saturation times are 2, 13 and 122 years for β values equal to 200, 20 and 2, respectively.

The saturation distribution within the BHK (Figure 8-8) illustrates how groundwater enters the BHK from the south-east where the vault intersects with stochastic feature ST10 (see Figure 3-8).

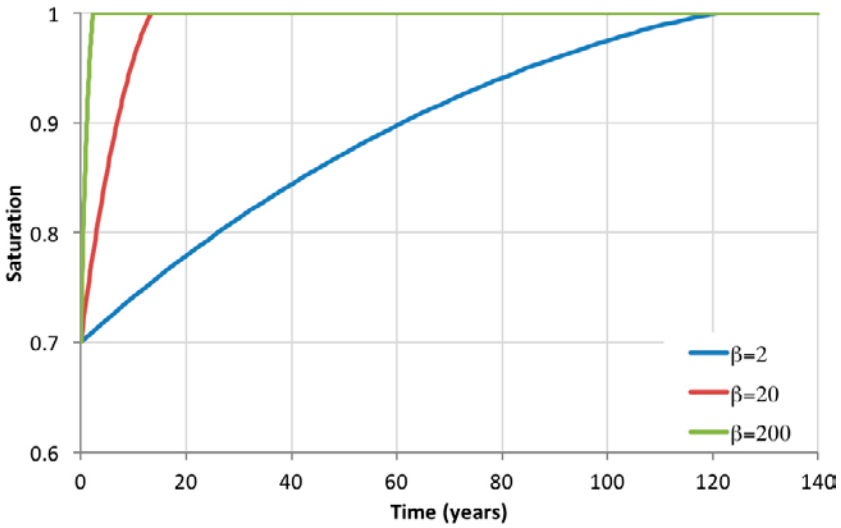

Figure 8-7. *Temporal evolution of the volume averaged effective saturation at the BHK for β = 2, 20 and 200.*

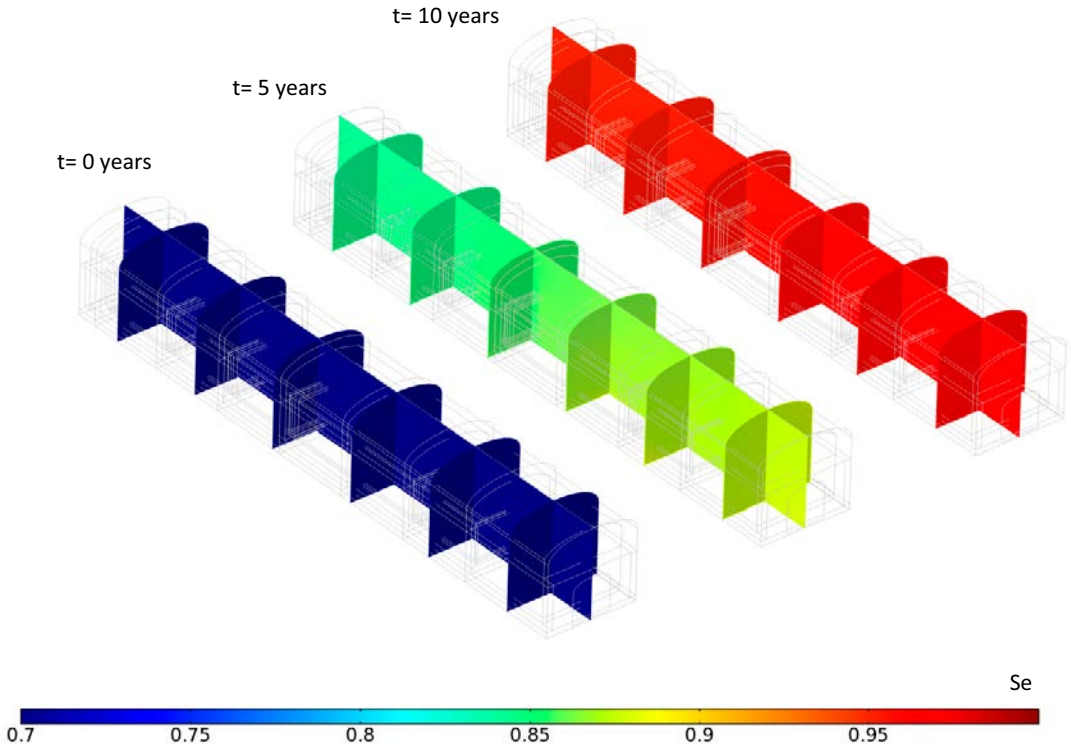

Figure 8-8. *Initial saturation in the BHK vault and saturation distribution at t = 5 and 10 years for β = 20 s/m³.*

8.7 Summary

The results of the simulations show that the saturation time for the BHA and BHK vaults differ about three orders of magnitude independently of the conductance value (Figure 8-9). This single parameter holds the uncertainty of the rock behaviour under unsaturated conditions. The results indicate that the depth of the rock unsaturated fringe, L, is critical to accurately compute the saturation time.

The BHA vault takes significantly longer than the BHK vault to become saturated (Figure 8-9 and Table 8-2). This is explained by the lower permeability of bentonite backfill compared to the concrete backfill. The permeability of the concrete backfill is higher than the permeability of the surrounding rock and similar to the permeability of the stochastic features that intersect the vault leading to a relatively fast saturation of the vault.

Table 8-2. Saturation time for BHK and BHA for different conductance values.

Conductance (β)	BHK saturation time (years)	BHA saturation time (years)
2	122	15 166
20	13.5	4 810
200	2.4	1 586

The presented estimates of saturation times can be related to previous investigations, concerning other repositories. Börgesson et al. (2015) modelled the saturation process of the Silo in SFR, assuming two different host rock representations. A multicomponent multiphase formulation implemented in the software Code_Bright (UPC 2003) was used for the simulations. The calculated time until full saturation of the EBS was between 13 and 53 years depending on modelling assumptions. This range is in agreement with the Silo saturation time of approximately 20 years found by Holmén and Stigsson (2001). These authors also estimated the saturation time for repository sections based on concrete barriers in the SFR. The saturation times for the BTF and BMA vaults were found to be less than a few years.

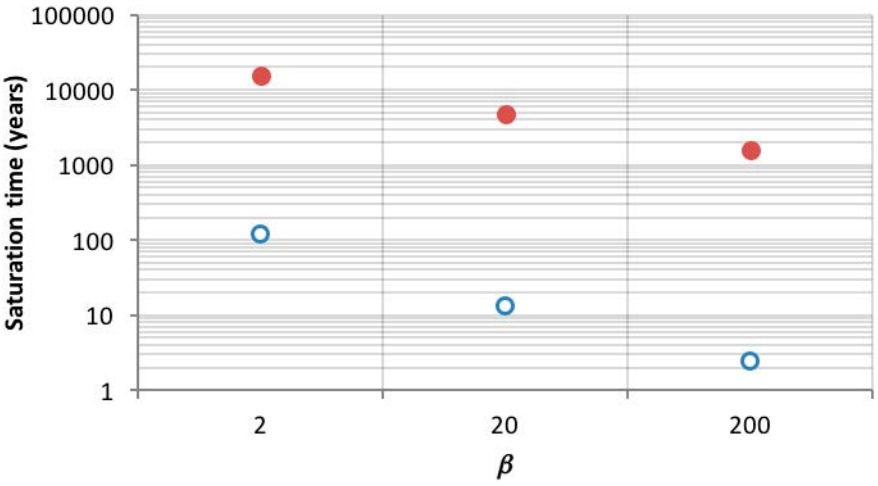

Figure 8-9. *Saturation time variation with the conductance β for the BHK (blue circles) and BHA (red circles).*

The limitations of the present numerical analysis lay in the uncertainty in the water pressure in the host rock around the vaults. The model is carried out in a vault scale model. Therefore, representative boundary conditions from a larger scale model are needed. In this case, the external pressure is obtained from a fully saturated model. The real system should have properties somewhere in between fully saturated and an open repository system (Börgesson et al. 2015). Here only boundary conditions from a fully saturated model have been used. Therefore, only one end of the spectrum has been evaluated.

A conductance parameter is introduced in the flow boundary condition to analyse the effect of the uncertainty in the host rock behaviour in unsaturated flow conditions. The rock is assumed to be fully saturated at a distance L from the vault. The conductance is inversely proportional to the depth of the host rock unsaturated fringe. A very large conductance represents the case of fully saturated rock and a low conductance implies a larger penetration depth of the unsaturated fringe (L).

The large span of estimated saturation times indicates that the depth of the rock unsaturated fringe, L, is critical to accurately compute the saturation time. Measuring the penetration of the unsaturated fringe around the tunnel before closure will help constrain the value of the conductance. Measured flow towards the tunnel after construction could also be used to calibrate the conductance value.

References

SKB's (Svensk Kärnbränslehantering AB) publications can be found at www.skb.com/publications.

Abarca E, Sampietro D, Miret M, von Schenck H, 2016. Initial modelling of the near-field hydrogeology. Exploring the influence of host rock characteristics and barrier properties. Report for the safety evaluation SE-SFL. SKB R-16-02, Svensk Kärnbränslehantering AB.

Amec Foster Wheeler, 2015. ConnectFlow version 11.2. Harwell, UK: Amec Foster Wheeler Nuclear UK Limited.

Bager D H, 2013. A study of consequences of freezing of concrete structures for storage of nuclear waste due to permafrost. SKB TR-12-13, Svensk Kärnbränslehantering AB.

Baroghel-Bouny V, Mainguy M, Lassabatere T, Coussy O, 1999. Characterization and identification of equilibrium and transfer moisture properties for ordinary and high-performance cementitious materials. Cement and Concrete Research 29, 1225–1238.

Bear J, 1972. Dynamics of fluids in porous media. New York: Dover.

Börgesson L, Åkesson M, Kristensson O, Malmberg D, Birgersson M, 2015. Modelling of critical H-M processes in the engineered barriers of SFR. SKB TR-14-27, Svensk Kärnbränslehantering AB.

COMSOL, 2015. COMSOL Multiphysics, version 5.1. Stockholm: COSMSOL AB.

Elfwing M, Evins L Z, Gontier M, Grahm P, Mårtensson P, Tunbrant S, 2013. SFL concept study. Main report. SKB TR-13-14, Svensk Kärnbränslehantering AB.

Gelhar L W, Axness C L, 1983. Three-dimensional stochastic analysis of macrodispersion in aquifers. Water Resources Research 19, 161–180.

Gelhar L W, Welty C, Rehfeldt K R, 1992. A critical review of data on field-scale dispersion in aquifers. Water Resources Research 28, 1955–1974.

Holmén J G, Stigsson M, 2001. Modelling of future hydrogeological conditions at SFR. SKB R-01-02, Svensk Kärnbränslehantering AB.

Höglund L O, 2014. The impact of concrete degradation on the BMA barrier functions. SKB R-13-40, Svensk Kärnbränslehantering AB.

Joyce S, Appleyard P, Hartley L, Tsitsopoulos V, Woollard H, Marsic N, Sidborn M, Crawford J, 2019. Groundwater flow and reactive transport modelling of temperate conditions. Report for the safety evaluation SE-SFL. SKB R-19-02, Svensk Kärnbränslehantering AB.

Liu Y, Wang J, Cao S, Chen L, 2013. Comparison of CODE-BRIGH and LAGAMINE for THM modeling. Long-term Performance of Engineered Barrier Systems (PEBS). Deliverable (D-N°:DB-WP3), European Commission.

Pintado X, Ledesma A, Lloret A, 2001. Backanalysis of thermos-hydraulic bentonite properties from laboratory tests. Engineering Geology 64, 91–115.

Saaltink M W, Ayora C, Olivella S, 2005. User's guide for RetrasoCodeBright (RCB). Department of Geotechnical Engineering and Geo-Sciences, Technical University of Catalonia (UPC), Barcelona, Spain.

Senger R, Lanyon B, Marschall P, Vomvoris S, Fujiwara A, 2008. Numerical modeling of the gas migration test at the Grimsel Test Site (Switzerland). Nuclear Technology 164, 155–168.

SKB, 2001. Project SAFE. Compilation of data for radionuclide transport analysis. SKB R-01-14, Svensk Kärnbränslehantering AB.

SKB, 2006. Long-term safety for KBS-3 repositories at Forsmark and Laxemar – a first evaluation. Main report of the SR-Can project. SKB TR-06-09, Svensk Kärnbränslehantering AB.

SKB, 2010. Data report for the safety assessment SR-Site. SKB TR-10-52, Svensk Kärnbränslehantering AB.

SKB, 2011. Site selection – siting of the final repository for spent nuclear fuel. SKB R-11-07, Svensk Kärnbränslehantering AB.

SKB, 2014. Data report for the safety assessment SR-PSU. SKB TR-14-10, Svensk Kärnbränslehantering AB.

UPC, 2003. CODE_BRIGHT: A 3D program for thermohydro-mechanical analysis in geological media. User's guide. Available at: https://deca.upc.edu/en/projects/code_bright/downloads/users_guide/view

van Genuchten M, 1980. A closed form equation for predicting the hydraulic conductivity of unsaturated soils. Soil Science Society of America Journal 44, 892–898.

Villar M V, Martín P L, Bárcena I, García-Siñeriz J L, Gómez-Espina R, Lloret A, 2012. Long-term experimental evidences of saturation of compacted bentonite under repository conditions. Engineering Geology 149–150, 57–69.

Åkesson M, Börgesson L, Kristensson O, 2010. SR-Site Data report. THM modelling of buffer, backfill and other system components. SKB TR-10-44, Svensk Kärnbränslehantering AB.

Appendix A

Consistent coupling of regional and near-field flow models

Introduction

The near-field groundwater flow model is fed by a regional groundwater flow model (Joyce et al. 2019) that is set up and solved with the ConnectFlow software (Amec Foster Wheeler 2015). The regional flow model supplies the repository scale model with pressure and density boundary conditions, initial conditions, and hydraulic properties of the bedrock (anisotropic permeability tensor and porosity). A benchmark exercise is presented here to illustrate that the models have been consistently coupled.

Interface ConnectFlow-COMSOL

VAL file

ConnectFlow generates an output file with extension VAL. In a VAL file, the nodal information of a computed simulation is provided. In this case the file used is named:

sfl_elaborated_r1_hrd_r0_hcd_regional_evolution_gflinear_amg_post_2000.val

The file contains the following variables:

Point_ID, x_coord, y_coord, z_coord, Pressure, Temperature, AL, Br, C, CA, Cl, F, Fe, K, Li, Mg, Mn, Na, S, Si, Sr, H, O, E, pH, pe, rho, mu, Q_darcy, kxx, kyy, kzz, phi.

Python script

A Python script was created to read the VAL file, filter the data, translate the system of coordinates to the local reference system of the COMSOL model and to write a text file readable by COMSOL:

1. **Coordinates translation**. The nodal coordinates in the VAL file are given in the reference system RT90. The COMSOL model was built in a local reference system. The following translation is applied to translate the coordinates in the RT90 system to the local COMSOL system.

   $X = X_{RT90} - X_0$
   $Y = Y_{RT90} - Y_0$
   where $X_0 = 1539000$ and $Y_0 = 6360000$

2. **Data filtering.** The VAL file contains data of a much larger domain. The Python script filters the data by coordinates. A box filter retrieves the values of the point data enclosed in a block domain which contains the near-field, specified by three corner points. The corner points used for filtering are:

   $X_{min} = 7175$ $X_{max} = 11725$
   $Y_{min} = 5625$ $Y_{max} = 8125$
   $Z_{min} = -1000$ $Z_{max} = -25$

3. **Writing a text file.** The script writes the necessary information for the repository-scale model into a text file. The coordinates are written in the COMSOL local reference system. This text file contains a header and N rows with point data with the following variables:

   x_coord, y_coord, z_coord, Pressure, Cl, rho, Q_darcy, kxx, kyy, kzz, phi

COMSOL file

The text files can be imported directly in a COMSOL file to be used later as interpolation function fields. A linear interpolation method is used to interpolate the variables into the finite element mesh in COMSOL. The interpolated function can then be used as material properties or boundary conditions in COMSOL.

Test of the consistent coupling

A COMSOL model is generated for a rock domain with no repository. The model contains an inner box at the repository location. That inner box does not have different material properties. It is used for meshing purposes to refine the mesh in this area, consistently with the ConnectFlow model, and as a post-processing domain to compute fluxes in and out of the box. This model has the same geometry as the ConnectFlow model that generated the VAL file.

The model domain is discretised in COMSOL in a finite element mesh of 1631679 tetrahedral elements. 976970 of these tetrahedral elements are located in the inner refined box.

The text file generated by the python script using the VAL file is imported in the COMSOL file and interpolated over the model mesh.

The rock permeability values from the text file (kxx, kyy, kzz) are used to define the anisotropic rock permeability field in the COMSOL model. Figure A-1 shows the comparison between the ConnectFlow permeability field imported into COMSOL and interpolated over the COMSOL mesh and the actual permeability field in ConnectFlow.

A density dependent flow model is generated in COMSOL. The dependent variable for the flow equation is the total pressure. The dependent variable for the transport equation is chloride mass fraction. Fluid density is computed as a function of the chloride mass fraction as explained in Section 3.3.1. The residual pressure and chloride mass fraction values from the text file are used to define the initial and boundary conditions. The total pressure is calculated as described in Section 3.3.

Prescribed total pressure and chloride mass fraction are imposed in all the outer boundaries and the density dependent flow simulation is run until a steady state solution is reached for pressure and chloride concentration.

The obtained results from the COMSOL simulation are compared with the results of the ConnectFlow model imported into COMSOL and interpolated over the COMSOL mesh.

Figure A-2 shows the residual pressures calculated in COMSOL and it is compared to the ConnectFlow results imported into COMSOL and interpolated over the COMSOL mesh. Figure A-3 shows the chloride mass fraction calculated in COMSOL and it is compared to the ConnectFlow results imported into COMSOL and interpolated over the COMSOL mesh. See Figure 3-13 and Figure 3-14 for details on the mesh resolution at different scales.

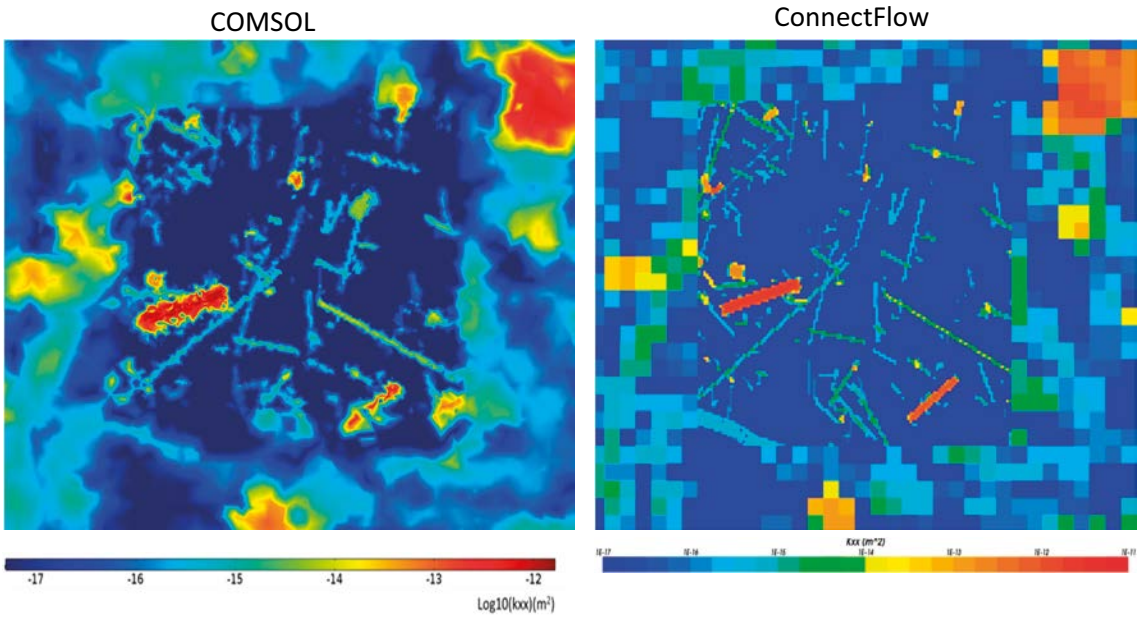

Figure A-1. *ConnectFlow permeability field imported in COMSOL and interpolated over the COMSOL mesh (left) and the actual permeability field in ConnectFlow (right).*

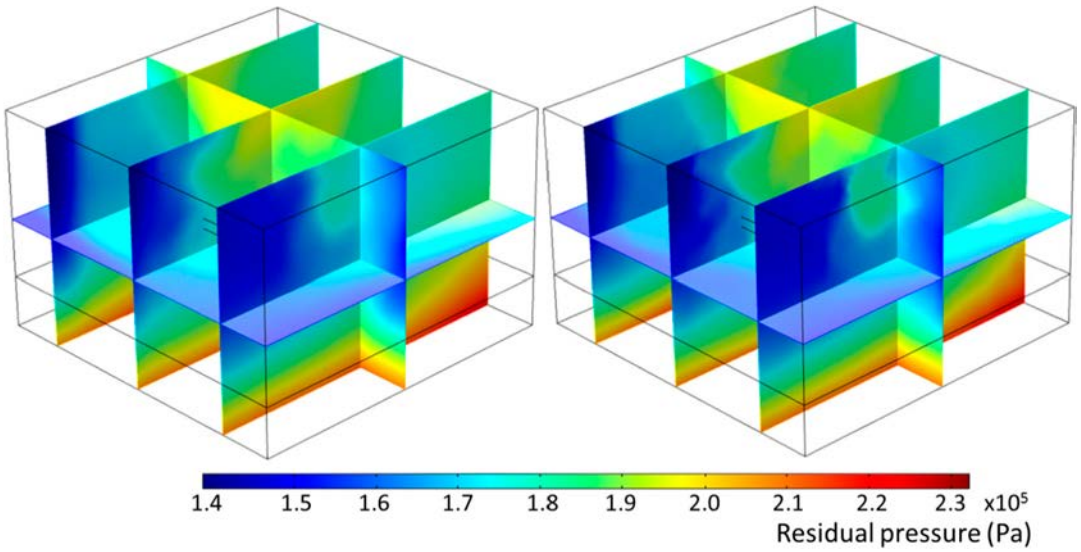

Figure A-2. *Comparison between the ConnectFlow (left) and COMSOL (right) residual pressure fields. The residual pressure is calculated in COMSOL as $p+\rho_0 gz$, where p is the total pressure (Pa), ρ_0 the freshwater density (kg/m^3), g the gravity (m^2/s) and z the elevation (m).*

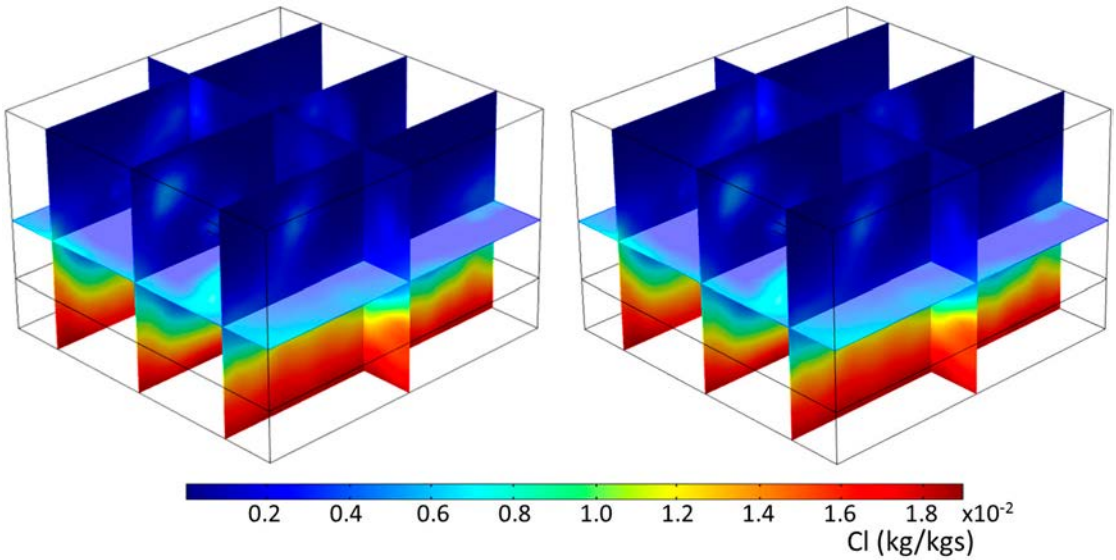

Figure A-3. *Comparison of the density field between ConnectFlow (left) and COMSOL (right). Density is expressed in terms of chloride mass fraction (kg/kg).*

A more quantitative evaluation of the consistency of the results is provided by the normalised histogram of the relative difference of the residual pressure over the model domain (Figure A-4) and for the relative difference of the chloride mass fraction over the model domain (Figure A-5). Note that the histograms have been normalised by the volume of the model domain. The relative error is calculated as:

$\varepsilon_p = (P_{CM}–P_{CF})/P_{CF}$

$\varepsilon_{Cl} = (Cl_{CM}–Cl_{CF})/Cl_{CF}$

where CM stands for COMSOL and CF for ConnectFlow.

Most of the model domain has a pressure relative difference lower than 2 %. The maximum computed difference is 8 % but this larger difference is restricted to a very small volume of the domain.

The difference in the chloride mass fraction is lower than 1 ‰ in most of the model domain.

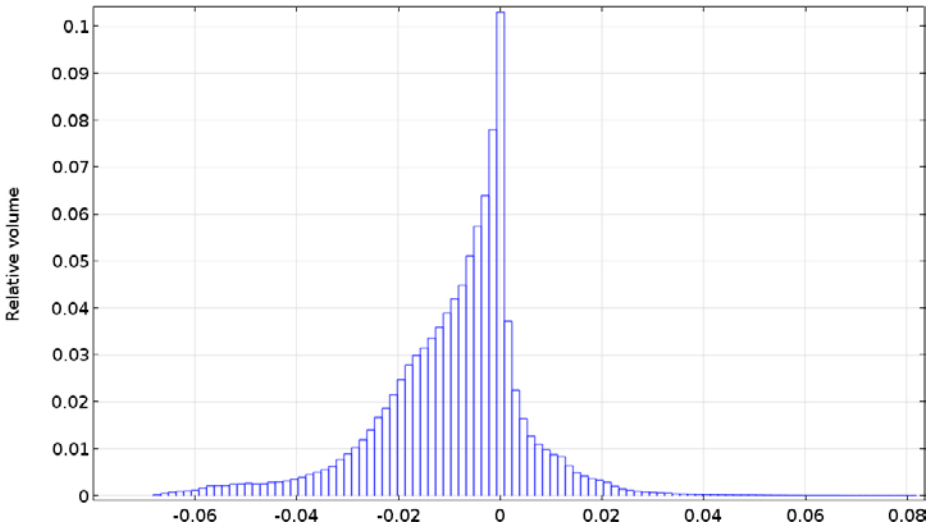

Figure A-4. *Normalised histogram of the relative difference between the residual pressure computed by COMSOL and the ConnectFlow results. The histogram has been normalised by the volume of the model domain.*

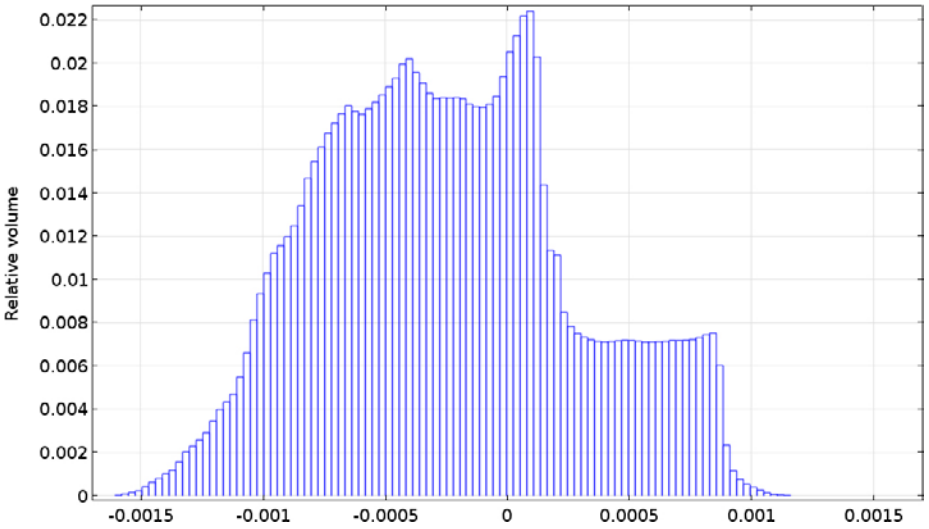

Figure A-5. *Normalised histogram of the relative difference between the chloride mass fraction computed by COMSOL and the ConnectFlow results. The histogram has been normalised by the volume of the model domain.*

Conclusions

The comparison exercise shows good agreement between the COMSOL results and the ConnectFlow results imported in COMSOL and interpolated over the COMSOL mesh.

Appendix B

Flows through vault compartments

Methodology

For each control volume, first, the groundwater flow is calculated with surface integrals over each of its 6 faces (Q_{face} (m^3/yr)). Positive values have been added up to compute the total groundwater flow crossing the control volume ($Q_{control\_volume,out}$ (m^3/yr)):

$$Q_{face} = \iint \vec{q} \cdot \vec{n}$$

$$Q_{control_{volume},in} = \sum_{Q_{face}<0} Q_{face}$$

$$Q_{control_{volume}out} = \sum_{Q_{face}>0} Q_{face}$$

The mass balance closing error has been calculated by comparing the positive values with the negative ones as follows:

$$\%\ Closing\ error = \frac{Q_{control\_volume,out} - Q_{control\_volume,in}}{Q_{control\_volume,in}}$$

The control volumes are labelled according to the axial sections in which they are contained (Figure 3-15).

Base Case

Table B-1. Calculated flow through the BHA waste and backfill sections for the base case. IDs refer to the vault section containing the control volume.

		Total flow (m^3/year)	Mass conservation error
Waste	1	3.33E-04	−0.14 %
	2	2.71E-04	0.36 %
	3	5.11E-04	−0.21 %
	4	2.69E-04	0.23 %
	5	1.66E-04	0.00 %
Backfill	0	7.15E-05	0.01 %
	1	2.50E-03	−0.02 %
	2	3.50E-04	0.28 %
	3	1.07E-03	−0.10 %
	4	1.59E-03	0.04 %
	5	3.93E-03	0.00 %
	6	5.97E-04	0.00 %

Table B-2. Calculated flow through BHK waste and backfill sections for the base case. IDs refer to the vault section containing the control volume.

		Total flow (m^3/year)	Mass conservation error
Waste	1	4.47E-02	0.01 %
	2	5.47E-02	−0.01 %
	3	2.42E-01	−0.01 %
	4	3.03E-01	0.00 %
	5	1.79E-01	0.01 %
	6	9.82E-02	0.00 %
Backfill	0	3.46E-02	0.01 %
	1	5.13E-02	0.02 %
	2	4.59E-02	0.01 %
	3	2.76E-01	0.00 %
	4	3.94E-01	0.01 %
	5	2.33E-01	0.01 %
	6	1.18E-01	0.00 %
	7	2.13E-01	0.01 %

Influence of the repository orientation

Table B-3. Calculated flow through the BHA waste and backfill sections for the case of 90° repository rotation and base case of degradation. IDs refer to the vault section containing the control volume.

		Total flow (m^3/year)	Mass conservation error
Waste	1	3.33E-04	−0.08 %
	2	7.20E-04	0.11 %
	3	9.29E-04	0.18 %
	4	6.12E-04	−0.37 %
	5	5.21E-04	0.01 %
Backfill	0	3.12E-03	0.00 %
	1	4.59E-03	−0.01 %
	2	2.28E-03	0.03 %
	3	7.87E-04	0.22 %
	4	3.51E-03	−0.06 %
	5	1.89E-03	0.00 %
	6	1.54E-02	0.00 %

Table B-4. Calculated flow through the BHK waste and backfill sections for the case of 90° repository rotation and base case of degradation. IDs refer to the vault section containing the control volume.

		Total flow (m^3/year)	Mass conservation error
Waste	1	6.62E-02	0.00 %
	2	1.69E-01	0.00 %
	3	1.99E-01	0.02 %
	4	1.65E-01	0.01 %
	5	2.16E-01	−0.02 %
	6	2.85E-01	0.00 %
Backfill	0	2.41E-02	0.00 %
	1	6.56E-02	0.00 %
	2	2.50E-01	0.01 %
	3	2.82E-01	0.02 %
	4	2.03E-01	0.01 %
	5	2.59E-01	−0.01 %
	6	3.53E-01	0.00 %
	7	1.14E-01	−0.01 %

Table B-5. Calculated flow through the BHA waste and backfill sections for the case of 180° repository rotation and base case of degradation. IDs refer to the vault section containing the control volume.

		Total flow (m^3/year)	Mass conservation error
Waste	1	9.36E-05	−0.04 %
	2	2.82E-04	−0.16 %
	3	2.81E-04	0.34 %
	4	3.14E-04	−0.15 %
	5	1.47E-04	0.01 %
Backfill	0	7.22E-04	0.00 %
	1	1.07E-03	0.00 %
	2	2.89E-04	−0.15 %
	3	3.21E-04	0.30 %
	4	9.61E-04	−0.05 %
	5	7.50E-03	0.00 %
	6	1.79E-03	0.00 %

Table B-6. Calculated flow through BHK waste and backfill sections for the case of 180° repository rotation and base case of degradation. IDs refer to the vault section containing the control volume.

		Total flow (m^3/year)	Mass conservation error
Waste	1	7.02E-02	0.00 %
	2	6.97E-02	0.01 %
	3	1.14E-01	0.01 %
	4	1.32E-01	−0.01 %
	5	9.67E-02	−0.01 %
	6	2.67E-02	0.05 %
Backfill	0	3.02E-02	−0.01 %
	1	8.95E-02	0.01 %
	2	8.87E-02	0.01 %
	3	1.54E-01	0.01 %
	4	1.74E-01	0.00 %
	5	1.31E-01	0.00 %
	6	3.55E-02	0.07 %
	7	2.32E-02	0.02 %

Table B-7. Calculated flow through BHA waste and backfill sections for the case of 270° repository rotation and base case of degradation. IDs refer to the vault section containing the control volume.

		Total flow (m^3/year)	Mass conservation error
Waste	1	2.04E-04	−0.16 %
	2	4.03E-04	0.13 %
	3	3.10E-04	−0.18 %
	4	2.79E-04	0.14 %
	5	4.87E-04	0.00 %
Backfill	0	2.42E-03	0.00 %
	1	1.09E-03	−0.03 %
	2	3.61E-03	0.02 %
	3	7.51E-03	−0.01 %
	4	1.01E-03	0.04 %
	5	4.28E-03	0.00 %
	6	9.61E-04	0.00 %

Table B-8. Calculated flow through BHK waste and backfill sections for the case of 270° repository rotation and base case of degradation. IDs refer to the vault section containing the control volume.

		Total flow (m^3/year)	Mass conservation error
Waste	1	2.26E-02	0.01 %
	2	1.58E-02	−0.02 %
	3	4.55E-02	−0.01 %
	4	1.02E-01	0.00 %
	5	1.20E-01	0.00 %
	6	7.59E-02	0.00 %
Backfill	0	1.43E-02	0.00 %
	1	3.19E-02	0.03 %
	2	1.69E-02	−0.02 %
	3	5.40E-02	0.00 %
	4	1.28E-01	0.00 %
	5	1.57E-01	0.00 %
	6	9.77E-02	0.00 %
	7	4.63E-02	−0.01 %

Degraded zone case

Table B-9. Calculated flow through BHA waste and backfill sections for the case of 0° repository rotation and degraded zone case of concrete degradation. IDs refer to the vault section containing the control volume.

		Total flow (m^3/year)	Mass conservation error
Waste	1	3.25E-04	−0.14 %
	2	2.44E-04	0.40 %
	3	4.93E-04	−0.22 %
	4	2.60E-04	0.24 %
	5	1.57E-04	0.00 %
Backfill	0	6.84E-05	0.01 %
	1	2.88E-03	−0.02 %
	2	3.25E-04	0.30 %
	3	7.49E-04	−0.15 %
	4	1.15E-03	0.05 %
	5	3.77E-03	0.00 %
	6	5.66E-04	0.00 %

Table B-10. Calculated flow through BHK waste and backfill sections for the case of 0° repository rotation and degraded zone case of concrete degradation. IDs refer to the vault section containing the control volume.

		Total flow (m^3/year)	Mass conservation error
Waste	1	1.97E-02	−0.01 %
	2	3.62E-02	−0.01 %
	3	1.14E-01	−0.01 %
	4	1.41E-01	0.00 %
	5	1.14E-01	0.01 %
	6	5.83E-02	−0.01 %
Backfill	0	1.93E-01	0.00 %
	1	1.40E-01	0.00 %
	2	9.68E-02	0.05 %
	3	7.11E-01	0.00 %
	4	1.37E+00	0.01 %
	5	1.02E+00	0.01 %
	6	3.82E-01	−0.01 %
	7	1.09E+00	0.00 %

Table B-11. Calculated flow through BHA waste and backfill sections for the case of 90° repository rotation and degraded zone case of concrete degradation. IDs refer to the vault section containing the control volume.

		Total flow (m^3/year)	Mass conservation error
Waste	1	3.14E-04	−0.09 %
	2	6.96E-04	0.11 %
	3	8.97E-04	0.19 %
	4	5.85E-04	−0.38 %
	5	5.06E-04	0.01 %
Backfill	0	3.00E-03	0.00 %
	1	4.39E-03	−0.01 %
	2	2.13E-03	0.04 %
	3	7.47E-04	0.23 %
	4	3.22E-03	−0.07 %
	5	1.52E-03	0.00 %
	6	1.45E-02	0.00 %

Table B-12. Calculated flow through BHK waste and backfill sections for the case of 90° repository rotation and degraded zone case of concrete degradation. IDs refer to the vault section containing the control volume.

		Total flow (m^3/year)	Mass conservation error
Waste	1	3.63E-02	0.00 %
	2	1.06E-01	−0.02 %
	3	1.37E-01	0.03 %
	4	1.26E-01	0.01 %
	5	1.63E-01	−0.03 %
	6	2.03E-01	0.00 %
Backfill	0	8.25E-02	0.00 %
	1	1.80E-01	0.01 %
	2	1.15E+00	0.01 %
	3	1.34E+00	0.03 %
	4	9.92E-01	0.01 %
	5	1.17E+00	−0.02 %
	6	1.76E+00	0.00 %
	7	6.24E-01	−0.01 %

Table B-13. Calculated flow through BHA waste and backfill sections for the case of 180° repository rotation and degraded zone case of concrete degradation. IDs refer to the vault section containing the control volume.

		Total flow (m^3/year)	Mass conservation error
Waste	1	9.35E-05	−0.04 %
	2	2.83E-04	−0.16 %
	3	2.81E-04	0.34 %
	4	3.15E-04	−0.15 %
	5	1.47E-04	0.01 %
Backfill	0	7.17E-04	0.00 %
	1	1.06E-03	0.00 %
	2	2.87E-04	−0.15 %
	3	3.19E-04	0.30 %
	4	9.54E-04	−0.05 %
	5	7.43E-03	0.00 %
	6	1.78E-03	0.00 %

Table B-14. Calculated flow through BHK waste and backfill sections for the case of 180° repository rotation and degraded zone case of concrete degradation. IDs refer to the vault section containing the control volume.

		Total flow (m^3/year)	Mass conservation error
Waste	1	2.71E-02	0.00 %
	2	3.12E-02	0.01 %
	3	5.07E-02	0.01 %
	4	5.55E-02	−0.01 %
	5	3.95E-02	0.01 %
	6	1.84E-02	0.07 %
Backfill	0	1.81E-01	−0.01 %
	1	2.53E-01	0.01 %
	2	2.60E-01	0.02 %
	3	4.85E-01	0.01 %
	4	4.87E-01	−0.01 %
	5	4.41E-01	0.01 %
	6	2.64E-01	0.05 %
	7	2.53E-01	−0.04 %

Table B-15. Calculated flow through BHA waste and backfill sections for the case of 270° repository rotation and degraded zone case of concrete degradation. IDs refer to the vault section containing the control volume.

		Total flow (m^3/year)	Mass conservation error
Waste	1	2.03E-04	−0.16 %
	2	4.02E-04	0.13 %
	3	3.10E-04	−0.18 %
	4	2.78E-04	0.14 %
	5	4.85E-04	−0.01 %
Backfill	0	2.40E-03	0.00 %
	1	1.08E-03	−0.03 %
	2	3.55E-03	0.02 %
	3	7.38E-03	−0.01 %
	4	9.90E-04	0.04 %
	5	4.16E-03	0.00 %
	6	9.30E-04	0.00 %

Table B-16. Calculated flow through BHK waste and backfill sections for the case of 270° repository rotation and degraded zone case of concrete degradation. IDs refer to the vault section containing the control volume.

		Total flow (m^3/year)	Mass conservation error
Waste	1	1.97E-02	−0.02 %
	2	1.65E-02	0.01 %
	3	2.65E-02	0.00 %
	4	5.62E-02	0.00 %
	5	7.40E-02	0.00 %
	6	5.38E-02	0.00 %
Backfill	0	1.61E-01	0.00 %
	1	1.37E-01	−0.01 %
	2	1.02E-01	0.02 %
	3	2.16E-01	0.02 %
	4	5.41E-01	0.00 %
	5	6.30E-01	0.00 %
	6	3.47E-01	0.00 %
	7	3.07E-01	0.00 %

Influence of the concrete barrier degradation

The influence of the concrete degradation has been studied for the 0° rotation. The results of the base case and degraded zone case are presented in the tables of the previous section.

Degraded case

Table B-17. Calculated flow through BHA waste and backfill sections for the degraded case of concrete backfill. IDs refer to the vault section containing the control volume.

		Total flow (m^3/year)	Mass conservation error
Waste	1	3.24E-04	−0.14 %
	2	2.44E-04	0.40 %
	3	4.93E-04	−0.22 %
	4	2.59E-04	0.24 %
	5	1.57E-04	0.00 %
Backfill	0	6.81E-05	0.01 %
	1	2.86E-03	−0.02 %
	2	3.23E-04	0.31 %
	3	7.43E-04	−0.15 %
	4	1.15E-03	0.05 %
	5	3.75E-03	0.00 %
	6	5.64E-04	0.00 %

Table B-18. Calculated flow through BHK waste and backfill sections for the degraded case of concrete backfill. IDs refer to the vault section containing the control volume.

		Total flow (m^3/year)	Mass conservation error
Waste	1	1.01E-01	0.00 %
	2	1.03E-01	0.00 %
	3	5.16E-01	0.00 %
	4	7.91E-01	0.00 %
	5	6.65E-01	0.01 %
	6	3.31E-01	−0.01 %
Backfill	0	1.68E-01	0.00 %
	1	9.93E-02	0.01 %
	2	4.76E-02	0.07 %
	3	8.43E-01	0.00 %
	4	1.80E+00	0.01 %
	5	1.44E+00	0.01 %
	6	6.76E-01	−0.01 %
	7	1.50E+00	−0.01 %

Appendix C

Control volume definition and flows for radionuclide transport calculations

Introduction

The simulations carried out with the near-field hydrogeological models provide groundwater flows through different control volumes faces for radionuclide transport calculations with ECOLEGO. This section details the surfaces where the flows are computed, how these flows are calculated and the delivery format to ECOLEGO.

Control volumes and their surfaces (faces) will be used to facilitate transfer of hydrological results from detailed near-field hydrological modelling to radionuclide transport calculation for SFL. The net-flow for each of the six faces of each control volume is calculated as a post-processing of the hydrological results and delivered in text files as input data to the radionuclide transport modelling.

Definition of the control volumes

Control volumes and their surfaces (faces) will be used to facilitate transfer of hydrological results from detailed near-field hydrological modelling to radionuclide transport calculation for SFL. Faces are numbered from 1–6 (Figure C-1):

- 1: The face at the top (roof) of the control volume.
- 2: The face at the bottom (floor) of the control volume.
- 3: The face with the highest y coordinate.
- 4 : The face with the highest x coordinate.
- 5 : The face with the lowest y coordinate.
- 6 : The face with the lowest x coordinate.

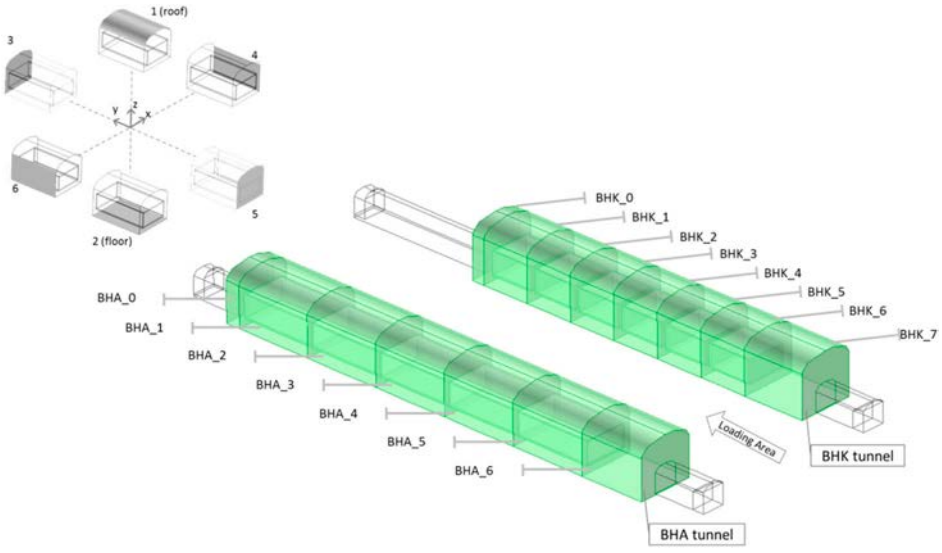

Figure C-1. *Labelling of the axial divisions and faces in the BHA and BHK vaults.*

BHA

The BHA is divided axially in 7 sections (Figure C-1). Sections are labelled from 0 to 6.

Sections 1 to 5 contain waste compartments and are divided into 5 control volumes each, according to Figure C-2. These control volumes are labelled as:

Wa: Waste control volume.

T: Top backfill.

B: Bottom backfill.

W: West backfill.

E: East backfill.

Sections 0 and 6 contain only backfill material. Section 6 corresponds to the loading area. Section 0 and 6 are divided into 3 control volumes:

T: Top backfill = Top backfill in sections 1–6 (Figure C-2).

B: Bottom backfill = Bottom backfill in sections 1–6 (Figure C-2).

M: Middle backfill = Waste + East + West compartments in sections 1–6 (Figure C-2).

The total number of control volume in the BHA vaults is 31.

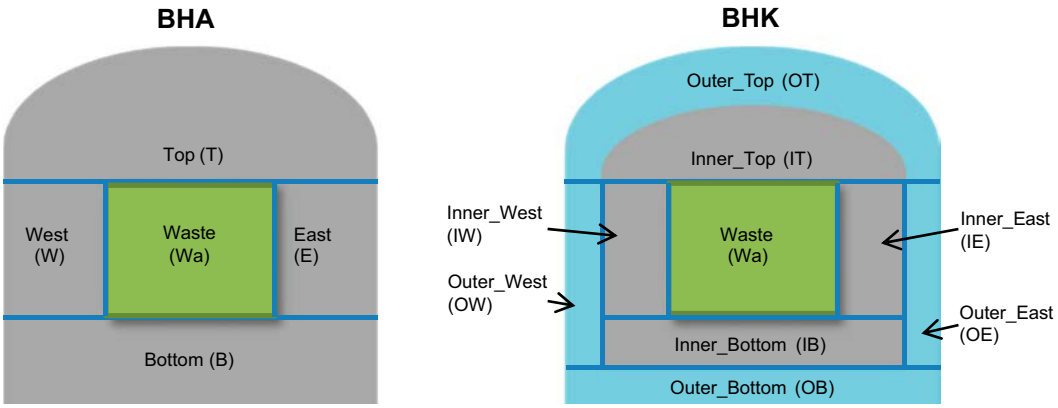

Figure C-2. *Labelling of the different divisions.*

BHK

The BHK is divided axially in 8 sections (Figure C-1). Sections are labelled from 0 to 7. The axial sections divide the backfill in the middle point of the space between waste caissons. Thus, each control volume will have 0.75 m of backfill at each end in the axial direction. For symmetry reasons, the sections 1 and 6 have also a 0.75 m-thick backfill portion in the contact with sections 0 and 7, respectively.

Sections 1 to 6 contain waste compartments and are divided into 11 control volumes each. In a transverse cross section traversing the waste, 9 control volumes are defined according to Figure C-2. These control volumes are labelled as:

Wa: Waste control volume.

IT: Inner Top backfill.

IB: Inner Bottom backfill.

IM: Inner West backfill.

IE: Inner East backfill.

OT: Outer Top backfill.

OB: Outer Bottom backfill.

OM: Outer West backfill.

OE: Outer East backfill.

Two additional control volumes are defined in the axial direction of the vault (Figure C-3). They correspond to the backfill material between waste caissons. Each section contains two of these control volumes, labelled:

N: Northern backfill.

S: Southern backfill.

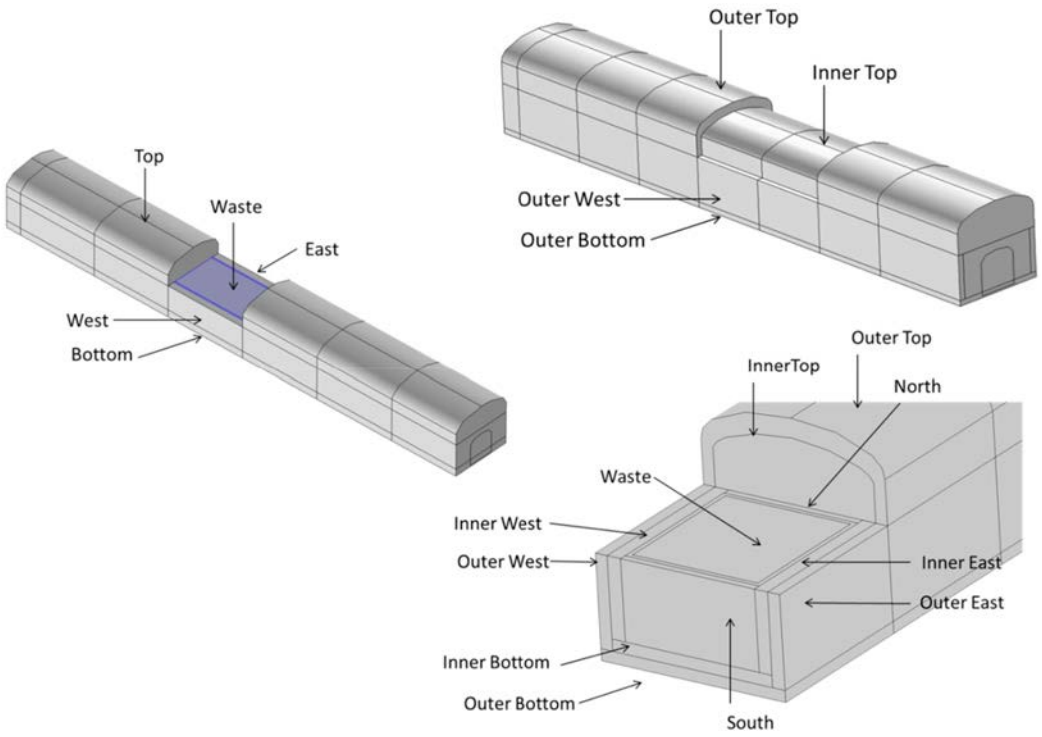

Figure C-3. *Detail of the divisions of the control volumes for the BHA (left) and BHK (right) vaults.*

Sections 0 and 7 contain only backfill material. Section 7 corresponds to the loading area. Section 0 and 7 are divided into 6 control volumes (Figure C-4):

IT: Inner Top backfill = Inner Top backfill in sections 1–6 (Figure C-2).

IB: Inner Bottom backfill = Inner Bottom backfill in sections 1–6 (Figure C-2).

IM: Inner Middle backfill = Waste + Inner West + Inner East + Inner Bottom backfill in sections 1–6 (Figure C-2).

OT: Outer Top backfill = Outer Top backfill in sections 1–6 (Figure C-2).

OB: Outer Bottom backfill = Outer Bottom backfill in sections 1–6 (Figure C-2).

OM: Outer Middle backfill (Figure C-4):= Waste + Inner West + Inner East + Inner Bottom in sections 1–6 (Figure C-2).

The total number of control volume in the BHK vaults is 78.

Calculation of the flow through faces

For each control volume, the groundwater flow is calculated with surface integrals over each of the 6 faces of the volume (Q_{face} (m^3/yr)). Positive values have been added up representing the groundwater flow crossing the control volume ($Q_{control\_volume,out}$(m^3/yr)):

$$Q_{face} = \iint \vec{q} \cdot \vec{n}$$

$$Q_{control_{volume},in} = \sum_{Q_{face}<0} Q_{face}$$

$$Q_{control_{volume}out} = \sum_{Q_{face}>0} Q_{face}$$

In order to check the accuracy of the results the mass balance closing error has been calculated by comparing the positive values with the negative ones as follows:

$$\%\ Closing\ error = \frac{Q_{control\_volume,out} - Q_{control\_volume,in}}{Q_{control\_volume,in}}$$

The sign convention for the results delivered to the radionuclide transport calculations is such that a positive value for a flow over a face of a control volume represents a flow out from that volume, and hence a negative value represents a flow in to the control volume.

The final notation to refer the different control surfaces is:

“Vault” _ “Section-number”_ “Control-volume-name”_ “Face-number” e.g. BHK _1_OT _1

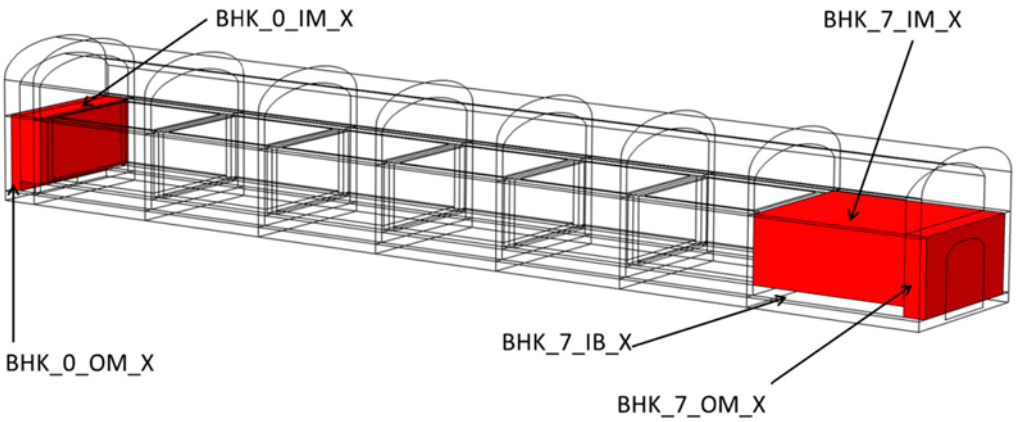

Figure C-4. *Detail of the divisions in the borders of the control volumes for the BHK vault.*

Files provided to ECOLEGO

The deliverables of the groundwater flows consist of two .txt file, one per vault, labelled with the name of the vault for each simulated case. Files are composed by two columns, the first column contains the name of the surface evaluated, following the notation presented above. The second column gives the value of groundwater flow crossing the surface in m^3/s. The two text files for the base case are presented below.

BHA.dat for the Base case

Control_volume Flow (m^3/s)

BHA_0_T_1 -8.531260228926400054e-13
BHA_0_T_2 -4.436507682388374723e-12
BHA_0_T_3 9.353213582365807409e-13
BHA_0_T_4 -4.496122643275641900e-14
BHA_0_T_5 4.495384887462942642e-12
BHA_0_T_6 -9.615475858517773983e-14
BHA_0_M_1 4.436507682388374723e-12
BHA_0_M_2 -6.820354166892742737e-12
BHA_0_M_3 4.239419527632668859e-13
BHA_0_M_4 -7.970259353747110188e-14
BHA_0_M_5 2.277258586620903630e-12
BHA_0_M_6 -2.377242642074888060e-13
BHA_0_B_1 6.820354166892742737e-12
BHA_0_B_2 1.188202103082115682e-12
BHA_0_B_3 -2.813437371542097036e-13
BHA_0_B_4 -2.227548058967659164e-13
BHA_0_B_5 -7.184776524950143809e-12
BHA_0_B_6 -3.197169335901271940e-13
BHA_1_T_1 -9.871130048096403959e-13
BHA_1_T_2 6.310049753023052732e-12
BHA_1_T_3 -4.495384887462942642e-12
BHA_1_T_4 8.052131663099846921e-15
BHA_1_T_5 -2.564813855522209408e-14
BHA_1_T_6 -8.100546656727014561e-13
BHA_1_W_1 -4.277497998672326201e-12
BHA_1_W_2 -5.503579640477260571e-12
BHA_1_W_3 -1.563259721012300084e-13
BHA_1_W_4 -5.354306016390490836e-14
BHA_1_W_5 1.547911447888398883e-13
BHA_1_W_6 9.836155655444954225e-12
BHA_1_Wa_1 -4.393630200784318121e-12
BHA_1_Wa_2 1.049873840146299618e-11
BHA_1_Wa_3 -1.873895801040832642e-12
BHA_1_Wa_4 -1.127275620811124175e-12
BHA_1_Wa_5 -3.142976469312230163e-12
BHA_1_Wa_6 5.354306016390490836e-14
BHA_1_E_1 2.361078446433594821e-12
BHA_1_E_2 -4.153993033439980954e-12
BHA_1_E_3 -2.470368134788444134e-13
BHA_1_E_4 8.183397543805153562e-13
BHA_1_E_5 9.431941883041995286e-14
BHA_1_E_6 1.127275620811124175e-12
BHA_1_B_1 -8.411657275457785871e-13
BHA_1_B_2 7.887972687190226171e-11
BHA_1_B_3 7.184776524950143809e-12
BHA_1_B_4 -1.010209594037267025e-11
BHA_1_B_5 -1.615455243438826554e-12
BHA_1_B_6 -7.350589539660524007e-11
BHA_2_T_1 -1.371349884301084911e-12
BHA_2_T_2 2.367968484776948072e-12
BHA_2_T_3 2.564813855522209408e-14
BHA_2_T_4 -2.358947013947646500e-13
BHA_2_T_5 -5.401077490334031252e-13
BHA_2_T_6 -2.465736329884285081e-13
BHA_2_W_1 -9.762632800887016279e-13
BHA_2_W_2 8.674533422823775407e-13
BHA_2_W_3 -1.547911447888398883e-13
BHA_2_W_4 5.227410769945445700e-13
BHA_2_W_5 1.477865187876901626e-13
BHA_2_W_6 -4.069440907343686547e-13
BHA_2_Wa_1 3.356232350539722295e-12
BHA_2_Wa_2 2.098336775662403932e-12
BHA_2_Wa_3 3.142976469312230163e-12
BHA_2_Wa_4 -3.858326511146735532e-12
BHA_2_Wa_5 -4.247619518339278930e-12
BHA_2_Wa_6 -5.227410769945445700e-13

BHA_2_E_1 -4.747937555227962277e-12
BHA_2_E_2 1.453001943559525185e-12
BHA_2_E_3 -9.431941883041995286e-14
BHA_2_E_4 -4.134316294180978849e-13
BHA_2_E_5 -5.568629779662988964e-14
BHA_2_E_6 3.858326511146735532e-12
BHA_2_B_1 -4.418792061504304335e-12
BHA_2_B_2 6.550837614031710918e-12
BHA_2_B_3 1.615455243438826554e-12
BHA_2_B_4 -2.180927091966255909e-12
BHA_2_B_5 8.609850347861787505e-13
BHA_2_B_6 -2.427578357968270724e-12
BHA_3_T_1 -9.733935368406530188e-13
BHA_3_T_2 1.323305419355488255e-12
BHA_3_T_3 5.401077490334031252e-13
BHA_3_T_4 -4.988571710897410867e-13
BHA_3_T_5 1.533628919202177627e-13
BHA_3_T_6 -5.447366137615984852e-13
BHA_3_W_1 -3.946413586292272275e-12
BHA_3_W_2 2.084479349410512693e-12
BHA_3_W_3 -1.477865187876901626e-13
BHA_3_W_4 3.109628378354508007e-12
BHA_3_W_5 -2.117049255941327615e-13
BHA_3_W_6 -8.882622493012880288e-13
BHA_3_Wa_1 1.195663156481434978e-11
BHA_3_Wa_2 -1.013404875992691144e-11
BHA_3_Wa_3 4.247619518339278930e-12
BHA_3_Wa_4 -2.096942662256205146e-12
BHA_3_Wa_5 -8.289597645905402649e-13
BHA_3_Wa_6 -3.109628378354508007e-12
BHA_3_E_1 -9.333523397877596660e-12
BHA_3_E_2 6.281495487222526204e-12
BHA_3_E_3 5.568629779662988964e-14
BHA_3_E_4 8.834151664832098035e-13
BHA_3_E_5 1.591490679380148942e-14
BHA_3_E_6 2.096942662256205146e-12
BHA_3_B_1 1.768073923293886068e-12
BHA_3_B_2 3.009488447014229063e-11
BHA_3_B_3 -8.609850347861787505e-13
BHA_3_B_4 -2.933253529257689759e-11
BHA_3_B_5 8.980900526361389777e-13
BHA_3_B_6 -2.567540693977512210e-12
BHA_4_T_1 4.609031150527293369e-12
BHA_4_T_2 2.013467671405989674e-12
BHA_4_T_3 -1.533628919202177627e-13
BHA_4_T_4 -1.528292851468348200e-13
BHA_4_T_5 -5.437402224135727028e-12
BHA_4_T_6 -8.787717174674011095e-13
BHA_4_W_1 1.957998906733388428e-12
BHA_4_W_2 -1.479726919754683793e-12
BHA_4_W_3 2.117049255941327615e-13
BHA_4_W_4 -2.695337337286827096e-12
BHA_4_W_5 2.306434662412565700e-13
BHA_4_W_6 1.774725545090061576e-12
BHA_4_Wa_1 -8.556925386043776132e-12
BHA_4_Wa_2 3.102615043681442689e-12
BHA_4_Wa_3 8.289597645905402649e-13
BHA_4_Wa_4 1.071341694459566198e-12
BHA_4_Wa_5 8.385833096806671058e-13
BHA_4_Wa_6 2.695337337286827096e-12
BHA_4_E_1 4.585458807904396010e-12
BHA_4_E_2 -3.754792654158867738e-12
BHA_4_E_3 -1.591490679380148942e-14
BHA_4_E_4 4.097336848786759430e-14
BHA_4_E_5 2.156245410951462462e-13
BHA_4_E_6 -1.071341694459566198e-12
BHA_4_B_1 2.131904530232109650e-12
BHA_4_B_2 4.591677901035794593e-11
BHA_4_B_3 -8.980900526361389777e-13
BHA_4_B_4 -1.861162045132862500e-12
BHA_4_B_5 -2.443198898882829273e-13
BHA_4_B_6 -4.504510836901183272e-11
BHA_5_T_1 -3.477110793999898783e-12
BHA_5_T_2 9.876531105188607474e-13
BHA_5_T_3 5.437402224135727028e-12
BHA_5_T_4 -2.441135979428804275e-14
BHA_5_T_5 -6.150170652015007537e-13
BHA_5_T_6 -2.308589332441643518e-12
BHA_5_W_1 -7.443708762180466438e-12
BHA_5_W_2 -5.852846712507423792e-12

BHA_5_W_3 -2.306434662412565700e-13
BHA_5_W_4 6.68324906828558 1394e-13
BHA_5_W_5 3.727679858108609752e-13
BHA_5_W_6 1.248610366561391291e-11
BHA_5_Wa_1 -1.474884290777114420e-12
BHA_5_Wa_2 5.264033909724260527e-12
BHA_5_Wa_3 -8.385833096806671058e-13
BHA_5_Wa_4 -1.319341404752837740e-12
BHA_5_Wa_5 -9.627561049225599029e-13
BHA_5_Wa_6 -6.683249068285581394e-13
BHA_5_E_1 7.930939942438764741e-12
BHA_5_E_2 -9.144000490563815285e-12
BHA_5_E_3 -2.156245410951462462e-13
BHA_5_E_4 1.540665640416251294e-13
BHA_5_E_5 -4.473409917401270296e-14
BHA_5_E_6 1.319341404752837740e-12
BHA_5_B_1 9.732813293346985012e-12
BHA_5_B_2 1.177369040047992195e-10
BHA_5_B_3 2.443198898882829273e-13
BHA_5_B_4 1.635558433247251220e-13
BHA_5_B_5 3.469007078964843390e-12
BHA_5_B_6 -1.313465836574465525e-10
BHA_6_T_1 -1.791755098335514728e-12
BHA_6_T_2 -2.344187697178973137e-13
BHA_6_T_3 6.150170652015007537e-13
BHA_6_T_4 2.907593063583659547e-14
BHA_6_T_5 1.139869044962254718e-12
BHA_6_T_6 2.420602570820731930e-13
BHA_6_M_1 2.344187697178973137e-13
BHA_6_M_2 -1.445616185575862254e-12
BHA_6_M_3 6.347222182857132904e-13
BHA_6_M_4 5.759247463902318193e-14
BHA_6_M_5 7.444178566274415664e-14
BHA_6_M_6 4.443503053440765742e-13
BHA_6_B_1 1.445616185575862254e-12
BHA_6_B_2 1.783323186823530100e-11
BHA_6_B_3 -3.469007078964843390e-12
BHA_6_B_4 -5.437901406533680224e-13
BHA_6_B_5 -1.248259663217559321e-13
BHA_6_B_6 -1.514123513840690805e-11

BHK.dat for the Base case

Control_volume Flow (m^3/s)

BHK_0_OT_1 -9.347264670746301953e-10
BHK_0_OT_2 6.458779930524569202e-10
BHK_0_OT_3 -1.451800086181614950e-10
BHK_0_OT_4 1.774699491570603486e-10
BHK_0_OT_5 1.786044939433483696e-10
BHK_0_OT_6 -1.076525359868944910e-11
BHK_0_IT_1 -5.181493449412497995e-10
BHK_0_IT_2 3.131802217619437626e-10
BHK_0_IT_3 -1.786044939433483696e-10
BHK_0_IT_4 8.602002283909113811e-11
BHK_0_IT_5 3.001517269694300029e-10
BHK_0_IT_6 -2.667957109278798976e-12
BHK_0_W_1 -2.317710303244792938e-11
BHK_0_W_2 1.370462613328532629e-11
BHK_0_W_3 1.108547178451108529e-12
BHK_0_W_4 5.475795228217183508e-12
BHK_0_W_5 6.051494853751201544e-12
BHK_0_W_6 -3.165398508546204477e-12
BHK_0_OM_1 -1.431748921228232298e-10
BHK_0_OM_2 5.942551844987699377e-11
BHK_0_OM_3 -1.496179262575594544e-11
BHK_0_OM_4 1.177801066215245154e-10
BHK_0_OM_5 -1.864381964517802435e-11
BHK_0_OM_6 -4.233309359311178347e-13
BHK_0_IM_1 -3.131802217619437626e-10
BHK_0_IM_2 1.210261998278299534e-10
BHK_0_IM_3 -7.839275762076808736e-12
BHK_0_IM_4 2.827343769972998262e-10
BHK_0_IM_5 -7.610431310251925554e-11
BHK_0_IM_6 -6.631194214220940124e-12
BHK_0_E_1 -4.472871868574784983e-11
BHK_0_E_2 3.133339791242391368e-11
BHK_0_E_3 -2.934407720080216517e-11
BHK_0_E_4 5.449956665787292100e-10

BHK_0_E_5 -5.225138265867779890e-11
BHK_0_E_6 -4.500015009647526490e-10
BHK_0_OB_1 -2.186650454274359481e-10
BHK_0_OB_2 1.753537838236264115e-10
BHK_0_OB_3 3.450823049114617069e-11
BHK_0_OB_4 5.963331903335594352e-11
BHK_0_OB_5 -5.598433398799127409e-11
BHK_0_OB_6 5.164700445461673420e-12
BHK_0_IB_1 -1.210261998278299534e-10
BHK_0_IB_2 1.142015029318497127e-10
BHK_0_IB_3 2.648309540725492840e-11
BHK_0_IB_4 4.948701734592822988e-11
BHK_0_IB_5 -7.071763933910529300e-11
BHK_0_IB_6 1.578729921934886114e-12
BHK_1_OT_1 -1.432792640137552222e-09
BHK_1_OT_2 1.453851194874846899e-09
BHK_1_OT_3 -8.863923449153208534e-11
BHK_1_OT_4 8.463688902920402378e-11
BHK_1_OT_5 2.454425097253592176e-11
BHK_1_OT_6 -4.172114100523821034e-11
BHK_1_IT_1 -1.333403518648788405e-09
BHK_1_IT_2 1.554114195594663964e-09
BHK_1_IT_3 -3.001517269694300029e-10
BHK_1_IT_4 5.809107684847618094e-11
BHK_1_IT_5 7.515626587919328796e-11
BHK_1_IT_6 -5.406068608532576798e-11
BHK_1_OW_1 -5.331012752519492679e-11
BHK_1_OW_2 2.700909844407832750e-11
BHK_1_OW_3 -6.051494853751201544e-12
BHK_1_OW_4 4.710863914151276887e-11
BHK_1_OW_5 8.350273550712091184e-12
BHK_1_OW_6 -2.310954629722373114e-11
BHK_1_IW_1 -7.720304297729582553e-11
BHK_1_IW_2 2.303792411571401067e-11
BHK_1_IW_3 -1.427418188825002214e-11
BHK_1_IW_4 1.082754776610280285e-10
BHK_1_IW_5 1.749829378082597756e-11
BHK_1_IW_6 -5.733578106954069286e-11
BHK_1_N_1 -8.246069321309981856e-11
BHK_1_N_2 3.537238988493414232e-11
BHK_1_N_3 1.728805906408251567e-11
BHK_1_N_4 6.448409615167387191e-11
BHK_1_N_5 -2.759723107184460217e-11
BHK_1_N_6 -7.084505634572119882e-12
BHK_1_Wa_1 -1.394503760509918892e-09
BHK_1_Wa_2 5.830156680188941238e-10
BHK_1_Wa_3 2.759723107184460217e-11
BHK_1_Wa_4 4.970747350815161892e-10
BHK_1_Wa_5 3.085636055981428301e-10
BHK_1_Wa_6 -1.042862202029181300e-10
BHK_1_S_1 -9.503855176603043209e-12
BHK_1_S_2 1.387064349527430540e-11
BHK_1_S_3 -3.085636055981428301e-10
BHK_1_S_4 4.452403680733017162e-12
BHK_1_S_5 2.966490852850165181e-10
BHK_1_S_6 3.095248176462054173e-12
BHK_1_IE_1 -7.290353693084609293e-11
BHK_1_IE_2 8.614821855681182124e-11
BHK_1_IE_3 7.309043592668696557e-11
BHK_1_IE_4 4.634466162385536132e-10
BHK_1_IE_5 1.624967512561057026e-11
BHK_1_IE_6 -5.660112349139227721e-10
BHK_1_OE_1 -7.116793946401387044e-11
BHK_1_OE_2 7.474790889474235449e-11
BHK_1_OE_3 5.225138265867779890e-11
BHK_1_OE_4 5.117492146732583164e-10
BHK_1_OE_5 7.434516975337009438e-12
BHK_1_OE_6 -5.750004164338045448e-10
BHK_1_OB_1 -6.195143814364926406e-10
BHK_1_OB_2 4.392295643117199364e-10
BHK_1_OB_3 5.598433398799127409e-11
BHK_1_OB_4 9.623656475347785297e-11
BHK_1_OB_5 1.763990683854719925e-11
BHK_1_OB_6 1.043524531439935503e-11
BHK_1_IB_1 -7.414448440716278493e-10
BHK_1_IB_2 5.177573740976734094e-10
BHK_1_IB_3 7.071763933910529300e-11
BHK_1_IB_4 1.115538001952511901e-10
BHK_1_IB_5 3.119494305429343543e-11
BHK_1_IB_6 1.022714192802788361e-11

BHK_2_OT_1 -8.19950918398240027e-10
BHK_2_OT_2 1.42231845598007497e-09
BHK_2_OT_3 -2.45442509725359218e-11
BHK_2_OT_4 -1.08912273758125483e-10
BHK_2_OT_5 -4.24993907887191336e-10
BHK_2_OT_6 -4.40303304808726525e-11
BHK_2_IT_1 -1.05578371156924913e-09
BHK_2_IT_2 1.51847562351478973e-09
BHK_2_IT_3 -7.51562658791932880e-11
BHK_2_IT_4 -1.58419845221799061e-10
BHK_2_IT_5 -1.74727812742271819e-10
BHK_2_IT_6 -5.45718932144535072e-11
BHK_2_OW_1 -4.92972195959121490e-11
BHK_2_OW_2 2.17714787229536805e-11
BHK_2_OW_3 -8.35027355071209118e-12
BHK_2_OW_4 3.20652368699482883e-11
BHK_2_OW_5 3.22837809025053997e-11
BHK_2_OW_6 -2.84731766825799234e-11
BHK_2_IW_1 -6.59913956443397897e-11
BHK_2_IW_2 2.00754564072609083e-11
BHK_2_IW_3 -1.74982937808259776e-11
BHK_2_IW_4 3.36945230569727002e-11
BHK_2_IW_5 7.04743763468313986e-11
BHK_2_IW_6 -4.07530342119168180e-11
BHK_2_N_1 -2.73429063723016829e-11
BHK_2_N_2 -9.31635820362795264e-13
BHK_2_N_3 -2.96649085285016518e-10
BHK_2_N_4 -4.18362118893798622e-12
BHK_2_N_5 3.35309998589859925e-10
BHK_2_N_6 -6.20283383223314710e-12
BHK_2_Wa_1 -1.24171730656280269e-09
BHK_2_Wa_2 4.70326884826326035e-10
BHK_2_Wa_3 -3.35309998589859925e-10
BHK_2_Wa_4 -1.14821287905776585e-10
BHK_2_Wa_5 1.26349658015757987e-09
BHK_2_Wa_6 -4.18473611725496089e-11
BHK_2_S_1 -4.93497866405769273e-11
BHK_2_S_2 4.52401184602352736e-11
BHK_2_S_3 -1.26349658015757987e-09
BHK_2_S_4 -5.87293190500795518e-13
BHK_2_S_5 1.25386981297644598e-09
BHK_2_S_6 1.43556719478099992e-11
BHK_2_IE_1 -1.34074228294769527e-10
BHK_2_IE_2 3.55877407056760499e-11
BHK_2_IE_3 -1.62496751256105703e-11
BHK_2_IE_4 -6.76014455838049914e-11
BHK_2_IE_5 6.27441632647665300e-11
BHK_2_IE_6 1.19592202285215328e-10
BHK_2_OE_1 -1.04245786378655857e-10
BHK_2_OE_2 4.16682374844702821e-11
BHK_2_OE_3 -7.43451697533700944e-12
BHK_2_OE_4 9.86735636182290985e-12
BHK_2_OE_5 1.73088496871050729e-11
BHK_2_OE_6 4.28321088677351109e-11
BHK_2_OB_1 -4.84939591684446628e-10
BHK_2_OB_2 3.73167583810166667e-10
BHK_2_OB_3 -1.76399068385471993e-11
BHK_2_OB_4 2.33067707855947451e-11
BHK_2_OB_5 9.86136891437111279e-11
BHK_2_OB_6 7.49823149672092691e-12
BHK_2_IB_1 -5.70298564579136091e-10
BHK_2_IB_2 4.21499875477022604e-10
BHK_2_IB_3 -3.11949430542934354e-11
BHK_2_IB_4 2.47693671606997750e-11
BHK_2_IB_5 1.46543203853960597e-10
BHK_2_IB_6 8.68779734196855718e-12
BHK_3_OT_1 -7.28802867774573019e-09
BHK_3_OT_2 7.77381688412076618e-09
BHK_3_OT_3 4.24993907887191336e-10
BHK_3_OT_4 -8.21374300818928921e-10
BHK_3_OT_5 -3.71342457609610757e-11
BHK_3_OT_6 -5.24911992709255663e-11
BHK_3_IT_1 -6.39494143258812841e-09
BHK_3_IT_2 6.74122413996840609e-09
BHK_3_IT_3 1.74727812742271819e-10
BHK_3_IT_4 -6.30173743238425663e-10
BHK_3_IT_5 2.59238564675876922e-10
BHK_3_IT_6 -1.50321167687426056e-10
BHK_3_OW_1 -2.40579753782408807e-10
BHK_3_OW_2 4.65188798336444252e-11

BHK_3_OW_3 -3.228378090250539972e-11
BHK_3_OW_4 2.457034363511236248e-10
BHK_3_OW_5 3.676062279284830803e-11
BHK_3_OW_6 -5.611801651749767262e-11
BHK_3_IW_1 -3.428683725471114660e-10
BHK_3_IW_2 6.606566530109063729e-11
BHK_3_IW_3 -7.047437634683139860e-11
BHK_3_IW_4 5.021800435728046059e-10
BHK_3_IW_5 8.727232616914015782e-11
BHK_3_IW_6 -2.421587530400137421e-10
BHK_3_N_1 -1.179656653201490690e-10
BHK_3_N_2 -2.635830553901510210e-11
BHK_3_N_3 -1.253869812976445978e-09
BHK_3_N_4 -4.042219684775595044e-11
BHK_3_N_5 1.461508330944695946e-09
BHK_3_N_6 -2.285902880883244788e-11
BHK_3_Wa_1 -5.710097047457065489e-09
BHK_3_Wa_2 5.832983742079931553e-09
BHK_3_Wa_3 -1.461508330944695946e-09
BHK_3_Wa_4 6.733482555649108379e-11
BHK_3_Wa_5 1.759151205887912173e-09
BHK_3_Wa_6 -4.874190534042466790e-10
BHK_3_S_1 -1.359315487876054272e-10
BHK_3_S_2 2.112056573903684324e-10
BHK_3_S_3 -1.759151205887912173e-09
BHK_3_S_4 7.264489262848549692e-11
BHK_3_S_5 1.603135451931927372e-09
BHK_3_S_6 8.098038640274364296e-12
BHK_3_IE_1 -4.343615058564743571e-10
BHK_3_IE_2 3.024853655767996977e-10
BHK_3_IE_3 -6.274416326476652997e-11
BHK_3_IE_4 1.923700612828271201e-10
BHK_3_IE_5 1.018038365441399227e-10
BHK_3_IE_6 -9.955752133722067551e-11
BHK_3_OE_1 -3.578007868243626888e-10
BHK_3_OE_2 2.468627906800376241e-10
BHK_3_OE_3 -1.730884968710507288e-11
BHK_3_OE_4 4.380470770799171128e-10
BHK_3_OE_5 7.042077309543960910e-11
BHK_3_OE_6 -3.802289914947110632e-10
BHK_3_OB_1 -6.499524294830945079e-09
BHK_3_OB_2 6.464203182596101153e-09
BHK_3_OB_3 -9.861368914371112790e-11
BHK_3_OB_4 1.193124029961969310e-10
BHK_3_OB_5 1.168806245868690537e-11
BHK_3_OB_6 2.964531610165933614e-12
BHK_3_IB_1 -6.386382124809152765e-09
BHK_3_IB_2 6.206142624317261505e-09
BHK_3_IB_3 -1.465432038539605974e-10
BHK_3_IB_4 1.878589302118834262e-10
BHK_3_IB_5 1.424614047029979528e-10
BHK_3_IB_6 -3.544683311109880260e-12
BHK_4_OT_1 -9.656790615884327269e-09
BHK_4_OT_2 9.333021454734453583e-09
BHK_4_OT_3 3.71342457609610757 1e-11
BHK_4_OT_4 9.629898314186205081e-12
BHK_4_OT_5 5.428015326568273226e-10
BHK_4_OT_6 -2.659190589446268276e-10
BHK_4_IT_1 -8.161391221492049918e-09
BHK_4_IT_2 7.911119696916780822e-09
BHK_4_IT_3 -2.592385646758769220e-10
BHK_4_IT_4 3.084201711948769489e-11
BHK_4_IT_5 1.015019299968040078e-09
BHK_4_IT_6 -5.365251257194125281e-10
BHK_4_OW_1 -4.331608557546842961e-10
BHK_4_OW_2 3.576948125666244131e-11
BHK_4_OW_3 -3.676062279284830803e-11
BHK_4_OW_4 6.449788670650283682e-10
BHK_4_OW_5 9.000827624929143550e-11
BHK_4_OW_6 -3.008308829362450114e-10
BHK_4_IW_1 -6.268269135647831188e-10
BHK_4_IW_2 5.416380864241531281e-11
BHK_4_IW_3 -8.727232616914015782e-11
BHK_4_IW_4 1.140458778455669878e-09
BHK_4_IW_5 1.600706362214584044e-10
BHK_4_IW_6 -6.405669399996818542e-10
BHK_4_N_1 -2.360327648279728746e-10
BHK_4_N_2 1.273025824511616964e-10
BHK_4_N_3 -1.603135451931927372e-09
BHK_4_N_4 2.360621332635209511e-11

BHK_4_N_5 1.728331238902968989e-09
BHK_4_N_6 -4.007049242550839238e-11
BHK_4_Wa_1 -6.759255879045543106e-09
BHK_4_Wa_2 5.408177662193418029e-09
BHK_4_Wa_3 -1.728331238902968989e-09
BHK_4_Wa_4 1.418940751252605903e-09
BHK_4_Wa_5 2.783903449307702494e-09
BHK_4_Wa_6 -1.123872569535132602e-09
BHK_4_S_1 -4.906600241161051803e-11
BHK_4_S_2 1.641554497968578336e-10
BHK_4_S_3 -2.783903449307702494e-09
BHK_4_S_4 4.023415222067387916e-11
BHK_4_S_5 2.605080351153424753e-09
BHK_4_S_6 2.348428350497181772e-11
BHK_4_IE_1 -2.399381370668626160e-10
BHK_4_IE_2 3.197394667886385078e-10
BHK_4_IE_3 -1.018038365441399227e-10
BHK_4_IE_4 1.360740416452735832e-09
BHK_4_IE_5 1.440291439627744840e-10
BHK_4_IE_6 -1.482781116799632572e-09
BHK_4_OE_1 -2.327862688878177553e-10
BHK_4_OE_2 1.767702503458446563e-10
BHK_4_OE_3 -7.042077309543960910e-11
BHK_4_OE_4 1.650131062290834039e-09
BHK_4_OE_5 6.877191719875441509e-11
BHK_4_OE_6 -1.592478824833730807e-09
BHK_4_OB_1 -5.923065006380987421e-09
BHK_4_OB_2 5.631102349082881330e-09
BHK_4_OB_3 -1.168806245868690537e-11
BHK_4_OB_4 1.168268225668456639e-10
BHK_4_OB_5 1.875330011684683773e-10
BHK_4_OB_6 -7.314553106166654631e-13
BHK_4_IB_1 -6.073538969872476316e-09
BHK_4_IB_2 5.710525274778487102e-09
BHK_4_IB_3 -1.424614047029979528e-10
BHK_4_IB_4 2.317384083809944573e-10
BHK_4_IB_5 2.781138615174489414e-10
BHK_4_IB_6 -4.411927065346427527e-12
BHK_5_OT_1 -2.249542365178359742e-09
BHK_5_OT_2 2.777269482897404435e-09
BHK_5_OT_3 -5.428015326568273226e-10
BHK_5_OT_4 -2.081724201100668475e-11
BHK_5_OT_5 9.796527973400674985e-11
BHK_5_OT_6 -6.219258164732522393e-11
BHK_5_IT_1 -2.318253710197116020e-09
BHK_5_IT_2 3.295712152353702572e-09
BHK_5_IT_3 -1.015019299968040078e-09
BHK_5_IT_4 -4.331718759384626471e-11
BHK_5_IT_5 2.530218520802314839e-10
BHK_5_IT_6 -1.722427734563930087e-10
BHK_5_OW_1 -1.708301400587793733e-10
BHK_5_OW_2 1.451377219551035501e-10
BHK_5_OW_3 -9.000827624929143550e-11
BHK_5_OW_4 -1.282009330800437827e-10
BHK_5_OW_5 2.541469768212389372e-11
BHK_5_OW_6 2.184825808178439352e-10
BHK_5_IW_1 -2.427360125768830796e-10
BHK_5_IW_2 2.298821040043629237e-10
BHK_5_IW_3 -1.600706362214584044e-10
BHK_5_IW_4 9.084383951265945935e-11
BHK_5_IW_5 4.954553148811907085e-11
BHK_5_IW_6 3.253566318973063888e-11
BHK_5_N_1 -2.104342829586904851e-10
BHK_5_N_2 4.524412295307401052e-11
BHK_5_N_3 -2.605080351153424753e-09
BHK_5_N_4 -3.683683341834033882e-11
BHK_5_N_5 2.864480840925527048e-09
BHK_5_N_6 -5.738914876178324898e-11
BHK_5_Wa_1 -2.747889234459731650e-09
BHK_5_Wa_2 4.650305136163083958e-09
BHK_5_Wa_3 -2.864480840925527048e-09
BHK_5_Wa_4 -3.796340605895358939e-12
BHK_5_Wa_5 1.027104035226748180e-09
BHK_5_Wa_6 -6.168106146989059599e-11
BHK_5_S_1 6.786988546086766762e-12
BHK_5_S_2 1.175232443500576236e-10
BHK_5_S_3 -1.027104035226748180e-09
BHK_5_S_4 1.675401917988488407e-11
BHK_5_S_5 8.578089074237923685e-10
BHK_5_S_6 2.822637071901437269e-11

BHK_5_IE_1 -1.014396109044784648e-10
BHK_5_IE_2 1.667487284293925661e-10
BHK_5_IE_3 -1.440291439627744840e-10
BHK_5_IE_4 6.526268902687703266e-12
BHK_5_IE_5 4.831136355033346958e-11
BHK_5_IE_6 2.38791548443508645 8e-11
BHK_5_OE_1 -7.262567159127647044e-11
BHK_5_OE_2 1.302996837086408322e-10
BHK_5_OE_3 -6.877191719875441509e-11
BHK_5_OE_4 -4.069942413242562926e-13
BHK_5_OE_5 2.357690785800890923e-11
BHK_5_OE_6 -1.207451491617196785e-11
BHK_5_OB_1 -5.583317459342627538e-09
BHK_5_OB_2 5.769950459052354900e-09
BHK_5_OB_3 -1.875330011684683773e-10
BHK_5_OB_4 -1.181047497841879998e-11
BHK_5_OB_5 1.563167642530648278e-11
BHK_5_OB_6 -2.908288651887724657e-12
BHK_5_IB_1 -5.209703335899970830e-09
BHK_5_IB_2 5.307880053678879252e-09
BHK_5_IB_3 -2.781138615174489414e-10
BHK_5_IB_4 5.548246013484278318e-12
BHK_5_IB_5 7.871473044097509846e-11
BHK_5_IB_6 9.566526989031303396e-11
BHK_6_OT_1 -5.102160257844750317e-10
BHK_6_OT_2 1.053380597488565428e-09
BHK_6_OT_3 -9.796527973400674985e-11
BHK_6_OT_4 -9.375209744411826126e-12
BHK_6_OT_5 -3.735425134560810040e-10
BHK_6_OT_6 -6.232865210487383883e-11
BHK_6_IT_1 -7.903314232955039151e-10
BHK_6_IT_2 1.922897018215229211e-09
BHK_6_IT_3 -2.530218520802314839e-10
BHK_6_IT_4 -5.133909725290661054e-11
BHK_6_IT_5 -7.380298110471138398e-10
BHK_6_IT_6 -9.022897654011167650e-11
BHK_6_OW_1 -6.045412955265908472e-11
BHK_6_OW_2 5.214734551944937957e-11
BHK_6_OW_3 -2.541469768212389372e-11
BHK_6_OW_4 -7.893559477394010540e-11
BHK_6_OW_5 -3.318088756440394702e-11
BHK_6_OW_6 1.458340597751740607e-10
BHK_6_IW_1 -9.739457983801274888e-11
BHK_6_IW_2 1.460239408499134518e-10
BHK_6_IW_3 -4.954553148811907085e-11
BHK_6_IW_4 5.850107467771134206e-11
BHK_6_IW_5 -6.429444396471417943e-11
BHK_6_IW_6 6.704800701588733518e-12
BHK_6_N_1 -4.966496306401726715e-11
BHK_6_N_2 7.657597045748409831e-11
BHK_6_N_3 -8.578089074237923685e-10
BHK_6_N_4 -8.930800254238567179e-12
BHK_6_N_5 8.386974856318909974e-10
BHK_6_N_6 1.127184439617099698e-12
BHK_6_Wa_1 -1.569451565206605559e-09
BHK_6_Wa_2 3.112444676941712912e-09
BHK_6_Wa_3 -8.386974856318909974e-10
BHK_6_Wa_4 -5.083161811033391646e-11
BHK_6_Wa_5 -6.317315303645002811e-10
BHK_6_Wa_6 -2.173776003912645083e-11
BHK_6_S_1 -1.141468343196390767e-10
BHK_6_S_2 4.987177381210251289e-11
BHK_6_S_3 6.317315303645002811e-10
BHK_6_S_4 -1.491338808823196097e-11
BHK_6_S_5 -5.146623582239208298e-10
BHK_6_S_6 -3.789049907820210261e-11
BHK_6_IE_1 -9.223907578695051416e-11
BHK_6_IE_2 1.346582650271847773e-10
BHK_6_IE_3 -4.831136355033346958e-11
BHK_6_IE_4 -3.006230292044601017e-11
BHK_6_IE_5 -3.872203142341942139e-11
BHK_6_IE_6 7.467580645280440907e-11
BHK_6_OE_1 -6.102697084738512306e-11
BHK_6_OE_2 1.063817445705760136e-10
BHK_6_OE_3 -2.357690785800890923e-11
BHK_6_OE_4 -2.029178638949718341e-11
BHK_6_OE_5 -2.536686363723774305e-11
BHK_6_OE_6 2.388209534815726003e-11
BHK_6_OB_1 -3.647777051863481461e-09
BHK_6_OB_2 3.705491251193602782e-09

BHK_6_OB_3 -1.56316764253064827e-11
BHK_6_OB_4 -6.29917137696224133e-12
BHK_6_OB_5 2.91658560905859512e-12
BHK_6_OB_6 -3.86753207140192824e-11
BHK_6_IB_1 -3.51957462708839727e-09
BHK_6_IB_2 3.48924796177345386e-09
BHK_6_IB_3 -7.87147304409750985e-11
BHK_6_IB_4 6.18020757228874691e-12
BHK_6_IB_5 3.06527337608496322e-11
BHK_6_IB_6 7.22307940723513153e-11
BHK_7_OT_1 -4.28054306702158567e-09
BHK_7_OT_2 4.30892780658810072e-09
BHK_7_OT_3 2.39675873798707953e-10
BHK_7_OT_4 -2.16707446085150495e-10
BHK_7_OT_5 3.41792387855896528e-11
BHK_7_OT_6 -8.57492083567188179e-11
BHK_7_IT_1 -3.33982858342339772e-09
BHK_7_IT_2 2.68357663451293243e-09
BHK_7_IT_3 7.38029811047113840e-10
BHK_7_IT_4 -1.98214940454340831e-10
BHK_7_IT_5 1.33866396573735164e-10
BHK_7_IT_6 -1.77394055108060978e-11
BHK_7_W_1 -1.42856831339720542e-10
BHK_7_W_2 1.46391325571316233e-10
BHK_7_W_3 3.31808875644039470e-11
BHK_7_W_4 7.40534592801377633e-10
BHK_7_W_5 -2.09219993511888552e-11
BHK_7_W_6 -7.56323029717890036e-10
BHK_7_OM_1 -3.77742680457392132e-10
BHK_7_OM_2 5.14598144247802038e-10
BHK_7_OM_3 -1.37038522526601853e-10
BHK_7_OM_4 -5.78222811824788725e-11
BHK_7_OM_5 1.86567308703644424e-10
BHK_7_OM_6 -1.28567743201835040e-10
BHK_7_IM_1 -2.68357663451293243e-09
BHK_7_IM_2 2.86694233414693296e-09
BHK_7_IM_3 6.17678833612054999e-10
BHK_7_IM_4 -4.53407836636287392e-10
BHK_7_IM_5 1.37809491432033497e-10
BHK_7_IM_6 -4.85583172761535599e-10
BHK_7_E_1 -2.32545365402444636e-10
BHK_7_E_2 1.97407275931269251e-10
BHK_7_E_3 2.53668636372377431e-11
BHK_7_E_4 -6.90592968652912473e-10
BHK_7_E_5 1.53082312385257425e-10
BHK_7_E_6 5.47263126918332647e-10
BHK_7_OB_1 -3.91917522740003997e-09
BHK_7_OB_2 4.77740921420024939e-09
BHK_7_OB_3 -2.91658560905859512e-12
BHK_7_OB_4 -5.05772923499704373e-10
BHK_7_OB_5 -1.33032345577715950e-10
BHK_7_OB_6 -2.16513941409193509e-10
BHK_7_IB_1 -2.86694233414693296e-09
BHK_7_IB_2 3.06077848164965633e-09
BHK_7_IB_3 -3.06527337608496322e-11
BHK_7_IB_4 -3.60330090995657811e-11
BHK_7_IB_5 -7.70968905431823529e-13
BHK_7_IB_6 -1.26383676838006323e-10

Arkitektkopia AB, Bromma, 2019

SKB is responsible for managing spent nuclear fuel and radioactive waste produced by the Swedish nuclear power plants such that man and the environment are protected in the near and distant future.

skb.se